NET ECOSYSTEM EXCHANGE OF CARBON DIOXIDE AND WATER VAPOR FLUXES IN WINTER WHEAT AND CANOLA UNDER CONVENTIONAL TILL AND NO-TILL SYSTEMS

By

Priyanka Manjunatha

Bachelor of Engineering in Civil Engineering
NMAMIT Nitte University
Karkala, Karnataka
2013

Master of Science in Civil Engineering
University of Texas at Tyler
Tyler, Texas
2015

Submitted to the Faculty of the
Graduate College of the
Oklahoma State University
in the partial fulfillment of
the requirements for
the Degree of
MASTER OF SCIENCE
May, 2019

NET ECOSYSTEM EXCHANGE OF CARBON DIOXIDE

AND WATER VAPOR FLUXES IN WINTER WHEAT AND

CANOLA UNDER CONVENTIONAL TILL AND NO-TILL SYSTEMS

Thesis Approved:

Thesis Adviser

Dr. Alexandre Caldeira Rocateli

Dr. Pradeep Wagle

Dr. Saleh Taghvaeian

ACKNOWLEDGEMENTS

I would like to thank my major advisor, Dr. Alexandre Caldeira Rocateli for his immense support, guidance, and encouragement during my graduate studies at Oklahoma State University.

I would like to thank Dr. Pradeep Wagle, Dr. Prasanna Gowda, and Dr. Saleh Taghvaeian for serving on my committee and providing suggestions. A special thanks to Dr. Pradeep Wagle for his excellent guidance and patience during my research work at the USDA-ARS, Grazinglands Research Laboratory.

I would like to thank the Department of Plant and Soil Sciences, and Department head, Dr. Jeff Edwards, for providing me an opportunity to pursue my master's degree at Oklahoma State University.

I also like to thank my husband, Suraj Thakur, for his support and my deepest gratitude to my family and friends who were unconditionally supportive throughout my studies.

Name: PRIYANKA MANJUNATHA

Date of Degree: MAY 2019

Title of Study: NET ECOSYSTEM EXCHANGE OF CARBON DIOXIDE AND WATER VAPOR FLUXES IN WINTER WHEAT AND CANOLA UNDER CONVENTIONAL TILL AND NO-TILL SYSTEMS

Major Field: CROP SCIENCE

Abstract: It is crucial to understand the impacts of climatic and crop factors, and management practices on carbon and water dynamics of Wheat (*Triticum aestivum* L.) and Canola (*Brassica napus* L.) ecosystems for long-term water planning and improved resource use efficiencies. Net ecosystem exchange (NEE) of CO_2 and H_2O was measured using eddy covariance systems over neighboring wheat and canola fields with different tillage practices such as conventional till (CT) and no-till (NT) in El Reno, Oklahoma, USA. In addition, wheat fields received different grazing managements such as grain only and graze-grain. The objectives of this study were to determine the seasonality of NEE, evapotranspiration (ET), and ecosystem water use efficiency (EWUE) over wheat and canola ecosystems in response to biophysical factors and management practices. In wheat ecosystems, the results revealed that large differences in ET and EWUE were attributed to different climatic conditions and grazing management. Large differences in CO_2 fluxes and ET during the canola growing season were caused by differences in stand establishment after winter dormancy rather than by tillage practices. The cumulative wheat ET was 459 mm for CT and 469 mm for NT under grain-only wheat and 365 mm for CT and 404 mm for NT under graze-grain wheat. The growing season EWUE was 3.49 (CT) and 3.27 (NT) g C mm^{-1} ET for the grain-only and 2.82 (CT) g C mm^{-1} ET and 2.99 (NT) g C mm^{-1} ET for the graze-grain wheat fields. Daily ET reached 6 mm at CT and NT fields for grain-only wheat and 4.6 mm (CT) and 5.3 mm (NT) for graze-grain wheat.

The seasonal sums of NEE were -346 g C m^{-2} and -188 g C m^{-2} at the CT and NT canola fields. Cumulative seasonal ET during the growing season was similar for both fields (429 mm for CT and 415 mm for NT). The EWUE at the growing season scale was 2.97 and 2.78 g C mm^{-1} ET for CT and NT canola fields, respectively. The maximum NEE (7-day average) reached -5.19 ± 0.49 and -4.66 ± 0.35 g C m^{-2} d^{-1} at CT and NT canola fields, respectively. Magnitude of daily canola ET (7-day average) reached 4.69 ± 0.42 mm d^{-1} and 4.28 ± 0.36 mm d^{-1} at CT and NT canola fields, respectively. This research showed the similar seasonal ET between CT and NT management and higher EWUE at CT field for grain-only wheat field under favorable conditions. The CT canola field was a strong carbon sink at the season scale. The ET were similar between CT and NT canola fields, however the higher EWUE was observed at CT field. However, long-term measurements are required to understand the influence of tillage practices and climatic conditions on carbon and ET dynamics.

TABLE OF CONTENTS

LIST OF TABLES

TABLES IN CHAPTER III

Table Page

TABLES IN CHAPTER IV

Table Page

LIST OF FIGURES

FIGURES IN CHAPTER III

Figure Page

FIGURES IN CHAPTER IV

Figure Page

CHAPTER I

INTRODUCTION

Background

Over the past century, the states of the earth's atmosphere and biosphere have experienced much change. Since the dawn of the industrial revolution, the mean global carbon dioxide (CO_2) concentration has risen from about 280 ppm to over 400 ppm (Tans and Keeling, 2014), mainly due to the burning of fossil fuels. The CO_2 abundance is expected to reach 600 ppm in the next century, even if growth of fossil fuel use is slow (Rotty and Marland, 1980). Rising atmospheric CO_2 concentration and other greenhouse gases (GHG) are believed to be partially responsible for climate change (West and Marland, 2002) and have a direct and positive impact on the photosynthesis, growth, and other physiological processes of C3 plant species (Wang et al., 2013). Under climate change, both air and soil temperature are subjected to rise directly affecting cereal crops production. Future agricultural systems is fated to face problems such as extreme temperature and drought stress which may detrimentally impact crop production (Wang et al., 2013). Therefore, more information on carbon, water, and energy fluxes, and interactions among earth surface, atmosphere, and plants is needed. (Baldocchi et al., 2001).

The hydrologic balance of terrestrial ecosystems is gaining interest in recent years (Aubinet et al., 1999) because drought is globally increasing in area and intensity in the last five decades (Dai et al., 2004). Drought is a major concern since it is expected to influence the terrestrial hydrologic cycle in the near future (Wagle and Kakani, 2014). In the hydrological balance, evapotranspiration (ET, combination of loss of water from soil (evaporation) and plants (transpiration) to the atmosphere) is the second largest term after precipitation in most cases, consuming about 50–90% of precipitation (Ford et al., 2007). Increase in food production has to be achieved to support the growing global population. Unfortunately, this higher food production demand must be achieved under reduced water availability (Singh et al., 2007). Furthermore, another concern in future is how elevated CO_2 concentration may affect crop ET (Hunsaker et al., 2000). Increase in ET may affect plants growth and yield. Therefore, in order to understand the role of global climate change on crop water use, ET is an essential component of the energy and water budgets in grassland and agricultural ecosystems (Verma et al., 1989; Hunsaker et al., 2000).

Objectives

The objectives of these studies were to: 1) determine the seasonality of Net ecosystem exchange of carbondioxide (NEE) and its components [(Gross primary photosynthesis (GPP) and ecosystem exchange (ER)] from conventional till and no-till wheat and canola systems, 2) quantify seasonal variations in ET, EWUE, and energy partitioning in wheat and canola crop under conventional till and no-till systems, 3) investigate the response of CO_2 and H_2O fluxes to changes in major environmental factors, and 4) compare difference in water use between conventional till and no-till systems.

References

Aubinet, M., Grelle, A., Ibrom, A., Rannik, Ü., Moncrieff, J., Foken, T., ... & Clement, R. (1999). Estimates of the annual net carbon and water exchange of forests: the EUROFLUX methodology. In *Advances in ecological research* (Vol. 30, pp. 113-175). Academic Press.

Baldocchi, D., Falge, E., Gu, L., Olson, R., Hollinger, D., Running, S., ... & Fuentes, J. (2001). FLUXNET: A new tool to study the temporal and spatial variability of ecosystem-scale carbon dioxide, water vapor, and energy flux densities. *Bulletin of the American Meteorological Society*, *82*(11), 2415-2434.

Dai, A., Trenberth, K. E., & Qian, T. (2004). A global dataset of Palmer Drought Severity Index for 1870–2002: Relationship with soil moisture and effects of surface warming. *Journal of Hydrometeorology*, *5*(6), 1117-1130.

Dlugokencky, E., & Tans, P. (2014). Trends in atmospheric carbon dioxide, National Oceanic & Atmospheric Administration, Earth System Research Laboratory (NOAA/ESRL).

Ford, C. R., Hubbard, R. M., Kloeppel, B. D., & Vose, J. M. (2007). A comparison of sap flux-based evapotranspiration estimates with catchment-scale water balance. *Agricultural and Forest Meteorology*, *145*(3-4), 176-185.

Hunsaker, D. J., Kimball, B. A., Pinter Jr, P. J., Wall, G. W., LaMorte, R. L., Adamsen, F. J., ... & Brooks, T. J. (2000). CO2 enrichment and soil nitrogen effects on wheat evapotranspiration and water use efficiency. *Agricultural and Forest Meteorology*, *104*(2), 85-105.

Rotty, R. M., & Marland, G. (1980). Constraints on fossil fuel use. In *Interactions of Energy and Climate* (pp. 191-212). Springer, Dordrecht.

Singh, R. P., Huerta-Espino, J., Sharma, R., Joshi, A. K., & Trethowan, R. (2007). High yielding spring bread wheat germplasm for global irrigated and rainfed production systems. *Euphytica*, *157*(3), 351-363.

West, T. O., & Marland, G. (2002). Net carbon flux from agricultural ecosystems: methodology for full carbon cycle analyses. *Environmental Pollution*, *116*(3), 439-444.

Wagle, P., & Kakani, V. G. (2014). Seasonal variability in net ecosystem carbon dioxide exchange over a young Switchgrass stand. *Gcb Bioenergy*, *6*(4), 339-350.

Wang, L., Feng, Z., & Schjoerring, J. K. (2013). Effects of elevated atmospheric CO2 on physiology and yield of wheat (Triticum aestivum L.): a meta-analytic test of current hypotheses. *Agriculture, ecosystems & environment*, *178*, 57-63.

CHAPTER II

LITERATURE REVIEW

Ecosystem level flux measurements

Flux is defined as how much of something moves through a unit area per unit time. Flux measurements are widely used in order to estimate the exchange of heat, water vapor (H_2O), carbon dioxide (CO_2), methane (CH_4), and other trace gases. Flux is dependent on various factors, including the number of elements crossing the area, the size of the area being crossed, and the amount of time it takes to cross the area. Flux is measured from single-point measurement and represents the entire ecosystem exchange (Burba, 2013). The eddy flux (F) is expressed as follow:

$$F \approx \overline{\rho_a w}' s' \qquad (1)$$

where F is flux, ρa is the mean air density, w is the vertical wind speed, and s the mixing ratio. The over bar denotes temporal averaging (i.e., 30-min).

Flux Measurement Techniques

Various methods like Bowen ratio energy balance (BREB), surface renewal (SR), scintillometer, and eddy covariance (EC) are used to measure fluxes over terrestrial surfaces. Bowen ratio energy balance method (BREB) is a practical and relatively reliable micrometeorological method (Allen et al., 2011), which is often used to measure latent heat (LE) and sensible heat (H). This concept enables solving the energy balance equation by measuring simple gradients of air temperature and vapor pressure in the near-surface layer above the evaporating surface. The method works best when soil water is an evapotranspiration (ET) limiting factor (Bowen, 1926). However, when the Bowen ratio is small, the method will be useful at fetch-to-height ratios as low as 20:1 (Heilman et al., 1989). The BREB method has following advantages: 1) it measures ET over both potential and non-potential surfaces, 2) the gradient-based fluxes are averaged over a medium sized area (200–100,000 m^2), 3) the system is quite robust, and 4) the instrumentation is relatively less expensive (Allen et al., 2011). The BREB method returns good results when employed in large extent, relatively smooth and uniform wetlands (Drexler et al., 2004). The disadvantage of this method is that it assumes equal transfer coefficients for H and LE which may not be true during stable (inversion) conditions (Drexler et al., 2004). The accuracy of ET depends substantially on the representativeness and accuracy of net radiation (Rn) and soil heat flux (G) (Allen et al., 2011). However, due to certain disadvantages such as need for an extensive study site having sufficient fetch, system inaccuracy and labor intense, BREB is currently considered as an outdated methodology.

Surface Renewal (SR) is based on analyzing the short-term energy transfer between canopy elements and air parcels during the turbulent exchange process. Therefore, it is less dependent on fetch, which make the SR methodology useful for calculating ET for locations with

fetch limitations such as edges of wetlands and small wetland patches. The advantages of this system are portability, easy maintenance, and relatively low costs. The main disadvantage of the SR method is that it must be calibrated against an independent measure of H flux density (Drexler et al., 2004).

The scintillometer is used to measure H and it consists of an optical transmitter and a receiver at the ends of an atmospheric propagation path. Scintillometer measurements require assumptions related to Monin–Obukhov stability functions, the estimation of mean shear stress (or friction velocity), and some empirical corrections related to the frequency spectrum. Some advantages of this device is it is relatively simple to operate and maintain, consistency in application (Kleissl et al., 2008), the integration of H over large distances (i.e., few hundreds of meters up to 10 km), with weighting toward the center of the transect (Meijninger et al., 2002). The disadvantages are it measures only the magnitude of H, it may require some post-processing correction, and the device is relatively expensive (Allen et al., 2011). This technique is currently being used.

The most commonly used and highly accurate method to measure fluxes such CO_2, H_2O, H, and LE fluxes is through in-situ EC towers that utilize a sonic anemometer with an CO_2 and H_2O gas analyzer to produce 30-minute flux averages from 10-20 Hz data (Baldocchi et al., 2000; Burba, 2013).

The first EC measurements that focused on CO_2 exchange occurred in the early 1970s (Desjardins, 1974; Desjardins and Lemon, 1974). This set of studies was performed over corn (*Zea mays* L.) using a propeller anemometer and a modified closed-path infrared gas analyzer, with a capacitance detector; a set of sensors with relatively slow time constants on the order of 0.5 s. There was almost ~40% error of CO_2 flux from these measurements, so the next

technological improvements came nearly a decade later and were reliant on the commercial availability of sonic anemometers and the development of rapid-responding open path infrared gas analyzers (Bingham et al., 1978; Jones et al., 1978; Brach et al., 1981; Ohtaki and Matsui, 1982). Open-path CO_2 sensors were a key innovation because they are able to acquire CO_2 fluctuations as rapidly as ten times or even higher per second.

In recent years, the EC technique has emerged as an alternative way to assess ecosystem carbon exchange and H_2O fluxes (Running et al., 1999; Canadell et al., 2000; Geider et al., 2001). This technique provides unique measurements of CO_2, H_2O, and energy fluxes between the biosphere and the atmosphere at the ecosystem scale. Assuming perfect turbulent mixing these measurements are typically integrated over periods of half an hour (Goulden et al., 1996) building the basis to calculate carbon and water balances from daily to annual timescales. A clear advantage is that if the water vapor covariance flux is measured, it provides a direct measure of LE. In addition, if Rn, G, and H are measured at the same time, energy balance closure can be computed to provide some verification of the measurements and fluxes are averaged over medium-sized (50 m-200 m) areas. If all of the energy balance components are measured accurately and there is no horizontal advection, then Rn – G = H+LE. None of the other methods have this self-verification. The greatest disadvantages of using eddy covariance are the cost andthe complexity and sensitivity of instruments to damage. Eddy covariance instrumentation generally requires high maintenance to ensure good results (Drexler et al., 2004).

Chamber techniques have been the most commonly used approach to measure greenhouse gases (GHGs) (Rochette and Hutchinson, 2005). Chambers can be linked to the Infrared gas analyzer (IRGA) equipment and measurements can be taken either by using open or closed chambers. In closed systems, sample material is enclosed in a sealed chamber and the

changes in the gas concentration in the enclosed air over time are used to estimate the fluxes. Outside air is continuously introduced into the chamber in the open systems and fluxes are estimated by the products of the airflow rate and differences in gas concentrations between inflowing and out flowing air (Teitel et al., 2011). The main disadvantage of using chambers are: 1) it provides measurements over a small surface area (Koskinen et al., 2014) and 2) data collection is made manually resulting in discontinuous and short-spanned data (Gagnon et al., 2016) which further could be misleading for data interpretation. Therefore, this technique might not be suitable for the fields with well-established canopies because single measurements will not be adequate to predict the strongly modified wind and concentration profiles (IFIA, 2019).

The Eddy Covariance Technique, Theory, and Flux Computations

The Eddy Covariance method is a micrometeorological technique, which provides a direct measure of net carbon between vegetated canopies and the atmosphere (Baldocchi et al., 1988; Foken and Wichura, 1996; Baldocchi et al., 2000). The EC method is capable of measuring ecosystem CO_2 exchange across a spectrum of times scales, ranging from hours to years with minimal disturbance of the underlying vegetation (Baldocchi et al., 2001). The atmosphere contains turbulent motions of upward and downward moving air that transports trace gases such as CO_2. The EC technique samples these turbulent motions to determine the net difference of material moving across the canopy-atmosphere interface (Baldocchi, 2003). The EC technique produces a direct measure of net ecosystem carbon exchange (NEE) and H_2O fluxes across the canopy-atmosphere interface by using the micrometeorological theory to interpret measurements of the covariance between vertical wind velocity and scalar concentration fluctuations (Baldocchi et al., 1988; Verma, 1990; Desjardins, 1992; Lenschow,

1995). Some assumptions made in EC method are: 1) flat terrain, 2) homogeneous canopy height and structure, 3) instruments should face the predominant wind, and 4) the site location should be large enough to place the tower to provide adequate footprint. Violation of these assumptions can cause systematic errors in the interpretation of the eddy covariance measurements (Baldocchi et al., 1988; Foken and Wichura, 1996; Massman and Lee, 2002).

CO_2 Fluxes

In EC technique, CO_2 commonly measured using infrared gas analyzer (IRGA) in either open or closed configuration. The CO_2 detector has a filter at the 4.26 µm absorption band, and the gas analyzer is usually placed at or slightly below the sonic anemometer level (Burba, 2013).

The flux of CO_2 and water vapor (H_2O flux) is given by (Webb *et al.*, 1981)

$$F = \bar{\rho} * \overline{w' * s'} \quad (2)$$

where ρ is the density of the dry air, w' is vertical wind speed, and s' is dry mole fraction. The bar above the product of the fluctuations denotes time averaging.

H_2O fluxes or Evapotranspiration (ET)

Total ET for a 30-min period (mm 30-min-1) is calculated from EC measured H_2O fluxes (mmol $m^{-2}s^{-1}$) as follows:

$$ET = (H2O\ flux*18.01528*1800)/10^6 \quad (3)$$

where H_2O is measured using infrared gas analyzer (IRGA) in either open or closed configuration.

Ecosystem water use efficiency (EWUE) is the net carbon uptake per amount of water lost from the ecosystem, which is a useful methodology to quantify the functionality in semiarid

shrubs and grassland communities (Emmerich, 2007). According to Emmerich (2007), EWUE is determined from the ratio of daily daytime NEE of CO_2 to daily nighttime ET (g CO_2 18 per mm H_2O) that is summoned for the growing season. For the maximum regression equation, day times with maximum CO_2 uptake with minimum ET were selected, and the slopes for the maximum EWUE were selected to compare EWUE between plant communities. The slope of NEE vs. ET and gross primary production (GPP) vs. ET using half-hourly measurement of the day was used to determine EWUE (Kuglitsch et al., 2008). Kuglitsch et al. 2008 reported that GPP and ET were strongly associated than NEP and ET since NEP depends on respiration and respiration is not tightly coupled with ET. On seasonal scale, EWUE is estimated from the slope of the regression of daily daytime NEE or GPP vs. ET and daily or monthly EWUE can be calculated from the ratio of daily or monthly integrals of GPP or NEE to ET (Baldocchi et al., 2001).

Latent heat flux (LE)

Latent Heat Flux is the stored heat energy in water, which is the same as ET. When the LE flux is positive, ET is occurring meaning that energy is transferred from the surface to the air. When the LE flux is negative, condensation is occurring which means that energy is transferred from the air to the surface. In this case, the surface warms up and the energy can be used to warm the subsurface. LE flux is negative usually during the night. LE flux is determined from the average values of wind speed and vapor density. LE flux is corrected for oxygen effects (Tanner and Greene, 1989) and density differences caused by heat and vapor transfer (Webb et al., 1980). Mathematical equation to estimate LE is

$$LE = \lambda \rho_a \overline{w' * q'} \qquad (4)$$

where λ is latent heat of vaporization, ρ is the density of the dry air, w' is vertical wind speed, and q is water vapor.

Sensible heat flux (H)

Sensible Heat flux is defined as the energy required to change the temperature of a substance with no phase change. If H is negative, the dominant direction of energy flow is from the air to the earth's surface, which means that air is losing energy and the earth's surface is gaining energy. If the H is positive, the dominant direction of energy flow is from the earth's surface to the air, which means the air is gaining energy and the surface of the earth is losing energy. Sensible-heat flux is determined by the covariance of instantaneous departures from the average values of wind speed and air temperature. Sensible heat flux can be estimated by the following equation.

$$H = \rho_a C_p \overline{w' * T'} \quad (5)$$

where ρ is the air density, Cp is specific heat, w' is vertical wind speed and T' is the temperature.

Energy Balance Closure (EBC)

Measurements of latent- and sensible- heat flux, combined with measurements of net radiation and subsurface-heat flux allow the estimation of an energy budget. The evaluation of energy budget using data collected at EC sites provides an indication of instrument efficiency in measuring the available energy (Berger et al., 2001).

Processing and screening of fluxes

Some of the basic corrections used in data processing includes Webb Pearman and Leuning (WBL) method, quality control, friction velocity (U*) correction, and EBC. The post processing data includes statistical analysis for quality control, determination of the appropriate averaging period (Vickers and Mahrt, 2003), correction for sonic temperature (Schotanus et al., 1983), density effects (Webb et al., 1980), and tilt correction (Mahrt et al., 2001). Time series data can be processed using Quality Control (QC) Software, version 3.0 (Vickers and Mahrt, 1997).

The data processing includes processing the real-time, instantaneous data (at 10-20 Hz), processing averaged data (0.5 to 2 hours), quality control, and long-term integration and analysis. Some of the main element of the data processing are correcting the time delay, screening, gap filling and partitioning (Burba, 2013). Several Software packages that are used for processing of eddy fluxes are TK3, Alteddy, ECPack, EddySoft, EdiRE eth-flux, TUDD, S + packages, ECO2S and eddy pro.

Time delay

The delay between the two-time series is mainly caused by differences in electronic signal treatment, spatial separation between wind and scalar sensors, and air travel through the tubes in closed-path eddy covariance systems. Time delays caused by electronic signal treatment (signal conversion and computation) are generally relatively small, constant and can thus be considered directly. The air parcel needs some time to pass both of the instruments, which depends on wind speed, wind direction, and the distance between the sensors (Aubinet et al., 2012).

Data screening

The EC method underestimates all the fluxes in stable conditions. This underestimation acts as a selective systematic error (Moncrieff et al., 1996) and could lead to a strong overestimation of net ecosystem exchange (NEE) at stable nighttime conditions and also at night, the turbulent flux is sensitive to the friction velocity (u*). The nighttime flux error leads to overestimation of a carbon sequestration and it also underestimates the flux-climate relationships such as photosynthetically active photon flux density (PPFD). Unreliable flux data during calm periods are excluded in order to avoid this error. During screening, negative nighttime NEE (as no photosynthesis occurs during the night) during low wind velocity is removed. Sensible heat and LE fluxes are filtered to keep in the ranges of -200 to 500 Wm^{-2} and –200 to 800 Wm^{-2}, respectively (Sun et al., 2010). Physically unreasonable CO_2 fluxes beyond ±3.5 SD (standard deviation) are removed (Wagle and Kakani, 2014).

The different types of data screening methods are: the statistical outlier method, the artificial time series method (Press et al., 1989), normal (Gaussian) distribution, the prediction model, and self-contained model (Hojstrup, 1993).

Velocity friction (u*)

Uncertainties and Drawbacks of u*

Varying footprints can be a source of errors and uncertainties that can affect data quality, particularly if the ecosystem is inhomogeneous and patchy (Göckede et al., 2006). At night, EC systems located above terrestrial ecosystems may report little or no CO_2 exchange even when such exchanges are known to be occurring. These flux deficits occur under stable, low-wind conditions when turbulence is not well developed (Hollinger et al., 1994; Goulden et al., 1996;

Aubinet et al., 1999; Massman and Lee, 2002; Gu et al., 2005; Barr et al., 2006). Therefore, the ecosystem respiration (ER) is underestimated and the carbon sequestration is overestimated (Moncrieff et al., 1996). Aubinet (2008) and Aubinet et al. (2009) identified two primary causes of nighttime EC flux deficits: intermittent turbulence and advective transport. Nighttime flux deficits are a major source of uncertainty and potential bias in EC measurements of NEE. Because they affect the magnitude of the day-night difference altering the size of the daily and annual NEE integrals (Goulden et al., 1996; Barford et al., 2001) and the partitioning of NEE into ER and gross primary production (GPP) (Falge et al., 2001; Barr et al., 2006; Papale et al., 2006). The uncertainties associated with nighttime deficits typically overwhelm other methodological sources of uncertainty such as coordinate rotation, instrument noise, or calibration errors (Morgenstern et al., 2004, Loescher et al., 2006). The friction velocity is currently used as a criterion to discriminate low and well mixed periods. This approach is generally known as the u∗ correction. In general, diurnal variations in u* tend to synchronize with diurnal variations in temperature, particularly air temperature. The u* is higher during daytime and lower during nighttime. Since ER is strongly influenced by temperature, ER also exhibits diurnal cycles. Therefore, ER and u* are potentially positively correlated at diurnal timescales even though there may have no causal relationship between them. Interestingly, nighttime u* is out of phase with temperature and ER at seasonal time scales with lower u* in summer and higher u* in winter. Therefore, a negative correlation between ER and u* can be expected at seasonal time scales (Gu et al., 2005). Bootstrapping technique is used to assess the uncertainty of the u∗ threshold detection (Papale et al., 2006), values below the threshold are removed and the gaps filled. Also, an automated statistical method (Moving Point Test, MPT) can be used to determine the u* thresholds in nighttime eddy flux filtering. The potential

correlative changes between ER and u* must be removed before u* can be used as a filter criterion. Moving point test uses an iterative approach to simultaneously determining a valid temperature response function, which is used to normalize nighttime flux measurements, and identify u* thresholds based on the normalized fluxes (Gu et al., 2005).

First, an implicit application of the correction could lead to even bigger errors: indeed, during calm night conditions, the CO_2 can be either removed by advection or stored in the canopy air. Another problem with the u∗ correction is that it depends on the operator's subjectivity. The u∗ threshold used to discriminate well and poorly mixed data is generally chosen by visual inspection (Papale et al., 2006). Finally, the hypotheses underlying the u∗ correction are still debatable: firstly, it is based on the assumption that flux in calm conditions can be inferred from measurements made in windy conditions, which is not proven. Secondly, it supposes that measurements made during turbulent periods are free of errors which are questioned by recent experiment results (Cook et al., 2004; Massman et al., 2004; Wohlfahrt et al., 2005).

Gap filling

Data from EC are usually reported half-hourly, 24 hours a day, and 365 days a year. According to (Falge et al., 2001), gaps in EC data are unavoidable due to several reasons such as power issues, sensor malfunction, data rejection and unmet assumptions of EC system.. Therefore, gap-filling procedures need to be established for providing complete data sets. The gaps in observed data can cause at least three problems: (1) difficulty in annual estimation of NEE, LE and H; (2) biased relationships between NEE, LE and H with climatic variables; and (3) low quality data for modeling validation (Hui Wan et al., 2004). Several gap-filling

techniques that have been proposed in scientific literature are (1) mean diurnal variation method (MDV - an interpolation technique based on the temporal auto-correlation of fluxes), (2) look-up tables (LUT - is an empirical method in which missing values are gap filled with the average of valid measurements under similar meteorological conditions), (3) artificial neural networks (ANNs - an empirical nonlinear regression models), and (4) nonlinear regression relationships between the flux and environmental drivers (Aubinet et al., 2012). Empirical models have been employed in the majority of the studies to fill data gaps for daytime and nighttime. Since photosynthesis is mainly driven by light during daytime in the growing season, the hyperbolic relationship between GPP and PPFD is commonly used to fill gaps for daytime during the growing season (Flanagan et al., 2002). Linear interpolation between the values adjacent to the missing values is generally used for small gaps (2–3 half-hourly means missing) for missing meteorological variables (temperature and relative humidity) (Falge et al., 2001). An average value before and after the gap was used to fill half-hourly gaps (Wever et al., 2002). Interpolated values were used to fill two hour or fewer gaps (Flanagan et al., 2002). Diurnal values derived for each time stamp of the day based on 14-day means were used to fill gaps in H_2O flux data (Kochendorfer et al., 2011). Established monthly ET – ET0 regression models developed from existing data were used to fill gaps in a 30-min ET data set, and regression relationships between ET and Rn were employed if ET0 is unavailable (Sun et al., 2010). They used linear interpolation method during the unavailability of all meteorological variables. Diurnal variations were used to estimate missing data in the absence of empirical relationships due to missing meteorological data. The size of the dataset used to develop these relationships depends on the size of data gap (Falge et al., 2001; Flanagan et al., 2002).

The REddy Proc based on R package is also available online from the Max Planck Institute for Biogeochemistry, which is widely used to fill gaps in flux data. This tool fills gaps using similar methods as (Falge et al., 2001) and it considers the co-variation of fluxes with meteorological variables and the temporal auto-correction of the fluxes (Reichstein et al., 2005; Wagle et al., 2017). The gap filling service is provided for the variables like fluxes (including uncertainty estimates) for NEE, H, LE and meteorology data like Rg, VPD, rH, Tair (air temperature), and Tsoil (soil temperature).

Partitioning of NEE

Eddy covariance estimates net exchange of matter and energy. The NEE of CO_2 can be divided into two components: GPP (uptake of carbon by photosynthesis) and ER (carbon release from autotrophic and heterotrophic activities). It is represented by the following equation:

$$NEE = ER - GPP \quad (6)$$

Here ER is always positive and GPP is positive during daytime and zero at nighttime (no photosynthesis occurs at nighttime). In this equation, NEE is equal to ER when GPP is zero, resulting in positive values of NEE. However, during daytime, larger values of GPP than ER results in negative values of NEE. Therefore, the sign convention of NEE considered in this study is that CO_2 uptake by the ecosystem is negative and a net CO_2 release to the atmosphere is positive.

NEE flux partitioning is needed for a better understanding on how interannual and between-site variability of NEE is caused (Valentini et al., 2000; Reichstein et al., 2005). The EC system does not measure ER and GPP individually. Instead, it provides a balance between these

two terms. Therefore, flux-partitioning algorithms are necessary to estimate these component fluxes from measured NEE. Hyperbolic light-response curve is one of the simple and most commonly used methods to partition NEE into GPP and ER.

$$NEE = (\alpha * GPPmax * PPFD/\alpha * PPFD + GPPmax) + ER \quad (7)$$

where α is the apparent quantum yield [i.e., the initial slope of the light – response curve (mol CO2 mol^{-1} of photons)], GPPmax is the maximum canopy CO_2 uptake rate (μmol m^{-2} s^{-1}) at light saturation, PPFD is measured photosynthetic photon flux density (μmol m^{-2} s^{-1}), and ER is respiration rate.

Several factors such as temperature, VPD (vapor pressure deficit), and moisture stress influence the relationship between NEE and PFD. The CO_2 flux of canopy saturates relatively less than that of a single leaf because lower leaves in plant canopies may have a PPFD deficit while the upper leaves are PPFD saturated (Ruimy et al., 1995). The rectangular hyperbolic light-response function failed to describe NEE only as a function of PPFD in several ecosystems (Li et al., 2005; Wang et al., 2008; Pingintha et al., 2010). The failure reason was that the light-response function underestimates the daily peak of NEE before noon and overestimate NEE in the afternoon and failed to account for the reduction in NEE at high VPD in the afternoon (Lasslop et al., 2010; Wagle and Kakani, 2014). Wagle and Kakani (2014) used modified rectangular hyperbolic light VPD model which included limitation of VPD on photosynthesis, which was able to provide better estimate of GPP and daytime ER and reproduce asymmetrical diurnal NEE cycles. Lasslop et al. (2010) and Wagle and Kakani (2014) calculated GPPmax as the exponential decreasing function at high VPD to include the effect of VPD on photosynthesis as shown below:

$$GPPmax = GP0\exp(-K(VPD-VPD0)), \text{ if } VPD > VPD0 \quad (8)$$

GPPmax = GP0, if VPD < VPD0 (9)

Where k indicates the response of GPPmax to VPD. (Lasslop, et al. 2010) set VPD0 threshold as 1kPa.

Role of Vapor pressure deficit (VPD)

Vapor pressure deficit could be particularly important in non-irrigated crop production. Large VPD might be responsible for limitation of photosynthesis as demonstrated by Wagle and Kakani (2014). The authors demonstrated that the rectangular hyperbolic-light response curve failed to provide good fits when VPD >3kPa, and that the modified model provided good fits when considering VPD <3kPa. During dry period, higher NEE was noticed in the morning and then decreased at higher VPD at equal light levels (PPFD). Stomatal closure control of photosynthesis and reduction of carbon uptake at higher VPD causes asymmetric shapes of diurnal NEE cycles.

Daytime and nighttime Ecosystem Respiration (ER)

The ER is the release of CO_2 from the ecosystem to the atmosphere due to autotrophic (vegetation respiration) and heterotrophic (soil respiration) activities. According to Davidson et al. (2006), respiration is the second most important flux in the global carbon cycle after photosynthesis. Soil respiration is the release of CO_2 by roots, soil microorganism, and chemical oxidation of carbon compounds (Lloyd and Taylor, 1994). Understanding the response of ER to major environmental drivers is critical for estimating carbon sequestration and large-scale modeling research (Wagle and Kakani, 2014). During nighttime, NEE is considered equal to ER due to the absence of photosynthesis at night. According to Lalrammawia and Paliwal (2010),

the maximum ER occurred when the soil moisture content was maximum and decreased gradually with the gradual depletion of soil moisture. Researchers have employed various approaches in order to estimate ER, for instance, the use of the same ER during night and daytime, daytime ER can be estimated by the extrapolated functional relationships between nighttime NEE and temperature to daytime conditions (Xu et al., 2001). However dark respiration was estimated in the leaves of two woody species (*Heteromeles arbutifolia* Ait. and *Lepechinia fragans* Greene) and in all cases dark respiration in the light was lower than respiration in darkness due to light inhibition of dark respiration (Villar et al., 1994).

Falge et al. (1996) modeled daytime respiration. At low levels of light intensities, the relationship between NEE and PPFD is linear, but as a result of the reduction in CO_2 assimilation and higher respiration rates due to a lack of light-induced inhibition of dark respiration the linear relationship breaks and slope changes abruptly. Therefore, estimation of the linear relation of light curve to zero PPFD before the change in slope provides correct estimates of respiration for daytime (Villar et al., 1994; Bruhn et al., 2011). Generally, the intercept value of a hyperbolic light-response curve fit has been used in the majority of the studies to estimate ER using all daytime data.

Energy balance closure (EBC)

The accuracy of EC measurements is assessed from energy balance closure (EBC) test. The EBC is based on the first law of thermodynamics and determined by comparing turbulent heat fluxes (H+LE) with the available energy fluxes (Rn – G) as given below:

$$Rn - G = H + LE \quad (10)$$

where Rn is net radiation, G is soil heat flux, H is sensible heat flux, and LE is latent heat flux.

The sum of turbulent fluxes (H + LE) measured is always less than the available energy (Rn – G), as the EC system under-estimates H and LE fluxes (Twine et al., 2000). The EBC is currently about 80% for many field experiments and for the CO2 flux networks (Aubinet et al., 1999; Wilson et al., 2002). Therefore, it is obvious that experimental data could not close the energy balance at the Earth's surface.

It was assumed that the EC system would underestimate turbulent fluxes systematically. Improvements in the sensors and the flux correction methods helped to improve EBC over the past decade (Foken et al., 2004). Another possible reason for the lack of EBC could be the errors in available energy measurements or from neglecting heat storage in biomass (Cook et al., 2004; Desai et al., 2005). Various location of the footprints for the measurements of Rn and G, which are close to the EC tower, whereas H and LE which are larger and upwind of the tower may induce some divergence in EBC (Flanagan et al., 2002). It is recently reported that either the time-averaged fluxes (Finnigan et al., 2003) or spatially averaged fluxes including turbulent-organized structures (Kanda et al., 2004) can close the energy balance. According to these findings, the unclosed EBC problem is not related to errors involved in the EC system. Rather, the error is related to the atmospheric phenomena which EC systems fail to measure. So it can be concluded based on previous studies that the lack of EBC correction in the surface layer is not due to EC method but it is related to the heterogeneous terrain and its influence on the turbulent exchange (Foken et al., 2011). A common procedure to reduce problems with the relative EBC consists of eliminating observations with a (very) low u* (so-called "u* filtering"), (Aubinet et al., 1999).

Footprint

The footprint defines the field of view of the flux/concentration sensor and reflects the influence of the surface on the measured turbulent fluxes (or concentrations). A source area is a fraction of the surface (mostly upwind) containing effective sources and sinks contributing to a measurement point (Kljun et al., 2002). The footprint is then defined as the relative contribution from each element of the surface area source/sink to the measured vertical fluxes or concentrations (Leclerc and Thurtell, 1990; Schuepp et al., 1990). The footprint is sensitive to both atmospheric stability and surface roughness. Mathematically, the surface area of influence on the entire flux goes to infinity and thus one must always define the %-level for the source area (Schmid, 1994). Often 50%, 75%, or 90% source areas contributing to a point flux measurement are considered.

References

Allen, R. G., Pereira, L. S., Howell, T. A., & Jensen, M. E. (2011). Evapotranspiration information reporting: I. Factors governing measurement accuracy. *Agricultural Water Management*, *98*(6), 899-920.

Aubinet, M. (2008). Eddy covariance CO2 flux measurements in nocturnal conditions: an analysis of the problem. *Ecological Applications*, *18*(6), 1368-1378.

Aubinet, M., Moureaux, C., Bodson, B., Dufranne, D., Heinesch, B., Suleau, M., ... & Vilret, A. (2009). Carbon sequestration by a crop over a 4-year sugar beet/winter wheat/seed potato/winter wheat rotation cycle. *Agricultural and Forest Meteorology*, *149*(3-4), 407-418.

Aubinet, M., Vesala, T., & Papale, D. (Eds.). (2012). *Eddy covariance: a practical guide to measurement and data analysis*. Springer Science & Business Media.

Baldocchi, D., Finnigan, J., Wilson, K., & Falge, E. (2000). On measuring net ecosystem carbon exchange over tall vegetation on complex terrain. *Boundary-Layer Meteorology*, *96*(1-2), 257-291.

Baldocchi, D. D. (2003). Assessing the eddy covariance technique for evaluating carbon dioxide exchange rates of ecosystems: past, present and future. *Global change biology*, *9*(4), 479-492.

Baldocchi, D. D., Hincks, B. B., & Meyers, T. P. (1988). Measuring biosphere-atmosphere exchanges of biologically related gases with micrometeorological methods. *Ecology*, *69*(5), 1331-1340.

Baldocchi, D. D., Law, B. E., & Anthoni, P. M. (2000). On measuring and modeling energy fluxes above the floor of a homogeneous and heterogeneous conifer forest. *Agricultural and Forest Meteorology*, *102*(2-3), 187-206.

Balkovič, J., van der Velde, M., Skalský, R., Xiong, W., Folberth, C., Khabarov, N., ... & Obersteiner, M. (2014). Global wheat production potentials and management flexibility under the representative concentration pathways. *Global and Planetary Change*, *122*, 107-121.

Barford, C. C., Wofsy, S. C., Goulden, M. L., Munger, J. W., Pyle, E. H., Urbanski, S. P., ... & Moore, K. (2001). Factors controlling long-and short-term sequestration of atmospheric CO2 in a mid-latitude forest. *Science*, *294*(5547), 1688-1691.

Barr, A. G., Morgenstern, K., Black, T. A., McCaughey, J. H., & Nesic, Z. (2006). Surface energy balance closure by the eddy-covariance method above three boreal forest stands

and implications for the measurement of the CO2 flux. *Agricultural and Forest Meteorology*, *140*(1-4), 322-337.

Berger, B. W., Davis, K. J., Yi, C., Bakwin, P. S., & Zhao, C. L. (2001). Long-term carbon dioxide fluxes from a very tall tower in a northern forest: Flux measurement methodology. *Journal of Atmospheric and Oceanic Technology*, *18*(4), 529-542.

Bingham, G. E., Gillespie, C. H., & McQuaid, J. H. (1978). *Development of a miniature, rapid-response carbon dioxide sensor* (No. UCRL-52440). California Univ., Livermore (USA). Lawrence Livermore Lab..

Bowen, I. S. (1926). The ratio of heat losses by conduction and by evaporation from any water surface. *Physical review*, *27*(6), 779.

Brach, E. J., Desjardins, R. L., & St Amour, G. T. (1981). Open path CO2 analyser. *Journal of Physics E: Scientific Instruments*, *14*(12), 1415.

Bruhn, D., Mikkelsen, T. N., Herbst, M., Kutsch, W. L., Ball, M. C., & Pilegaard, K. (2011). Estimating daytime ecosystem respiration from eddy-flux data. *Biosystems*, *103*(2), 309-313.

Burba, G. (2013). *Eddy covariance method for scientific, industrial, agricultural and regulatory applications: A field book on measuring ecosystem gas exchange and areal emission rates*. LI-Cor Biosciences.

Canadell, J. G., Mooney, H. A., Baldocchi, D. D., Berry, J. A., Ehleringer, J. R., Field, C. B., ... & Running, S. W. (2000). Commentary: Carbon metabolism of the terrestrial biosphere: A multitechnique approach for improved understanding. *Ecosystems*, *3*(2), 115-130.

Chi, J., Waldo, S., Pressley, S., O'Keeffe, P., Huggins, D., Stöckle, C., ... & Lamb, B. (2016). Assessing carbon and water dynamics of no-till and conventional tillage cropping systems in the inland Pacific Northwest US using the eddy covariance method. *Agricultural and forest meteorology*, *218*, 37-49.

Ciais, P., Tans, P. P., Trolier, M., White, J. W. C., & Francey, R. J. (1996). A large northern hemisphere terrestrial CO 2 sink indicated by the 1 3 C 1 2 C ratio of atmospheric CO 2. *Oceanographic Literature Review*, *2*(43), 123-124.

Cook, B. D., Davis, K. J., Wang, W., Desai, A., Berger, B. W., Teclaw, R. M., ... & Heilman, W. (2004). Carbon exchange and venting anomalies in an upland deciduous forest in northern Wisconsin, USA. *Agricultural and Forest Meteorology*, *126*(3-4), 271-295.

Davidson, E. A., Janssens, I. A., & Luo, Y. (2006). On the variability of respiration in terrestrial ecosystems: moving beyond Q10. *Global Change Biology*, *12*(2), 154-164.

Desai, A. R., Bolstad, P. V., Cook, B. D., Davis, K. J., & Carey, E. V. (2005). Comparing net ecosystem exchange of carbon dioxide between an old-growth and mature forest in the upper Midwest, USA. *Agricultural and Forest Meteorology*, *128*(1-2), 33-55.

Desjardins, R. L. (1974). A technique to measure CO 2 exchange under field conditions. *International Journal of Biometeorology*, *18*(1), 76-83.

Desjardins, R. L. (1992). Review of techniques to measure CO 2 flux densities from surface and airborne sensors. In *Advances in Bioclimatology 1* (pp. 1-23). Springer, Berlin, Heidelberg.

Desjardins, R. L., & Lemon, E. R. (1974). Limitations of an eddy-correlation technique for the determination of the carbon dioxide and sensible heat fluxes. *Boundary-Layer Meteorology*, *5*(4), 475-488.

Drexler, J. Z., Snyder, R. L., Spano, D., & Paw U, K. T. (2004). A review of models and micrometeorological methods used to estimate wetland evapotranspiration. *Hydrological Processes*, *18*(11), 2071-2101.

Emmerich, W. E. (2007). Ecosystem water use efficiency in a semiarid shrubland and grassland community. *Rangeland Ecology & Management*, *60*(5), 464-470.

Epplin, F. M., & Peeper, T. F. (1998). Influence of planting date and environment on Oklahoma wheat grain yield trend from 1963 to 1995. *Canadian journal of plant science*, *78*(1), 71-77.

Falge, E., Baldocchi, D., Olson, R., Anthoni, P., Aubinet, M., Bernhofer, C., ... & Granier, A. (2001). Gap filling strategies for defensible annual sums of net ecosystem exchange. *Agricultural and forest meteorology*, *107*(1), 43-69.

Falge, E., Graber, W., Siegwolf, R., & Tenhunen, J. D. (1996). A model of the gas exchange response ofPicea abies to habitat conditions. *Trees*, *10*(5), 277-287.

Finnigan, J. J. (2004). A re-evaluation of long-term flux measurement techniques part II: coordinate systems. *Boundary-Layer Meteorology*, *113*(1), 1-41.

Flanagan, L. B., Wever, L. A., & Carlson, P. J. (2002). Seasonal and interannual variation in carbon dioxide exchange and carbon balance in a northern temperate grassland. *Global Change Biology*, *8*(7), 599-615.

Foken, T., Aubinet, M., Finnigan, J. J., Leclerc, M. Y., Mauder, M., & Paw U, K. T. (2011). Results of a panel discussion about the energy balance closure correction for trace gases. *Bulletin of the American Meteorological Society*, *92*(4), ES13-ES18.

Foken, T., Göockede, M., Mauder, M., Mahrt, L., Amiro, B., & Munger, W. (2004). Post-field data quality control. In *Handbook of micrometeorology* (pp. 181-208). Springer, Dordrecht.

Foken, T., & Wichura, B. (1996). Tools for quality assessment of surface-based flux measurements. *Agricultural and forest meteorology*, *78*(1-2), 83-105.

Gagnon, S., L'Hérault, E., Lemay, M., & Allard, M. (2016). New low-cost automated system of closed chambers to measure greenhouse gas emissions from the tundra. *Agricultural and forest meteorology*, *228*, 29-41.

Geider, R. J., Delucia, E. H., Falkowski, P. G., Finzi, A. C., Grime, J. P., Grace, J., ... & Platt, T. (2001). Primary productivity of planet earth: biological determinants and physical constraints in terrestrial and aquatic habitats. *Global Change Biology*, *7*(8), 849-882.

Göckede, M., Markkanen, T., Hasager, C. B., & Foken, T. (2006). Update of a footprint-based approach for the characterisation of complex measurement sites. *Boundary-Layer Meteorology*, *118*(3), 635-655.

Goulden, M. L., Munger, J. W., Fan, S. M., Daube, B. C., & Wofsy, S. C. (1996). Measurements of carbon sequestration by long-term eddy covariance: Methods and a critical evaluation of accuracy. *Global change biology*, *2*(3), 169-182.

Greb, B. W. (1979). Reducing drought effects on croplands in the west-central Great Plains.

Gu, L., Falge, E. M., Boden, T., Baldocchi, D. D., Black, T. A., Saleska, S. R., ... & Xu, L. (2005). Objective threshold determination for nighttime eddy flux filtering. *Agricultural and Forest Meteorology*, *128*(3-4), 179-197.

Hansen, N. C., Allen, B. L., Baumhardt, R. L., & Lyon, D. J. (2012). Research achievements and adoption of no-till, dryland cropping in the semi-arid US Great Plains. *Field Crops Research*, *132*, 196-203.

Heijmans, M. M., Arp, W. J., & Chapin III, F. S. (2004). Carbon dioxide and water vapour exchange from understory species in boreal forest. *Agricultural and Forest Meteorology*, *123*(3-4), 135-147.

Heilman, J. L., Brittin, C. L., & Neale, C. M. U. (1989). Fetch requirements for Bowen ratio measurements of latent and sensible heat fluxes. *Agricultural and Forest Meteorology*, *44*(3-4), 261-273.

Hojstrup, J. (1993). A statistical data screening procedure. *Measurement Science and Technology*, *4*(2), 153.

Hollinger, D. Y., Kelliher, F. M., Byers, J. N., Hunt, J. E., McSeveny, T. M., & Weir, P. L. (1994). Carbon dioxide exchange between an undisturbed old-growth temperate forest and the atmosphere. *Ecology*, *75*(1), 134-150.

Hui, D., Wan, S., Su, B., Katul, G., Monson, R., & Luo, Y. (2004). Gap-filling missing data in eddy covariance measurements using multiple imputation (MI) for annual estimations. *Agricultural and Forest Meteorology*, *121*(1-2), 93-111.

International Fertilizer Industry Association (IFIA). (2001). *Global estimates of gaseous emissions of NH3, NO and N2O from agricultural land*. Food and Agriculture Organization of the United Nations (FAO).

Jones, E. P., Ward, T. V., & Zwick, H. H. (1978). A fast response atmospheric CO2 sensor for eddy correlation flux measurements. *Atmospheric Environment (1967)*, *12*(4), 845-851.

Kanda, M., Inagaki, A., Letzel, M. O., Raasch, S., & Watanabe, T. (2004). LES study of the energy imbalance problem with eddy covariance fluxes. *Boundary-Layer Meteorology*, *110*(3), 381-404.

Keeling, R. F., Piper, S. C., & Heimann, M. (1996). Global and hemispheric CO2 sinks deduced from changes in atmospheric O2 concentration. *Nature*, *381*(6579), 218.

Kleissl, J., Gomez, J., Hong, S. H., Hendrickx, J. M. H., Rahn, T., & Defoor, W. L. (2008). Large aperture scintillometer intercomparison study. *Boundary-layer meteorology*, *128*(1), 133-150.

Kljun, N., Rotach, M. W., & Schmid, H. P. (2002). A three-dimensional backward Lagrangian footprint model for a wide range of boundary-layer stratifications. *Boundary-Layer Meteorology*, *103*(2), 205-226.

Kochendorfer, J., Castillo, E. G., Haas, E., & Oechel, W. C. (2011). Net ecosystem exchange, evapotranspiration and canopy conductance in a riparian forest. *Agricultural and Forest Meteorology*, *151*(5), 544-553.

Koskinen, M., Minkkinen, K., Ojanen, P., Kamarainen, M., Laurila, T., & Lohila, A. (2014). Measurements of CO2 exchange with an automated chamber system throughout the year: challenges in measuring night-time respiration on porous peat soil. *Biogeosciences*.

Kuglitsch, F. G., Reichstein, M., Beer, C., Carrara, A., Ceulemans, R., Granier, A., ... & Matteucci, G. (2008). Characterisation of ecosystem water-use efficiency of european forests from eddy covariance measurements. *Biogeosciences Discussions*, *5*(6), 4481-4519.

Lalrammawia, C., & Paliwal, K. (2010). Seasonal changes in net ecosystem exchange of CO_2 and respiration of Cenchrus ciliaris L. grassland ecosystem in semi-arid tropics: an eddy covariance measurement. *Current Science*, 1211-1218.

Lasslop, G., Reichstein, M., Papale, D., Richardson, A. D., Arneth, A., Barr, A., ... & Wohlfahrt, G. (2010). Separation of net ecosystem exchange into assimilation and respiration using a

light response curve approach: critical issues and global evaluation. *Global Change Biology*, *16*(1), 187-208.

Leclerc, M. Y., & Thurtell, G. W. (1990). Footprint prediction of scalar fluxes using a Markovian analysis. *Boundary-Layer Meteorology*, *52*(3), 247-258.

Lenschow, D. H. (1995). *Micrometeorological techniques for measuring biosphere-atmosphere trace gas exchange* (pp. 126-163). Oxford: Blackwell Science.

Li, S. G., Asanuma, J., Eugster, W., Kotani, A., Liu, J. J., Urano, T., ... & Sugita, M. (2005). Net ecosystem carbon dioxide exchange over grazed steppe in central Mongolia. *Global Change Biology*, *11*(11), 1941-1955.

Lloyd, J., & Taylor, J. A. (1994). On the temperature dependence of soil respiration. *Functional ecology*, 315-323.

Loescher, H. W., Law, B. E., Mahrt, L., Hollinger, D. Y., Campbell, J., & Wofsy, S. C. (2006). Uncertainties in, and interpretation of, carbon flux estimates using the eddy covariance technique. *Journal of Geophysical Research: Atmospheres*, *111*(D21).

Mahrt, L., Moore, E., Vickers, D., & Jensen, N. O. (2001). Dependence of turbulent and mesoscale velocity variances on scale and stability. *Journal of Applied Meteorology*, *40*(3), 628-641.

Massman, W. J., & Lee, X. (2002). Eddy covariance flux corrections and uncertainties in long-term studies of carbon and energy exchanges. *Agricultural and Forest Meteorology*, *113*(1), 121-144.

Massman, W., Lee, X., & Law, B. E. (2004). Handbook of micrometeorology. A guide for surface flux measurements and analysis. *Atmospheric and Oceanographic Sciences Library. 29.*

Meijninger, W. M. L., Hartogensis, O. K., Kohsiek, W., Hoedjes, J. C. B., Zuurbier, R. M., & De Bruin, H. A. R. (2002). Determination of area-averaged sensible heat fluxes with a large aperture scintillometer over a heterogeneous surface–Flevoland field experiment. *Boundary-Layer Meteorology*, *105*(1), 37-62.

Moffat, A. M., Papale, D., Reichstein, M., Hollinger, D. Y., Richardson, A. D., Barr, A. G., ... & Falge, E. (2007). Comprehensive comparison of gap-filling techniques for eddy covariance net carbon fluxes. *Agricultural and Forest Meteorology*, *147*(3-4), 209-232.

Moncrieff, J. B., Malhi, Y., & Leuning, R. (1996). The propagation of errors in long-term measurements of land-atmosphere fluxes of carbon and water. *Global change biology*, *2*(3), 231-240.

Morgenstern, K., Black, T. A., Humphreys, E. R., Griffis, T. J., Drewitt, G. B., Cai, T., ... & Livingston, N. J. (2004). Sensitivity and uncertainty of the carbon balance of a Pacific

Northwest Douglas-fir forest during an El Niño/La Niña cycle. *Agricultural and Forest Meteorology*, *123*(3-4), 201-219.

Ohtaki, E., & Matsui, T. (1982). Infrared device for simultaneous measurement of fluctuations of atmospheric carbon dioxide and water vapor. *Boundary-Layer Meteorology*, *24*(1), 109-119.

Papale, D., Reichstein, M., Aubinet, M., Canfora, E., Bernhofer, C., Kutsch, W., ... & Yakir, D. (2006). Towards a standardized processing of Net Ecosystem Exchange measured with eddy covariance technique: algorithms and uncertainty estimation. *Biogeosciences*, *3*(4), 571-583.

Patrignani, A., Godsey, C. B., Ochsner, T. E., & Edwards, J. T. (2012). Soil water dynamics of conventional and no-till wheat in the Southern Great Plains. *Soil Science Society of America Journal*, *76*(5), 1768-1775. Patrignani, A., Godsey, C. B., Ochsner, T. E., & Edwards, J. T. (2012). Soil water dynamics of conventional and no-till wheat in the Southern Great Plains. *Soil Science Society of America Journal*, *76*(5), 1768-1775.

Pingintha, N., Leclerc, M. Y., Beasley Jr, J. P., Durden, D., Zhang, G., Senthong, C., & Rowland, D. (2010). Hysteresis response of daytime net ecosystem exchange during drought. *Biogeosciences*, *7*(3), 1159-1170.

Press, W. H., Flannery, B. P., Teukolsky, S. A., & Vetterling, W. T. (1989). *Numerical recipes* (Vol. 2). Cambridge: Cambridge university press.

Reichstein, M., Falge, E., Baldocchi, D., Papale, D., Aubinet, M., Berbigier, P., ... & Grünwald, T. (2005). On the separation of net ecosystem exchange into assimilation and ecosystem respiration: review and improved algorithm. *Global Change Biology*, *11*(9), 1424-1439.

Rochette, P., & Hutchinson, G. L. (2005). Measurement of soil respiration in situ: chamber techniques.

Ruimy, A., Jarvis, P. G., Baldocchi, D. D., & Saugier, B. (1995). CO2 fluxes over plant canopies and solar radiation: a review. In *Advances in ecological research* (Vol. 26, pp. 1-68). Academic Press.

Running, S. W., Baldocchi, D. D., Turner, D. P., Gower, S. T., Bakwin, P. S., & Hibbard, K. A. (1999). A global terrestrial monitoring network integrating tower fluxes, flask sampling, ecosystem modeling and EOS satellite data. *Remote sensing of environment*, *70*(1), 108-127.

Schmid, H. P. (1994). Source areas for scalars and scalar fluxes. *Boundary-Layer Meteorology*, *67*(3), 293-318.

Schotanus, P., Nieuwstadt, F., & De Bruin, H. A. R. (1983). Temperature measurement with a sonic anemometer and its application to heat and moisture fluxes. *Boundary-Layer Meteorology*, *26*(1), 81-93.

Schuepp, P. H., Leclerc, M. Y., MacPherson, J. I., & Desjardins, R. L. (1990). Footprint prediction of scalar fluxes from analytical solutions of the diffusion equation. *Boundary-Layer Meteorology*, *50*(1-4), 355-373.

Stisen, S., Sandholt, I., Nørgaard, A., Fensholt, R., & Jensen, K. H. (2008). Combining the triangle method with thermal inertia to estimate regional evapotranspiration—Applied to MSG-SEVIRI data in the Senegal River basin. *Remote Sensing of Environment*, *112*(3), 1242-1255.

Sun, G., Noormets, A., Gavazzi, M. J., McNulty, S. G., Chen, J., Domec, J. C., ... & Skaggs, R. W. (2010). Energy and water balance of two contrasting loblolly pine plantations on the lower coastal plain of North Carolina, USA. *Forest Ecology and Management*, *259*(7), 1299-1310.

Tanner, B. D., & Greene, J. P. (1989). Measurement of sensible heat and water vapor fluxes using eddy correlation methods. *Final report prepared for US Army Dugway Proving Grounds, Dugway, Utah*, *17*.

Teitel, M., Atias, M., Schwartz, A., & Cohen, S. (2011). Use of a greenhouse as an open chamber for canopy gas exchange measurements: Methodology and validation. *Agricultural and forest meteorology*, *151*(10), 1346-1355.

Twine, T. E., Kustas, W. P., Norman, J. M., Cook, D. R., Houser, P., Meyers, T. P., ... & Wesely, M. L. (2000). Correcting eddy-covariance flux underestimates over a grassland. *Agricultural and Forest Meteorology*, *103*(3), 279-300.

Valentini, R., Matteucci, G., Dolman, A. J., Schulze, E. D., Rebmann, C. J. M. E. A. G., Moors, E. J., ... & Lindroth, A. (2000). Respiration as the main determinant of carbon balance in European forests. *Nature*, *404*(6780), 861.

Verma, S. B. (1990). Micrometeorological methods for measuring surface fluxes of mass and energy. *Remote sensing reviews*, *5*(1), 99-115.

Vickers, D., & Mahrt, L. (1997). Quality control and flux sampling problems for tower and aircraft data. *Journal of Atmospheric and Oceanic Technology*, *14*(3), 512-526.

Vickers, D., & Mahrt, L. (2003). The cospectral gap and turbulent flux calculations. *Journal of Atmospheric and Oceanic technology*, *20*(5), 660-672.

Villar, R., Held, A. A., & Merino, J. (1994). Comparison of methods to estimate dark respiration in the light in leaves of two woody species. *Plant physiology*, *105*(1), 167-172.

Wagle, P., & Kakani, V. G. (2014). Confounding effects of soil moisture on the relationship between ecosystem respiration and soil temperature in switchgrass. *Bioenergy Research*, *7*(3), 789-798.

Wagle, P., & Kakani, V. G. (2014). Growing season variability in evapotranspiration, ecosystem water use efficiency, and energy partitioning in switchgrass. *Ecohydrology*, *7*(1), 64-72.

Wagle, P., & Kakani, V. G. (2014). Seasonal variability in net ecosystem carbon dioxide exchange over a young Switchgrass stand. *Gcb Bioenergy*, *6*(4), 339-350.

Wagle, P., Xiao, X., Gowda, P., Basara, J., Brunsell, N., Steiner, J., & Anup, K. C. (2017). Analysis and estimation of tallgrass prairie evapotranspiration in the central United States. *Agricultural and Forest Meteorology*, *232*, 35-47.

Wang, L., Feng, Z., & Schjoerring, J. K. (2013). Effects of elevated atmospheric CO2 on physiology and yield of wheat (Triticum aestivum L.): a meta-analytic test of current hypotheses. *Agriculture, ecosystems & environment*, *178*, 57-63.

Wang, Y., Zhou, G., & Wang, Y. (2008). Environmental effects on net ecosystem CO2 exchange at half-hour and month scales over Stipa krylovii steppe in northern China. *agricultural and forest meteorology*, *148*(5), 714-722.

Webb, E. K., Pearman, G. I., & Leuning, R. (1980). Correction of flux measurements for density effects due to heat and water vapour transfer. *Quarterly Journal of the Royal Meteorological Society*, *106*(447), 85-100.

West, T. O., & Marland, G. (2002). A synthesis of carbon sequestration, carbon emissions, and net carbon flux in agriculture: comparing tillage practices in the United States. *Agriculture, Ecosystems & Environment*, *91*(1-3), 217-232.

Wever, L. A., Flanagan, L. B., & Carlson, P. J. (2002). Seasonal and interannual variation in evapotranspiration, energy balance and surface conductance in a northern temperate grassland. *Agricultural and Forest meteorology*, *112*(1), 31-49.

Williams, D. G., Cable, W., Hultine, K., Hoedjes, J. C. B., Yepez, E. A., Simonneaux, V., ... & Hartogensis, O. K. (2004). Evapotranspiration components determined by stable isotope, sap flow and eddy covariance techniques. *Agricultural and Forest Meteorology*, *125*(3-4), 241-258.

Wilson, K., Goldstein, A., Falge, E., Aubinet, M., Baldocchi, D., Berbigier, P., ... & Grelle, A. (2002). Energy balance closure at FLUXNET sites. *Agricultural and Forest Meteorology*, *113*(1), 223-243.

Wohlfahrt, G., Anfang, C., Bahn, M., Haslwanter, A., Newesely, C., Schmitt, M., ... & Cernusca, A. (2005). Quantifying nighttime ecosystem respiration of a meadow using eddy covariance, chambers and modelling. *Agricultural and Forest Meteorology*, *128*(3-4), 141-162.

Xu, M., DeBiase, T. A., Qi, Y., Goldstein, A., & Liu, Z. (2001). Ecosystem respiration in a young ponderosa pine plantation in the Sierra Nevada Mountains, California. *Tree Physiology*, *21*(5), 309-318.

CHAPTER III

DYNAMICS OF EVAPOTRANSPIRATION IN RAINFED WINTER WHEAT MANAGED UNDER DIFFERENT TILLAGE AND GRAZING SYSTEMS

Abstract

Evapotranspiration (ET) and energy fluxes were measured using the eddy covariance technique from rainfed winter wheat (*Triticum aestivum* L.) fields managed under different tillage and grazing systems in central Oklahoma, as a part of the United States Department of Agriculture (USDA) Long-Term Agroecosystem Research (LTAR) network. The objective of this study was to quantify and compare dynamics of ET during the 2016-2017 (grain-only) and 2017-2018 (graze-grain) growing seasons and summer fallow period (2017) between conventional (CT) and no-till (NT) winter wheat fields. Seasonal distributions of energy partitioning and ecosystem water use efficiency (EWUE) were also examined. Daily ET reached approximately 6 mm in both fields for grain-only wheat during the 2016-2017 growing season, while it reached 4.6 mm (CT) and 5.3 mm (NT) for graze-grain wheat during the 2017-2018 growing season. Similar canopy stands resulted in similar seasonal ET sums (459-469 mm) for the 2016-2017 growing season between CT and NT fields. However, slightly better canopy stands in NT caused slightly higher cumulative ET in NT (404 mm) than CT (365 mm) for the 2017-2018 growing season.

Daily ET reached up to 4.9 mm (CT) and 3.6 mm (NT) during fallow. The fallow period ET sum was ~1.5 times higher in CT field, indicating the role of residue on the surface as a barrier to minimize ET loss from NT field. The growing season scale EWUE was 3.49 g C mm^{-1} ET (CT) and 3.27 g C mm^{-1} ET (NT) for the 2016-2017 growing season and 2.82 g C mm^{-1} ET (CT) and 2.99 g C mm^{-1} ET (NT) for the 2017-2018 growing season. The ET measurement over a longer-term will provides more insights onto the impact of CT and NT on water use of wheat-based agroecosystems in the southern Great Plains of the United States.

1. Introduction

Wheat (*Triticum aestivum* L.) is an important cereal crop that serves as an essential food source for human and livestock (Balkovič et al., 2014). The forecast level of global production of wheat for 2018/2019 is 754.1 million tons (FAO, 2018). Since wheat production will remain crucial as an important component of human and livestock nutrition, increasing its production is essential for food security (Balkovič et al., 2014). In the United States, wheat ranks third among field crops in terms of acreage and production after maize (*Zea mays* L.) and soybean (*Glycine max* L.) (USDA-ERS, 2018).

The dominant cropping system in the U.S. Southern Great Plains (SGP) is continuous production of winter wheat (Redmon et al., 1995; Edwards et al., 2011). Wheat is grown in the region for the production of a range of commodities, including single (grain-only or forage-only) and dual purpose (both graze and grain) production (Hansen et al., 2012; Hossain et al., 2004). The winter wheat system is subject to failure in the SGP due to variable amounts of annual precipitation, which can range from 600 to 1000 mm (Hansen et al., 2012). Thus, it is common for farmers in the SGP to adopt wheat followed by summer fallow to secure enough soil moisture

at wheat planting. Normally, grain-only wheat is grown for eight to nine month periods (plant in October and harvest in June/July), with a 3-4 month period of summer fallow before the next wheat planting (Hansen et al., 2012). Management systems that include forage production (grazing-only, or graze-grain) plant wheat in early-September. This earlier planting provides biomass for grazing from mid-November through early-May of the following year in graze-out scenarios, and from mid-November to late February (before the development of first hollow stem) in graze-grain systems (Decker et al., 2009; Phillips et al., 1999).

Conventional tillage (CT) is the traditional management technique applied to winter wheat in the SGP (Hossain et al. 2004). It utilizes a range of different implements and timing of operations for an integrated chemical and mechanical weed control during the fallow period and preparation of seedbed. Conventional tillage potentially increases soil erosion, and decreases soil organic carbon (SOC) and aggregate stability (West and Marland, 2002). Half of Oklahoma's cropland wheat fields are classified as highly erodible land; thus erosion is a concern. Some authors cited that an 18-fold reduction in soil erosion can be achieved by shifting from CT to conservation tillage (e.g., reduced tillage or no-tillage (NT) (Epplin and Peeper, 1998; Patrignani et al., 2012). Furthermore, NT may increase water infiltration and soil water content during fallow periods (Bonfil et al., 1999). Even though CT is the main adopted winter wheat management in the SGP, NT system is adopted by several farmers and is gaining more attention in the last decades.

Evapotranspiration (ET) is an important component of the energy and water budgets at site-specific, regional, and global scales. Dynamics of ET are affected by various factors including weather conditions, crop characteristics, management practices, and environmental aspects (Allen et al., 1998). Projections of Climate Change represent a challenge for the agricultural

sector to produce more food with less water, which can be achieved by increasing crop water productivity (Zwart and Bastiaanssen, 2004). Climate change has some direct, e.g., change biological processes like respiration, and indirect impacts, e.g., change in management practices, in the ecosystem (Kaur et al., 2017; Lloyd and Taylor, 1994). Further, management practices applied in agricultural systems can alter water dynamics by changing crop performance (Van Wie et al., 2013). Hence, it is important to understand the impacts of climatic and crop factors, and management practices on dynamics of ET for long-term water planning in water limited areas (Zhang et al., 2011).

Ecosystem water use efficiency (EWUE, the ratio of net carbon uptake to loss of water from the ecosystem) is an important characteristic of ecosystem productivity (Niu et al., 2011). Because water loss from the ecosystem can involve different sources other than transpiration, upscaling of leaf level measurements to the ecosystem level causes additional complications that affect EWUE estimations (Ponton et al., 2006). Alternatively, EWUE can be determined at the ecosystem level from continuous and direct measurements of carbon dioxide (CO_2) and water vapor (H_2O) fluxes by eddy covariance (EC) system (Law et al., 2002).

A few studies have reported ET in winter wheat in the SGP. Howell et al. (1997) measured ET from an irrigated field of winter wheat under CT management in the southern High Plains of Texas using a lysimeter method. Burba and Verma (2005) measured ET from a rainfed field of winter wheat under CT management in north-central Oklahoma using an EC system. These previous studies have shown large differences in ET magnitudes (maximum ET was >10 mm d^{-1} for irrigated wheat and ~7 mm day^{-1} for rainfed wheat). However, comparative studies of ET measurements from paired fields of winter wheat managed under different forms of tillage and cropping systems (graze-only and graze-grain) under the diverse climatic conditions of the SGP

are lacking. In addition, earlier studies lacked thorough investigation of the dynamics of ET, EWUE, and energy partitioning.

In this paper, we evaluated EC measurements of ET from co-located CT and NT winter wheat fields during two growing seasons (2016-2017 grain-only and 2017-2018 graze-grain). Both seasons were followed by summer fallow. This study addresses the following questions: (1) What are the differences in ET patterns for the two growing seasons and a summer fallow period between co-located CT and NT fields under single (grain-only) and dual purpose (graze-grain) winter wheat production systems? (2) What are the seasonal distributions of EWUE and energy partitioning at those winter wheat fields? and, (3) How do H_2O fluxes respond to major climatic variables [photosynthetic photon flux density (PPFD), air temperature (T_a), and vapor pressure deficit (VPD)]?

2. Material and methods

2.1. Site description and weather conditions

The study sites were located at the United States Department of Agriculture – Agricultural Research Service (USDA-ARS), Grazinglands Research Laboratory (GRL) in El Reno, OK. Measurement of ET was obtained using EC systems from co-located winter wheat fields managed under CT (27.5 ha, Lat. 35.5598 and Long. -98.06231) and NT (18.7 ha, Lat. 35.5643 and Long. -98.0614) systems from November 2016 to May 2018. The soil type was classified as a fine-silty, mixed, superactive, thermic pahich, Haplustolls (dale soil series) (USDA-NRCS, 1999).

A multi-purpose winter wheat (variety Gallagher) was sown at 90 kg seed ha^{-1} in rows spaced ~19 cm apart during October 16-18, 2016 (for grain-only purpose) and September 23-24, 2017 (for graze-grain purpose). As a result of poor crop stand due to water logging after heavy rainfall

events in September and October 2017, the fields were replanted during November 9-13, 2017 (~67 kg ha^{-1} additional seed). Although graze-grain wheat fields are generally grazed from November to February, these fields were only grazed during January and February in 2018 because of late re-planting. The fields were harvested for grain in mid-June 2017 and 2018. All agricultural practices and management are presented in Table 1. The grain-only CT field received total of 194 kg N fertilizer while the grain only NT field received only 101 kg N fertilizer based on soil tests.

Average monthly temperature and rainfall for the study period are compared with the 30-Year means (1981-2010) in Table 2. Fields were rainfed and adjacent; therefore same climatic conditions in both fields were assumed. The site has a continental climate, with total rainfall during the study period (November 2016 to May 2018) of 1294 mm over two growing seasons, the 30-Year mean of total rainfall for the same period was 1494 mm. The fields received 6% more rainfall (502 mm) than the 30-Year mean (473 mm) during the 2016-2017 growing season (November 2016 – May 2017). In contrast, the crop experienced drought during the 2017-2018 growing season (October 2017 – May 2018), with total seasonal rainfall of 264 mm (44% less than the 30-year average). The fallow period (June - September 2017) received ~47 % more rainfall (529 mm) as compared to the 30-Year mean (359 mm). As compared to 30-Year mean, the fields received ~74% less rainfall from November 2016 to January 2017, but ~37% more rainfall from February to May 2017. Similarly, total rainfall was 49% lower from October 2017 to January 2018 and 57% lower from February to May 2018.

2.2. Eddy fluxes and biometric measurements

The EC systems were comprised of an open path infrared gas analyzer (LI- 7500-RS, LICOR, Lincoln, NE, USA) and a 3-D sonic anemometer (CSAT3, Campbell Scientific Inc.,

Logan, UT, USA). The sensors were mounted at a fixed height of a 2.5 m above the ground. Wind velocity and concentration of CO_2 and H_2O fluxes were collected at 10 Hz frequency. The following supplementary measurements were also collected: PPFD (using LI- 190, LICOR. Lincoln, NE, USA), soil temperature at 2 and 6 cm depths (using thermocouples), soil moisture at 5 cm depth (using Hydra probe, Stevens Water Monitoring Systems Inc., Portland, OR, USA), soil heat fluxes (G) at 8 cm depths (using HFT3, REBS Inc., Bellevue, WA, USA), and above canopy net radiation (R_n – using NRLite, Kipp & Zonen, Delft, The Netherlands).

Biometric measurements such as canopy height, percentage of canopy cover, leaf area index (LAI), and aboveground dry biomass were collected from five randomly located positions in both fields approximately at 16-day intervals that coincided with Landsat overpass dates. The LAI was measured using a LAI -2200C plant canopy analyzer (LICOR Inc., Lincoln, NE, USA) and biomass samples were collected destructively from 0.5 × 0.5 m quadrats.

2.3. Data processing, screening, and gap filling

The raw flux data from EC systems were processed using *EddyPro* (LICOR Inc., Lincoln, NE, USA) software to compute 30-min fluxes. The *EddyPro* provides a quality flag, ranging from 0 (best quality fluxes) to 2 (bad quality fluxes that should be excluded). In addition, unreliable fluxes and statistical outliers beyond ± 3.5 SD (standard deviation) were also discarded from 14-day running windows unless there were four or more consecutive values beyond ± 3.5 SD (Wagle and Kakani, 2014a). Sensible heat flux (H) from -200 to 500 Wm^{-2} and latent heat flux (LE) from -200 to 800 Wm^{-2} were filtered to keep them within reliable ranges (Wagle and Kakani, 2014b). The 30-min ET value was calculated from LE. The *REddyProc* (REddyProc, 2015) R–package from the Max Planck Institute for Biogeochemistry, Germany, was used to fill gaps in data and to partition net ecosystem CO_2 exchange (NEE) into gross

primary production (GPP) and ecosystem respiration (ER). This tool fills gaps using methods similar to Falge et al. (2001) and considers the co-variation of fluxes with meteorological variables and the temporal auto-correction of fluxes (Reichstein et al., 2005). Based on the relationship between T_a and nighttime NEE, the ER was estimated using the Lloyd and Taylor (1994) model.

2.4. Examining the response of H_2O fluxes to major climatic variables (PPFD, T_a, and VPD)

The response of H_2O fluxes to major climatic variables (PPFD, T_a, and VPD) were compared across two growing seasons separately. To examine the H_2O-PPFD relationship, daytime H_2O fluxes (PPFD > 5 μmol m^{-2} s^{-1}) for each season (2016-2017 and 2017-2018) were binned into 12 classes of PPFD (<100, 100-200, 200-400, 400-600, 600-800, 800-1000, 1000-1200, 1200-1400, 1400-1600, 1600-1800, 1800-2000, and >2000 μmol m^{-2} s^{-1}), 11 classes of T_a (<-5, -5-0, 0-4, 4-8, 8-12, 12-16, 16-20, 20-24, 24-28, 28-32, and >32 °C), and 10 classes of VPD (<0.5, 0.5-1, 1-1.5, 1.5-2, 2-2.5, 2.5-3, 3-3.5, 3.5-4, 4-4.5, and > 4.5 kPa).

2.5. Energy balance closure (EBC) and ecosystem water use efficiency (EWUE) estimations

The accuracy of EC measurements was assessed from energy balance closure (EBC) (Foken et al., 2004). The EBC was calculated from a linear regression of sum of turbulent fluxes (H+LE) vs. available energy (R_n-G) for 30-min fluxes for two growing seasons separately.

The EWUE is generally computed as the ratio of carbon gain (GPP) to water loss (ET). We computed monthly EWUE as the ratio of monthly sums of GPP to ET, and growing season EWUE as the ratio of growing season sums of GPP to ET (Wagle et al., 2016).

3. Results and discussion

3.1. LAI, above ground biomass, and canopy coverage

Dry biomass, canopy coverage, and LAI were higher during the 2016-2017 growing season than the 2017-2018 growing season due to grazing as part of the graze-grain component of the management sequence of paddocks, and lower rainfall in the 2017-2018 growing season (Fig. 1 and 2). Maximum LAI reached 7-7.5 m^2 m^{-2} in late March in 2017 and 3-3.3 m^2 m^{-2} in early May in 2018. The highest aboveground biomass of ~1.3 kg m^{-2} (equivalent to 13 t ha^{-1} in both fields) was observed in late April in 2017, while the greatest amount of biomass during the mid-May 2018 was only ~ 0.4 Kg m^{-2} (equivalent to 4 t ha^{-1} in both fields). The maximum canopy coverage during the 2016-2017 was > 95% and remained fairly constant from March to mid-April. However, the maximum canopy coverage reached only 58% (CT) and 74% (NT) during the 2017-2018 growing season.

Grain yield approximated 4.86 and 3.53 t ha^{-1} in 2017 and 1.67 and 1.55 t ha^{-1} in 2018 for CT and NT fields, respectively. Although lower grain yields can be expected in graze-grain fields compared to grain-only fields, graze-grain management does not usually result in such low levels of grain production in the SGP, if properly managed (Redmon et al., 1995). Grain yields were reduced by only 14% when compared between graze-grain and grain-only wheat fields (Edwards et al., 2011). The substantial lower yields observed in 2018 might be mostly attributed to the late re-seeding in early November after water logging conditions which limited good wheat root system development during Fall. The grain yields of 4.86 t ha^{-1} (CT) and 3.53 t ha^{-1} (NT) observed in in 2017 were higher than the average yield (~3.0 t ha^{-1}) recorded for Oklahoma, Texas, and Kansas in past years (Patrignani et al., 2014). However, some previous studies have reported higher yields in Oklahoma. Lollato and Edwards (2015) reported maximum yield of 7.11 t ha^{-1} for rainfed winter wheat during the 2012-2013 growing season at Chickasha, Oklahoma and 7.68 t ha^{-1} for irrigated winter wheat during the 2013-2014 growing

season at Stillwater, Oklahoma. Patrignani et al. (2012) reported maximum grain yields of 4.39 t ha^{-1} for CT and 4.45 t ha^{-1} for NT winter wheat during the 2009-2011 period at Lahoma, OK.

3.2. Energy balance closure and energy partitioning

The EBC for the November 2016 – September 2017 period was 0.74 for CT field and 0.76 for NT field (Fig. 3). For the 2017-2018 growing season (October 2017 – May 2018), it was 0.75 for CT field and 0.85 for NT field. The results showed that the measured turbulent fluxes (H+LE) accounted for 88-93% of the available energy (R_n-G). The EBC values of 0.75-0.76 in this study fell within the typical range (0.7-0.8) of EC experiments (Foken et al., 2006). The correction factor for EBC was not applied to correct underestimation of fluxes since causes of these energy imbalances are not well known. These imbalances may arise from errors in measurement of any of four components of energy balance and from neglecting stored energy in soil and biomass (Cook et al., 2004; Desai et al., 2005) or related to atmospheric phenomena which EC systems cannot measure (Foken, 2008).

Diurnal peak values (monthly average) of H and LE fluxes during the study period in CT and NT fields are presented in Figure 4. Diurnal peak values of H decreased as the growing season progressed, then increased after crop senescence and harvesting. In contrast, diurnal peak values of LE increased as the growing season progressed and decreased after crop senescence and harvesting. During the 2016-2017 growing season, diurnal peak H reached lows of 44 (NT) and 64 (CT) W m^{-2} and LE reached ~250 W m^{-2} during peak growth in April and May. During the period of summer fallow of 2017, diurnal peak H approximated 340 Wm^{-2} in both fields in June. Diurnal peak values of LE were approximately 56 (NT) and 99 (CT) W m^{-2} in July when the monthly rainfall was 22 mm, but increased to 253 (CT) and 113 (NT) W m^{-2} in August when the monthly rainfall was 252 mm. It was evident from Figure 4 that diurnal peak values of LE were

higher for CT than for NT wheat field during the entire fallow period (June-September 2017), illustrating the role of crop residues on reduction of ET.

During the dry 2017-2018 growing season, diurnal peak H reached lows of ~100 W m^{-2} in November and December, but increased to ~170 W m^{-2} from January to March and further increased beyond 200 W m^{-2} in April and May. As a result, H was the dominant turbulent flux even during the active growing season (February to May) in 2018 (Table 3) due to dry conditions.

Table 3 shows that 43-44% of R_n was converted to LE in both CT and NT fields during the 2016-2017 growing season, and LE was the dominant turbulent flux. In comparison, only 30-33% of R_n was converted to LE during the dry 2017-2018 growing season, and H was the dominant turbulent flux at the seasonal scale. For the active growing season (February-May), 46-51% of R_n was converted to LE and 22% of R_n was converted to H in 2017. In contrast, only 31-33% of R_n was converted to LE and 38-44% of R_n was converted to H in 2018. Some discrepancies in partitioning of R_n into H and LE between the two seasons can be attributed to the different managements. In addition, drought conditions in the 2017-2018 growing season caused higher proportion of H over LE. Several studies have shown that H can dominate over LE even during the active growing season under dry conditions (Veenendaal et al., 2004; Wagle and Kakani, 2014).

3.3. Diurnal and daily patterns of ET during growing seasons

Diurnal trends in ET during the 2016-2017 and 2017-2018 growing seasons for CT and NT fields are shown in Figures 5 and 6. The ET rates were higher in the 2016-2017 growing season due to more favorable climatic conditions and the management practice (grain-only) that was

applied. Peak diurnal ET reached 0.19-0.20 mm 30-min^{-1} in May 2017 and 0.13-0.16 mm 30-min^{-1} in May 2018.

Daily ET patterns for the study period is presented in Figure 7. Daily ET during the 2016-2017 growing season reached ~6.0 mm d^{-1} in both fields. Daily ET for the 2017-2018 growing season reached up to 4.6 mm d^{-1} and 5.3 mm d^{-1} in NT and CT fields, respectively. Lower magnitudes of daily ET in grazed fields than in grain-only fields was due to reduced transpiration from plants related to dry conditions and biomass removal by grazing. Burba and Verma (2005) reported maximum daily ET of ~7 mm during the growing season for rainfed winter wheat at Ponca City, Oklahoma. Slightly lower ET rates (~6 mm d^{-1} for grain-only wheat) occurred in our study as compared to 7.0 mm d^{-1} for rainfed winter wheat reported by Burba and Verma (2005). The differences in ET at these two locations can be attributed to amount of annual rainfall received. Total mean annual rainfall was higher (1258 mm) during their study period, compared to 1046 mm from October 2016 to September 2017 for the current study.

3.4. Daily patterns of ET during fallow

Daily ET during the fallow period ranged from 0.39 to 3.6 mm d^{-1} for NT field and 0.43 to 4.9 mm d^{-1} for CT field (Fig. 7). Lower ET rates under NT indicates reduced water evaporation from soil due to the residue on surface that retained the soil moisture. In contrast, higher rates of ET in CT infers more water loss through evaporation from soil that is exposed directly to the radiation. A previous study showed more water storage during the fallow period of winter wheat when herbicides were used to control weeds rather than CT practices (Smika and Wicks, 1968). Soil moisture played a key role on ET during the fallow period. For example, daily ET rates increased from 1.5 mm d^{-1} to 4.2 mm d^{-1} and 1.1 mm d^{-1} to 2.2 mm d^{-1} at CT and NT fields, respectively, after a 150 mm rainfall event during August 10-12, 2017.

3.6. Cumulative ET during the growing season and fallow period

Monthly sums of ET for the study period for NT and CT fields are provided in Table 4. Monthly ET for both fields was similar during the 2016-2017 growing season, ranging from 25-29 mm in December to ~115 in May. Monthly ET during the 2017-2018 growing season ranged from 12-19 mm in December-January to 85 mm (CT) and 113 mm (NT) in May. Dormancy of wheat and cold temperatures caused lower monthly sums of ET in winter. Cumulative ET during the most active growing period in 2017 (February-May) was approximately 80% of cumulative rainfall, while cumulative ET during the entire growing season (November 2016 – May 2017) was approximately 90% of the seasonal rainfall (502 mm). In comparison, cumulative ET during the fallow period was 28% (NT) and 41% (CT) of cumulative rainfall (528 mm). Cumulative ET during the most active growing period in 2018 (February-May) approximated 56-63% of the cumulative rainfall, while cumulative ET during the entire growing season (October 2017 - May 2018) was 66 % (NT) and 72% (CT) of the seasonal rainfall (265 mm). We observed similar seasonal ET sums (459-469 mm) for the 2016-2017 growing season between CT and NT fields, most likely due to similar stand characteristics as shown in Figure 1. However, ET sums were higher in NT (404 mm) than CT (365 mm) during the 2017-2018 growing season because of slightly better canopy stand in NT as shown in Figure 2.

Cumulative ET during the fallow period was substantially higher under CT (216 mm) than NT (146 mm) management (Table 5). The result is further supported by higher daily ET rates under CT management during the entire fallow period (Fig. 7). The fallow period ET sum was ~1.5 times higher under CT, indicating the role of residue on the surface that served as a barrier to minimize ET loss from NT field.

Annual ET for the November 2016 – October 2017 period for grain-only winter wheat in our study was 755 mm for CT field and 684 mm for NT field. Burba and Verma (2005) reported annual ET of 710-750 mm for grain-only winter wheat at Ponca City, Oklahoma. These results suggest that annual ET of 700-750 mm could be the baseline ET for grain-only winter wheat in the region.

3.6. Seasonal patterns of ecosystem water use efficiency (EWUE)

During the 2016 – 2017 growing season, the magnitude of EWUE (monthly sums of GPP/ET) for the study period is presented in Figure 8. The highest EWUE was observed in February 2017 (4.9 g C mm^{-1} ET for CT and 4.5 g C mm^{-1} ET for NT) in response to rapid increases in GPP relative to ET, caused by favorable environmental conditions for carbon uptake. The increase in GPP was 54% (CT) and 51% (NT) as compared to 28% increases in ET (both CT and NT) from January to February. The lowest EWUE was observed during late growing season in May (1.9 g C mm^{-1} ET for CT and 1.8 g C mm^{-1} ET for NT) because of the rapid decrease in carbon uptake with approaching crop senescence. The magnitude of monthly EWUE during the 2017-2018 growing season reached 5.6 g C mm^{-1} ET and 4.6 g C mm^{-1} ET in January at CT and NT fields, respectively. Lower monthly sums of ET that occurred in relation to significant carbon uptake caused higher EWUE (> 3.5 g C mm^{-1} ET) during winter months. Minimum monthly EWUE of ~ 2.4 g C mm^{-1} ET were observed in May at both fields.

At the growing season scale, overall EWUE was 3.49 g C mm^{-1} ET (CT) and 3.27 g C mm^{-1} ET (NT) for the 2016-2017 growing season and 2.82 g C mm^{-1} ET (CT) and 2.99 g C mm^{-1} ET (NT) for the 2017-2018 growing season. Slightly better canopy stands (Fig. 1 and 2) might have caused slightly higher EWUE in CT field for the 2016-2017 growing season and in NT field for

the 2017-2018 growing season. Results illustrated that the difference in canopy stand was the major determinant for growing season EWUE rather than the tillage system.

Different methods of calculating EWUE make directly comparisons of EWUE values among different studies complicated. Lollato and Edwards (2015) reported maximum water use efficiency of winter wheat in central Oklahoma between 7.8 to 12.6 kg ha^{-1} mm^{-1}, based on the ratio of grain yield to seasonal ET (ET derived from a soil water balance). When the same method was used to compute EWUE, values of 10.59 and 7.54 kg ha^{-1} mm^{-1} (2017) and 4.57 and 3.83 kg ha^{-1} mm^{-1} (2018) were obtained for CT and NT systems, respectively. Water use efficiency (based on grain-yield and ET) of dry land wheat ranged from 3.4 to 18.8 kg ha^{-1} mm^{-1} for CT and 4.7 to 14.8 kg ha^{-1} mm^{-1} for NT in Loess Plateau, central China (Zhang et al., 2013). The average water use efficiency (based on grain-yield and ET) was about 8.9 kg ha^{-1} mm^{-1} for the northern Great Plains of North America, while the maximum water use efficiency under favorable conditions for rainfed wheat worldwide was 22.3 kg ha^{-1} mm^{-1} (Sadras and Angus, 2006).

3.7. Response of H_2O flux to major climatic variables

The H_2O flux increased rapidly with increasing T_a, VPD, and PPFD, and reached a maximum at T_a of ~24°C and VPD of ~2.25 kPa in both fields during the 2016-2017 growing season (Fig. 9 and 10). Optimum values of T_a and VPD for the 2017-2018 growing season were approximately 29°C and 3.5 kPa in both fields. The H_2O flux decreased or plateaued beyond those optimum values of T_a and VPD. However, H_2O flux did not decline up to the observed ranges (>1900 µmol m-2 s-1) of PPFD.

To further examine the response of H_2O flux to T_a and VPD, diurnal trends of H_2O, T_a, and VPD were examined for two selected weeks (May 1-15) of both growing seasons (Fig. 11).

Daily H_2O patterns during 2017 were symmetrical in both fields, reaching maximum at 2:00-3:00 pm when T_a was ~24°C and VPD was ~2.25 kPa. In comparison, daily H_2O patterns were still symmetrical in both fields when T_a was ~28°C and VPD was ~2.7 kPa during 2018. Higher thresholds of T_a and VPD noted for the 2017-2018 growing season, compared to the 2016-2017 growing season, could be due to two drivers. First, optimum values of T_a and VPD are generally higher in dry seasons due to adaptation to dry conditions (Wagle and Kakani, 2014). Secondly, higher contribution of evaporation to ET due to sparse vegetation (lower biomass, LAI, and canopy cover) during the 2017-2018 growing season may have contributed for higher thresholds of T_a and VPD, since evaporation is not regulated by stomata and not sensitive to higher T_a and VPD (Ritchie, 1998). Lei and Yang (2010) reported a threshold VPD of ~2.5 kPa for H_2O flux for irrigated winter wheat in the North China Plain.

4. Conclusion

Cumulative ET was similar during the 2016-2017 growing season (grain-only wheat) in both systems (459 mm for CT and 469 mm for NT) due to identical canopy stands. However, cumulative ET for the fallow period (June – September 2017) was about 1.5 times higher for CT than NT system. Cumulative ET during the 2017-2018 growing season (graze-grain wheat) was 365 mm for CT and 404 mm for NT fields. Seasonal cumulative ET for the 2016-2017 growing season was approximately 90% of the seasonal cumulative precipitation in both fields. During the 2017-2018 growing season, cumulative ET was 72 % and 65 % of the seasonal cumulative precipitation in CT and NT fields, respectively. The growing season average EWUE was 3.49 and 3.27 g C mm^{-1} ET for the 2016-2017 growing season and 2.82 g C mm^{-1} ET and 2.99 g C

mm^{-1} ET for the 2017-2018 growing season for CT and NT fields, respectively. Large differences in ET and EWUE during two growing seasons were attributed to different climatic conditions, 2016-2017 growing season received higher amount of rainfall that resulted in higher ET and EWUE, whereas 2017-2018 growing season was dry with less rainfall that contributed less ET and EWUE. In grain-only management both evaporation and transpiration contributed to ET as a result ET was higher during the 2016-2017 growing season, and lower ET and EWUE during 2017-2018 graze-grain management was due to reduced transpiration from plants due to biomass removal by grazing. Evaluation of longer streams of data are necessary to understand variability in seasonal and fallow period ET of winter wheat in response to tillage systems and climatic conditions.

REFERENCES

Allen, R. G., Pereira, L. S., Raes, D., & Smith, M. (1998). Guidelines for computing crop water requirements-FAO Irrigation and drainage paper 56, FAO-Food and Agriculture Organisation of the United Nations, Rome (http://www. fao. org/docrep) ARPAV (2000), La caratterizzazione climatica della Regione Veneto, Quaderni per. *Geophysics*, *156*, 178.

Balkovič, J., van der Velde, M., Skalský, R., Xiong, W., Folberth, C., Khabarov, N., ... & Obersteiner, M. (2014). Global wheat production potentials and management flexibility under the representative concentration pathways. *Global and Planetary Change*, *122*, 107-121.

Bonfil, D. J., Mufradi, I., Klitman, S., & Asido, S. (1999). Wheat grain yield and soil profile water distribution in a no-till arid environment. *Agronomy Journal*, *91*(3), 368-373.

Cook, B. D., Davis, K. J., Wang, W., Desai, A., Berger, B. W., Teclaw, R. M., ... & Heilman, W. (2004). Carbon exchange and venting anomalies in an upland deciduous forest in northern Wisconsin, USA. *Agricultural and Forest Meteorology*, *126*(3-4), 271-295.

Decker, J. E., Epplin, F. M., Morley, D. L., & Peeper, T. F. (2009). Economics of five wheat production systems with no-till and conventional tillage. *Agronomy journal*, *101*(2), 364-372.

Desai, A. R., Bolstad, P. V., Cook, B. D., Davis, K. J., & Carey, E. V. (2005). Comparing net ecosystem exchange of carbon dioxide between an old-growth and mature forest in the upper Midwest, USA. *Agricultural and Forest Meteorology*, *128*(1-2), 33-55.

Epplin, F. M., & Peeper, T. F. (1998). Influence of planting date and environment on Oklahoma wheat grain yield trend from 1963 to 1995. *Canadian journal of plant science*, *78*(1), 71-77.

FAO. 2017. Food and Agriculture Organization statistics database. FAO, United Nations. http://www.fao.org/worldfoodssituatio/csdb/en/ (accessed June, 2018)

Foken, T. (2008). The energy balance closure problem: an overview. *Ecological Applications*, *18*(6), 1351-1367.

Foken, T., Göockede, M., Mauder, M., Mahrt, L., Amiro, B., & Munger, W. (2004). Post-field data quality control. In *Handbook of micrometeorology* (pp. 181-208). Springer, Dordrecht.

Foken, T., Wimmer, F., Mauder, M., Thomas, C., & Liebethal, C. (2006). Some aspects of the energy balance closure problem. *Atmospheric Chemistry and Physics*, *6*(12), 4395-4402.

Hansen, N. C., Allen, B. L., Baumhardt, R. L., & Lyon, D. J. (2012). Research achievements and adoption of no-till, dryland cropping in the semi-arid US Great Plains. *Field Crops Research*, *132*, 196-203.

Hossain, I., Epplin, F. M., Horn, G. W., & Krenzer Jr, E. G. (2004). Wheat production and management practices used by Oklahoma grain and livestock producers. *Oklahoma Agricultural Experimental Station, B-818. Oklahoma State University, Stillwater*.

Kaur, H., Huggins, D. R., Rupp, R. A., Abatzoglou, J. T., Stöckle, C. O., & Reganold, J. P. (2017). Agro-ecological class stability decreases in response to climate change projections for the Pacific Northwest, USA. *Frontiers in Ecology and Evolution*, *5*, 74.

Law, B. E., Falge, E., Gu, L. V., Baldocchi, D. D., Bakwin, P., Berbigier, P., ... & Goldstein, A. (2002). Environmental controls over carbon dioxide and water vapor exchange of terrestrial vegetation. *Agricultural and Forest Meteorology*, *113*(1), 97-120.

Lei, H., & Yang, D. (2010). Interannual and seasonal variability in evapotranspiration and energy partitioning over an irrigated cropland in the North China Plain. *Agricultural and Forest Meteorology*, *150*(4), 581-589.

Lloyd, J., & Taylor, J. A. (1994). On the temperature dependence of soil respiration. *Functional ecology*, 315-323.

Niu, S., Xing, X., Zhang, Z. H. E., Xia, J., Zhou, X., Song, B., ... & Wan, S. (2011). Water-use efficiency in response to climate change: from leaf to ecosystem in a temperate steppe. *Global Change Biology*, *17*(2), 1073-1082.

Patrignani, A., Godsey, C. B., Ochsner, T. E., & Edwards, J. T. (2012). Soil water dynamics of conventional and no-till wheat in the Southern Great Plains. *Soil Science Society of America Journal*, *76*(5), 1768-1775.

Patrignani, A., Lollato, R. P., Ochsner, T. E., Godsey, C. B., & Edwards, J. (2014). Yield gap and production gap of rainfed winter wheat in the southern Great Plains. *Agronomy Journal*, *106*(4), 1329-1339.

Phillips, W. A., Albers, R., Albin, R., & Hatfield, E. E. (1999). The Effect of Herbicide Application During the Winter on Forage Production, Animal Performance, and Grain Yield of Winter Wheat1. *The Professional Animal Scientist*, *15*(2), 141-147.

Ponton, S., Flanagan, L. B., Alstad, K. P., Johnson, B. G., Morgenstern, K. A. I., Kljun, N., ... & Barr, A. G. (2006). Comparison of ecosystem water-use efficiency among Douglas-fir forest, aspen forest and grassland using eddy covariance and carbon isotope techniques. *Global Change Biology*, *12*(2), 294-310.

Redmon, L. A., Horn, G. W., Krenzer, E. G., & Bernardo, D. J. (1995). A review of livestock grazing and wheat grain yield: Boom or bust?. *Agronomy Journal*, *87*(2), 137-147.

REddyProc. 2015. Department Biogeochemical Integration. https://www.bgc-jena.mpg.de/bgi/index.php/Services/REddyProcWebR.

Reichstein, M., Falge, E., Baldocchi, D., Papale, D., Aubinet, M., Berbigier, P., ... & Grünwald, T. (2005). On the separation of net ecosystem exchange into assimilation and ecosystem respiration: review and improved algorithm. *Global Change Biology*, *11*(9), 1424-1439.

Ritchie, J. T. (1998). Soil water balance and plant water stress. In *Understanding options for agricultural production* (pp. 41-54). Springer, Dordrecht.

Sadras, V. O., & Angus, J. F. (2006). Benchmarking water-use efficiency of rainfed wheat in dry environments. *Australian Journal of Agricultural Research*, *57*(8), 847-856.

Smika, D. E., & Wicks, G. A. (1968). Soil Water Storage During Fallow in the Central Great Plains as Influenced by Tillage and Herbicide Treatments 1. *Soil science society of America journal*, *32*(4), 591-595.

USDA-ERS. 2017. Overview of the United States Wheat production. https://www.ers.usda.gov/topics/crops/wheat/ (accessed June 25, 2018)

Van Wie, J. B., Adam, J. C., & Ullman, J. L. (2013). Conservation tillage in dryland agriculture impacts watershed hydrology. *Journal of hydrology*, *483*, 26-38.

Veenendaal, E. M., Kolle, O., & Lloyd, J. (2004). Seasonal variation in energy fluxes and carbon dioxide exchange for a broad-leaved semi-arid savanna (Mopane woodland) in Southern Africa. *Global Change Biology*, *10*(3), 318-328.

Wagle, P., & Kakani, V. G. (2014). Growing season variability in evapotranspiration, ecosystem water use efficiency, and energy partitioning in switchgrass. *Ecohydrology*, *7*(1), 64-72.

Wagle, P., & Kakani, V. G. (2014). Seasonal variability in net ecosystem carbon dioxide exchange over a young Switchgrass stand. *Gcb Bioenergy*, *6*(4), 339-350.

Wagle, P., Kakani, V. G., & Huhnke, R. L. (2016). Evapotranspiration and ecosystem water use efficiency of switchgrass and high biomass sorghum. *Agronomy Journal*, *108*(3), 1007-1019.

West, T. O., & Marland, G. (2002). A synthesis of carbon sequestration, carbon emissions, and net carbon flux in agriculture: comparing tillage practices in the United States. *Agriculture, Ecosystems & Environment*, *91*(1-3), 217-232.

Zhang, S., Sadras, V., Chen, X., & Zhang, F. (2013). Water use efficiency of dryland wheat in the Loess Plateau in response to soil and crop management. *Field Crops Research*, *151*, 9-18.

Zhang, X., Chen, S., Sun, H., Shao, L., & Wang, Y. (2011). Changes in evapotranspiration over irrigated winter wheat and maize in North China Plain over three decades. *Agricultural Water Management*, *98*(6), 1097-1104.

Zwart, S. J., & Bastiaanssen, W. G. (2004). Review of measured crop water productivity values for irrigated wheat, rice, cotton and maize. *Agricultural water management*, *69*(2), 115-133.

Table 1. Management practices in winter wheat fields during the study period.

Fields	Date	Event	Product	Rate
Grain-only CT field	9/6/2016	Fertilizer (broadcast)	Dry 46-00-00	112 kg ha^{-1}
	10/16/2016	Fertilizer in furrow	Dry 32-23-00	82 kg ha^{-1}
	3/3/2017	Herbicide	Chem-Surf 90, Quelex	
	8/13/2016	Tillage (tandem disc harrow)	10-13 cm	
	2016 (9/8, 10/8)	Tillage (field cultivator)	10-13 cm	
	10/15/2016	Seedbed preparation	8-10 cm	
Grain-only NT field	10/17/2016	Fertilizer (broadcast)	UAN 28%	19 kg ha^{-1}
	10/18/2016	Fertilizer in furrow	Dry 32-23-00	82 kg ha^{-1}
	3/3/2017	Herbicide	Chem-Surf 90, Quelex	
	10/17/2016	Seedbed preparation	5 cm	
Graze-grain CT field	9/23/2017	Fertilizer in furrow	Dry 29-29-00	94 Kg ha^{-1}
	2017 (6/28, 7/29, 9/5)	Tillage		
	9/23/2017	Seedbed preparation	8-10 cm	
Fields	Date	Event	Product	Rate
Graze-grain NT field	9/24/2017	Fertilizer in furrow	Dry 29-29-00	94 Kg ha^{-1}
	7/6/2017	Herbicide	Glyphosate	

Table 2. Monthly total rainfall and average air temperature (T_a) for the 2016-2018 study period in comparison with the 30-Year Normals (1981-2010).

Month	2016-2018		30-Year Normals	
	T_a (°C)	Rainfall (mm)	T_a (°C)	Rainfall (mm)
October 2016	18.57	15	15.91	95
November	11.98	15	9.25	59
December	2.60	23	3.62	46
January 2017	3.49	7	2.85	33
February	8.95	114	5.33	48
March	12.49	50	10.04	80
April	14.99	227	15.13	82
May	18.78	66	20.14	124
June	24.44	136	24.63	113
July	27.43	22	27.43	65
August	23.90	252	27.02	87
September	21.59	119	22.21	94
October	15.8	109	15.91	95
November	10.3	3	9.25	59
December	3.3	6	3.62	46
January 2018	1.8	3	2.85	33
February	3.29	39	5.33	48
March	10.91	9	10.04	80
April	11.92	50	15.13	82
May	23.12	46	20.14	124

Table 3. Partitioning of net radiation (R_n) into soil heat (G) and turbulent (sensible heat, H and latent heat, LE) fluxes.

Seasonal scale (November-May)				
Fields	2016-2017	R^2	2017-2018	R^2
CT	$G = 0.0852 X R_n - 5.6048$	0.38	$G = 0.1004 X R_n - 5.1844$	0.59
$H = 0.2342 X R_n - 19.718$		0.48	$H = 0.3883 X R_n - 2.9934$	0.70
$LE = 0.4379 X R_n + 38.918$		0.74	$LE = 0.2972 X R_n + 21.343$	0.67
NT	$G = 0.0605 X R_n - 4.5678$	0.38	$G = 0.0677 X R_n - 5.6722$	0.46
$H = 0.2986 X R_n – 21.539$		0.53	$H = 0.4458 X R_n - 2.2684$	0.68
$LE = 0.431 X R_n + 43.29$		0.71	$LE = 0.3297 X R_n + 28.184$	0.71
Active growing season (February-May)				
CT	$G = 0.0703 X R_n - 1.4328$	0.39	$G = 0.0931 X R_n - 2.6908$	0.63
$H = 0.2244 X R_n - 31.524$		0.55	$H = 0.38 X R_n - 9.1366$	0.73
$LE = 0.4624 X R_n + 51.014$		0.80	$LE = 0.3118 X R_n + 29.502$	0.71
NT	$G = 0.0473 X R_n - 2.2875$	0.36	$G = 0.0633 X R_n - 3.4019$	0.48
$H = 0.2206 X R_n - 31.64$		0.49	$H = 0.4384 X R_n - 2.8047$	0.69
$LE = 0.5136 X R_n + 52.308$		0.83	$LE = 0.3338 X R_n + 29.319$	0.73

Table 4. Monthly sums of evapotranspiration (ET, mm) and rainfall (mm) for the 2016-2018 study period.

Months	ET		Rainfall
	CT	NT	
November- 2016	42	38	15
December	25	29	23
January- 2017	31	31	7
February	49	49	114
March	93	97	50
April	107	110	227
May	113	116	66
June	34	27	136
July	42	26	22
August	96	56	252
September	44	37	119
October	79	68	109
November	27	36	3
December	18	24	6
January-2018	12	19	3
February	18	19	39
March	54	58	9
April	72	66	50
May	85	113	46

Table 5. Cumulative evapotranspiration and rainfall for the growing season (2017 and 2018) and fallow period (June – September 2017).

Period	Evapotranspiration		Rainfall
	Conventional till	No-till	
	---------- (mm) ----------		
2016-2017 growing season	459	468	501
Fallow	216	146	528
2017-2018 growing season	365	404	264
Total	1040	1019	1294

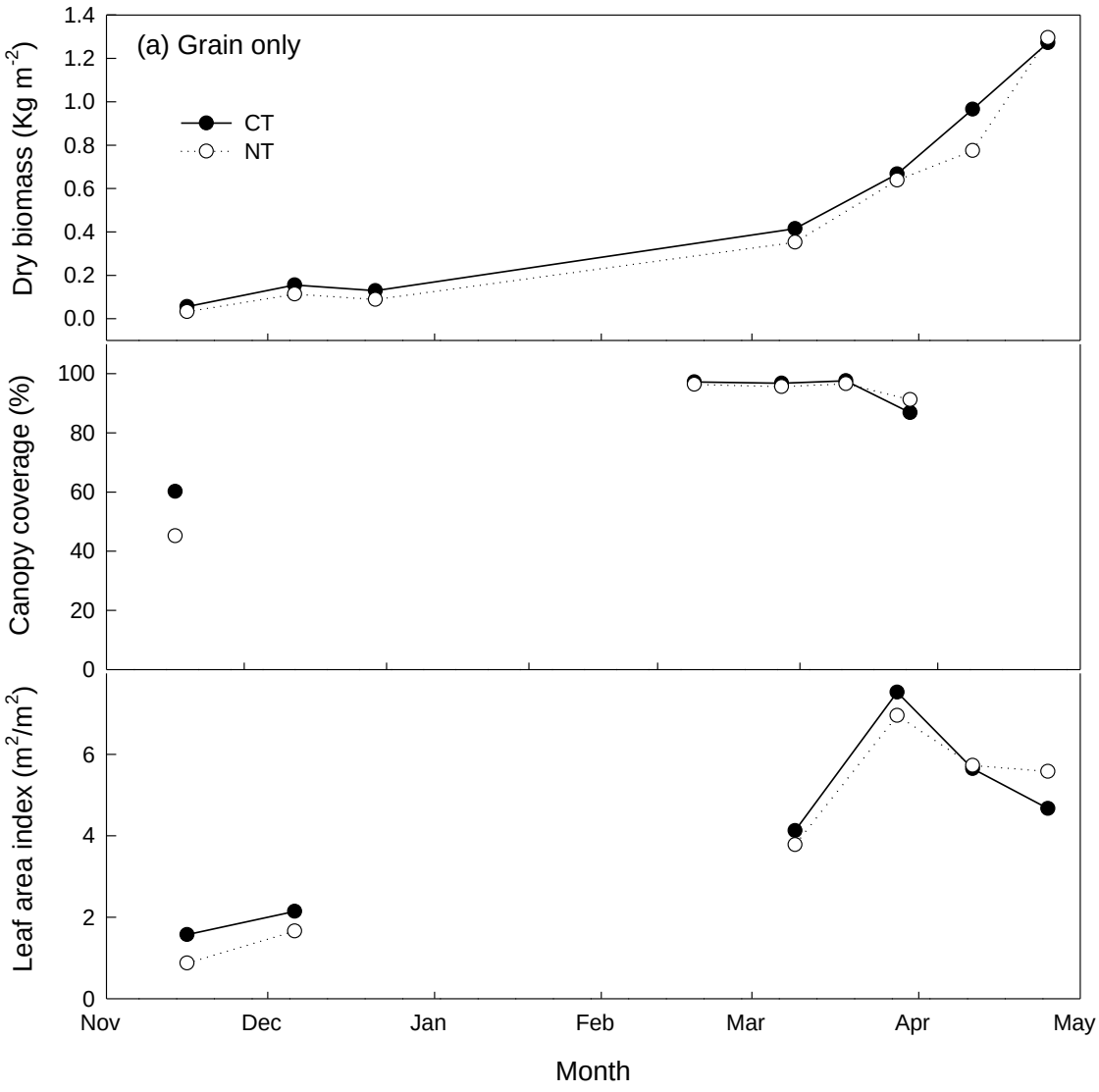

Fig. 1: Seasonal changes in aboveground dry biomass, percent of canopy coverage, and leaf area index for the 2016-2017 growing seasons in conventional (CT) and no-till (NT) winter wheat fields.

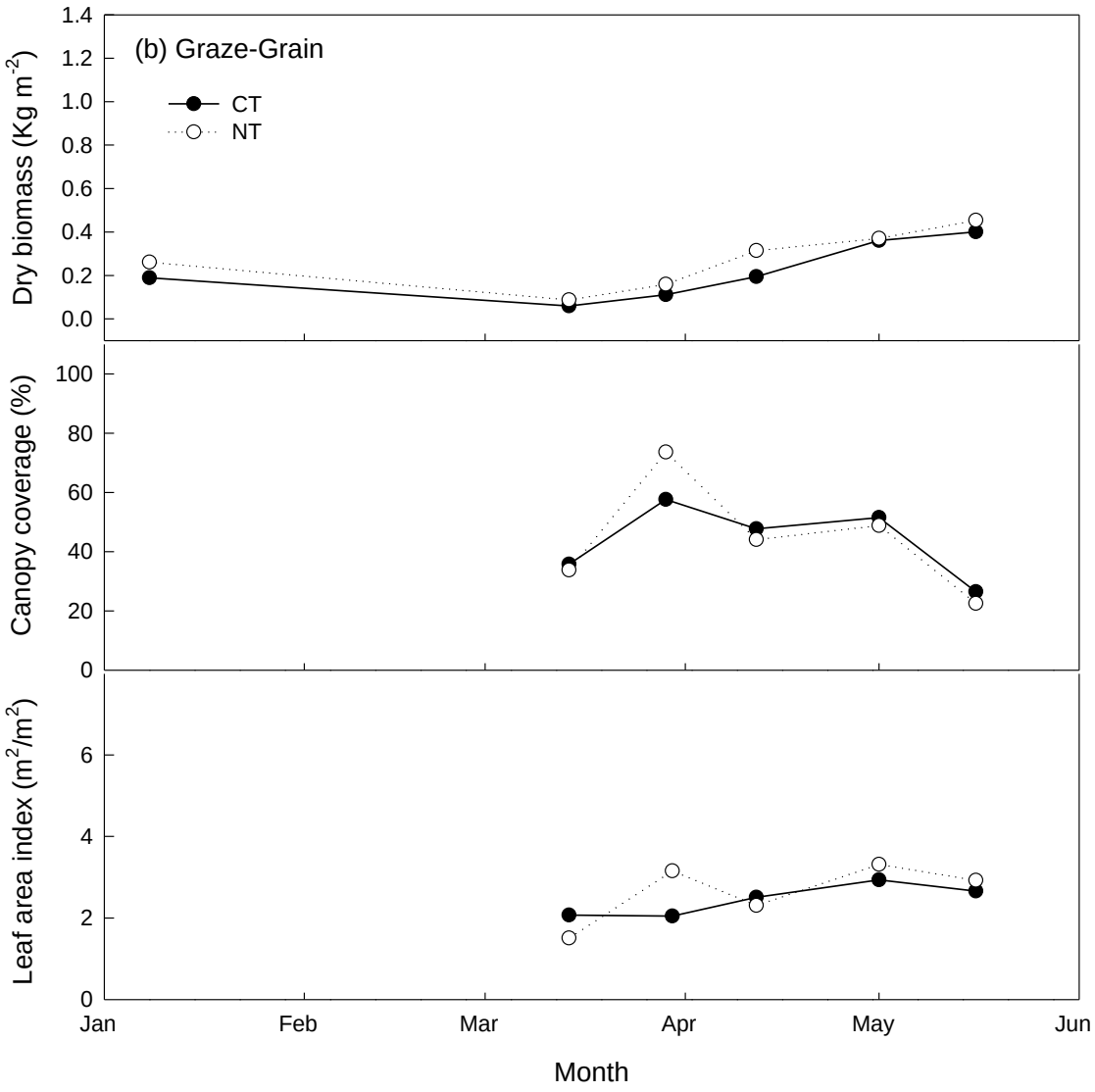

Fig. 2: Seasonal changes in aboveground dry biomass, percent of canopy coverage, and leaf area index for the 2017-2018 growing seasons in conventional (CT) and no-till (NT) winter wheat fields

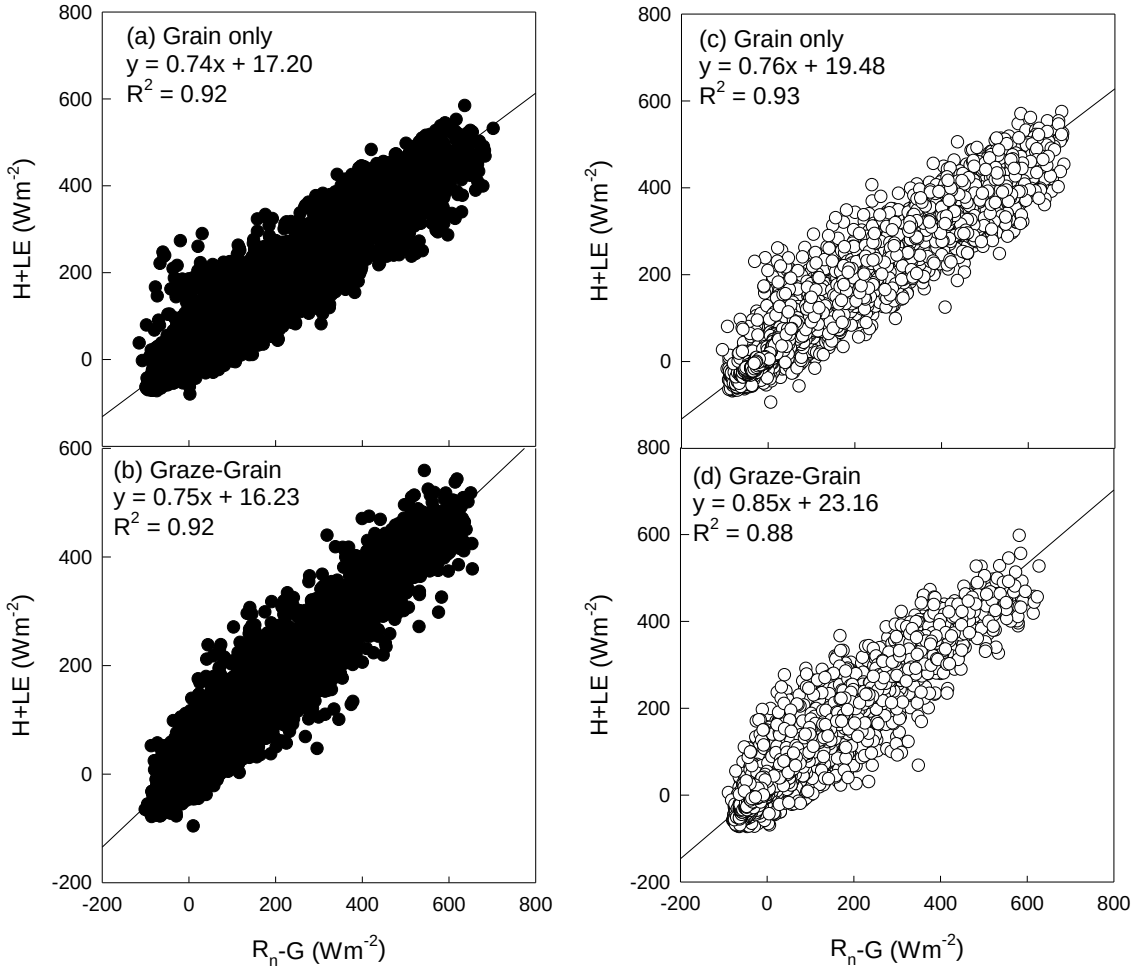

Fig. 3: Energy balance closure in conventional (CT – closed circles) and no-till (NT – open circles) winter wheat fields. Turbulent fluxes [sensible heat (H) and latent heat (LE)] were measured by eddy covariance and the available energy [net radiation (R_n) - soil heat flux (G)] was measured independent of eddy covariance.

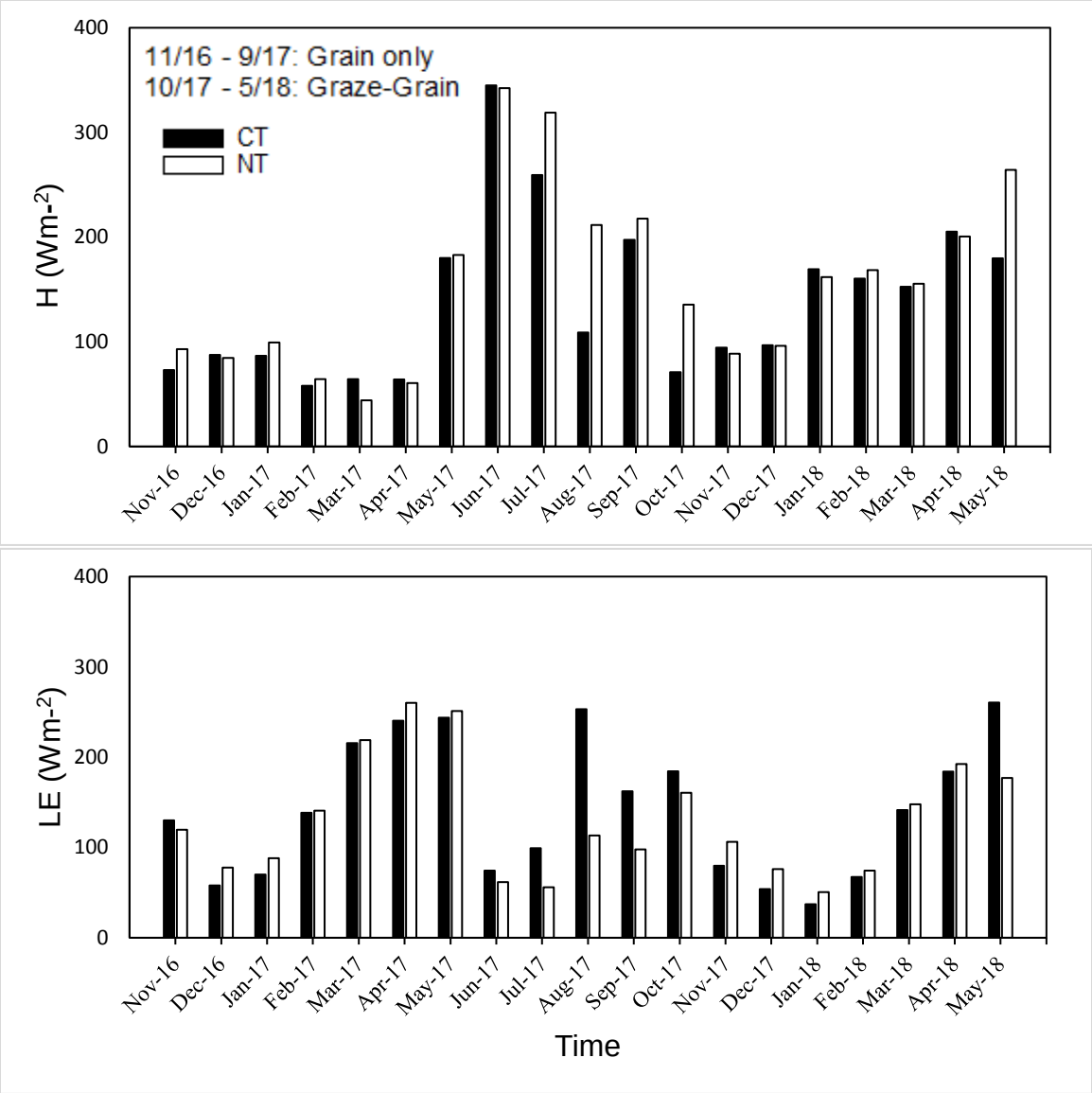

Fig. 4: Seasonal distribution of mean (monthly average) diurnal peaks of turbulent fluxes (sensible heat, H and latent heat, LE) for the 2016-2017 and 2017-2018 growing seasons and fallow period in conventional till (CT) and no-till (NT) winter wheat fields.

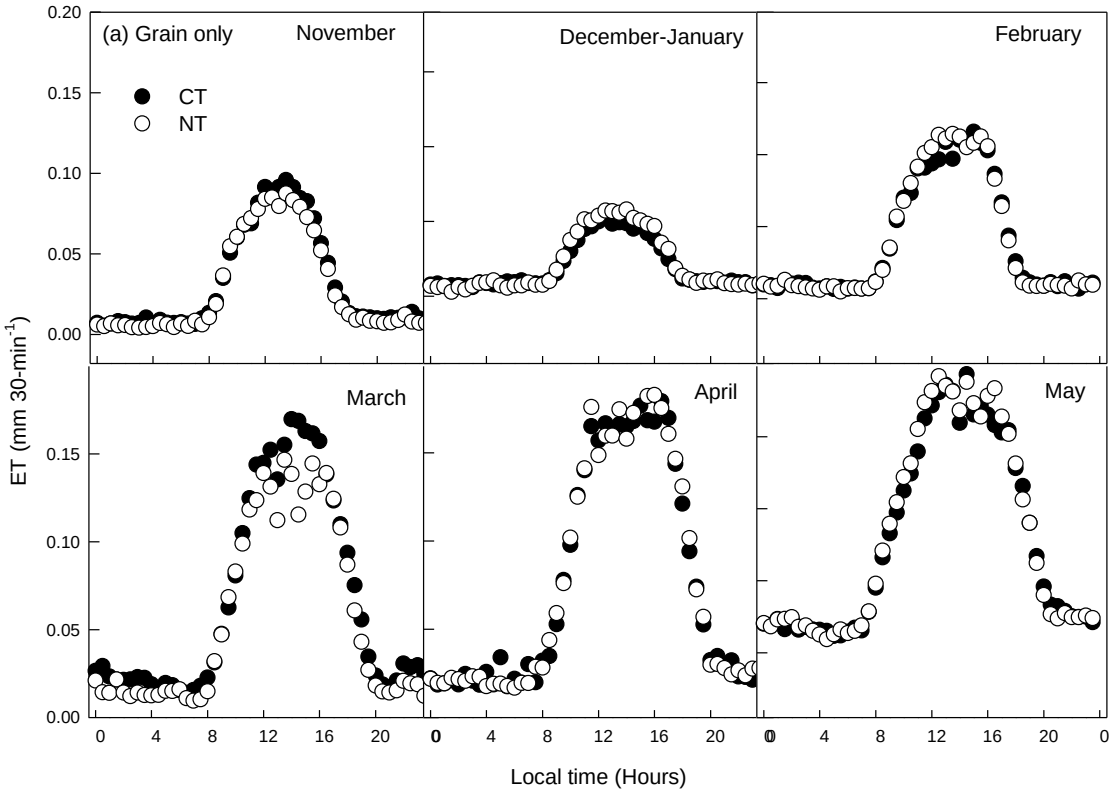

Fig. 5: Half-hourly binned diurnal courses of evapotranspiration (ET) for the 2016-2017 growing seasons in conventional till (CT) and no-till (NT) winter wheat fields. Each data point is a 30-min average value for the entire month.

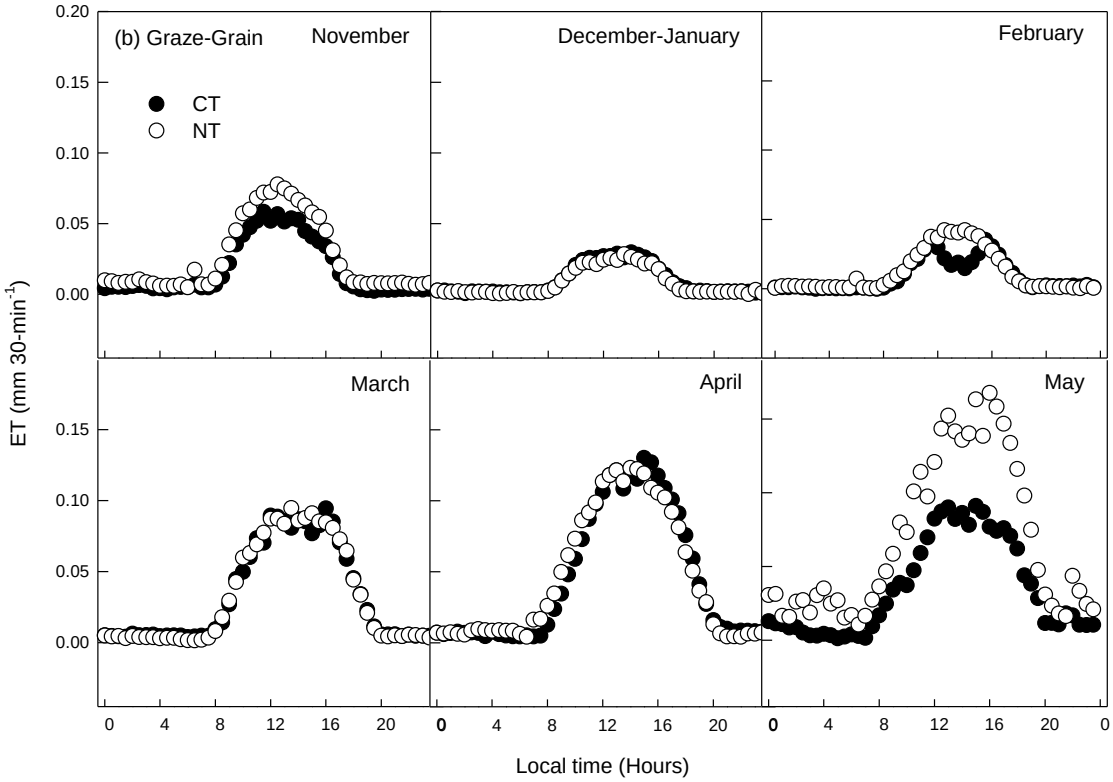

Fig. 6: Half-hourly binned diurnal courses of evapotranspiration (ET) for the 2017-2018 growing seasons in conventional till (CT) and no-till (NT) winter wheat fields. Each data point is a 30-min average value for the entire month.

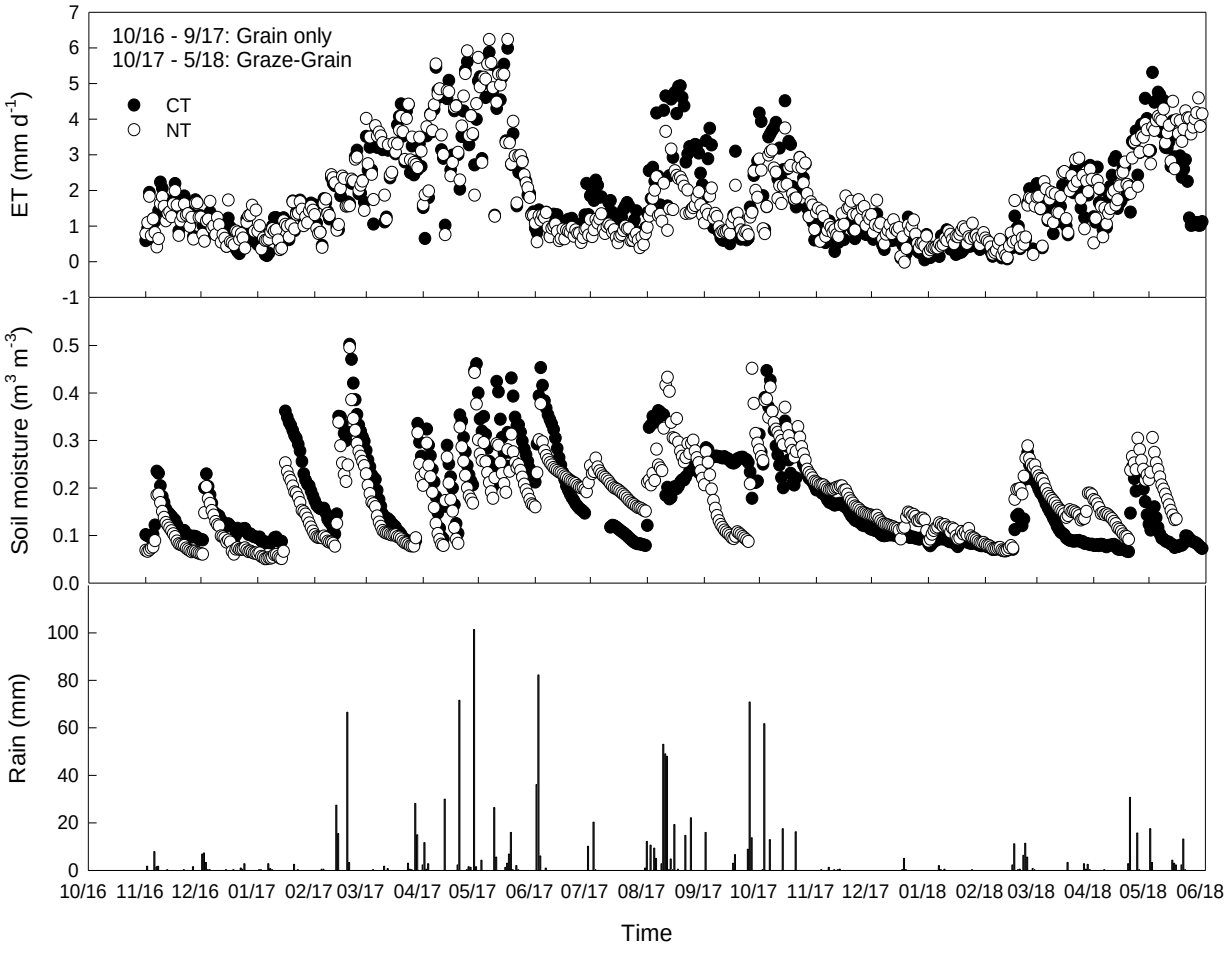

Fig. 7: Daily patterns of evapotranspiration (ET), soil moisture, and rainfall for the study period in conventional till (CT) and no-till (NT) winter wheat fields.

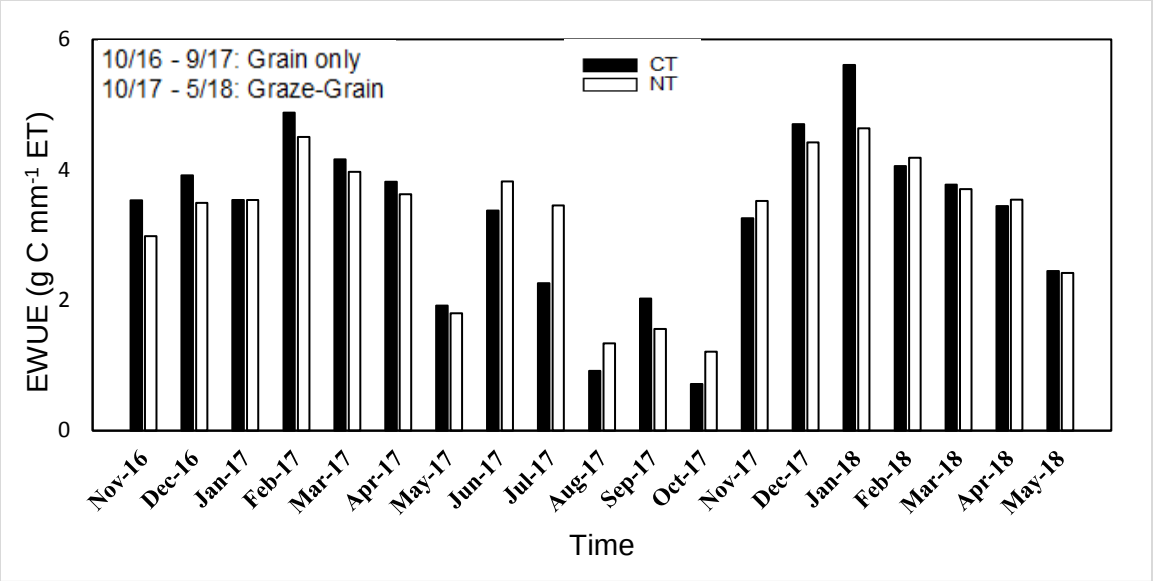

Fig. 8: Monthly values of ecosystem water use efficiency (EWUE = ratio of monthly cumulative gross primary production to evapotranspiration) for the 2016-2017 and 2017-2018 growing seasons in conventional till (CT) and no-till (NT) winter wheat fields.

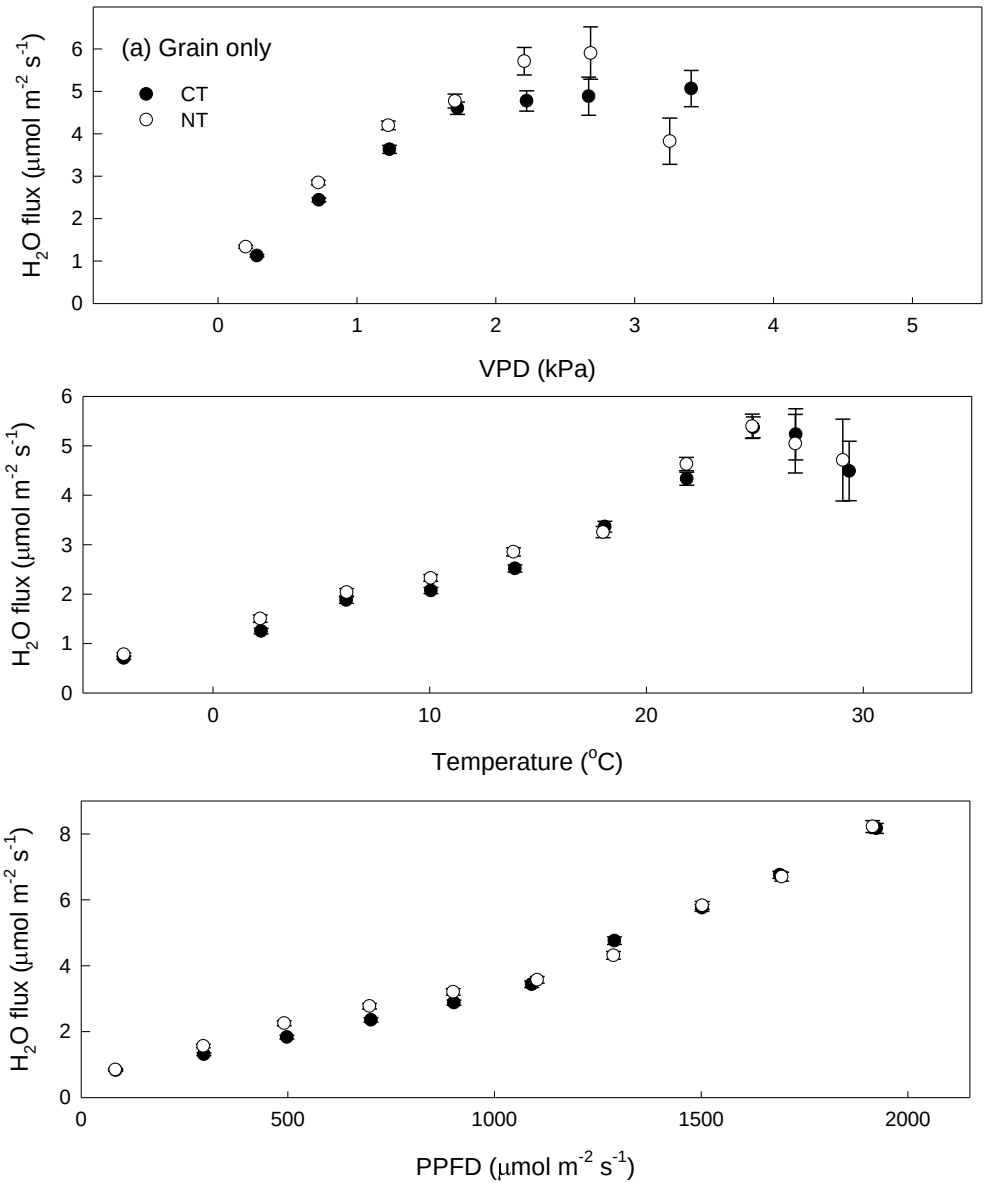

Fig. 9: Response of H_2O flux to vapor pressure deficit (VPD), air temperature (T_a), and photosynthetic photon flux density (PPFD) in conventional till (CT) and no-till (NT) winter wheat fields. Half-hourly H_2O fluxes for active growing seasons (November – April, 2017) were aggregated in classes of increasing PPFD, T_a, and VPD. Bars represent standard error of the means.

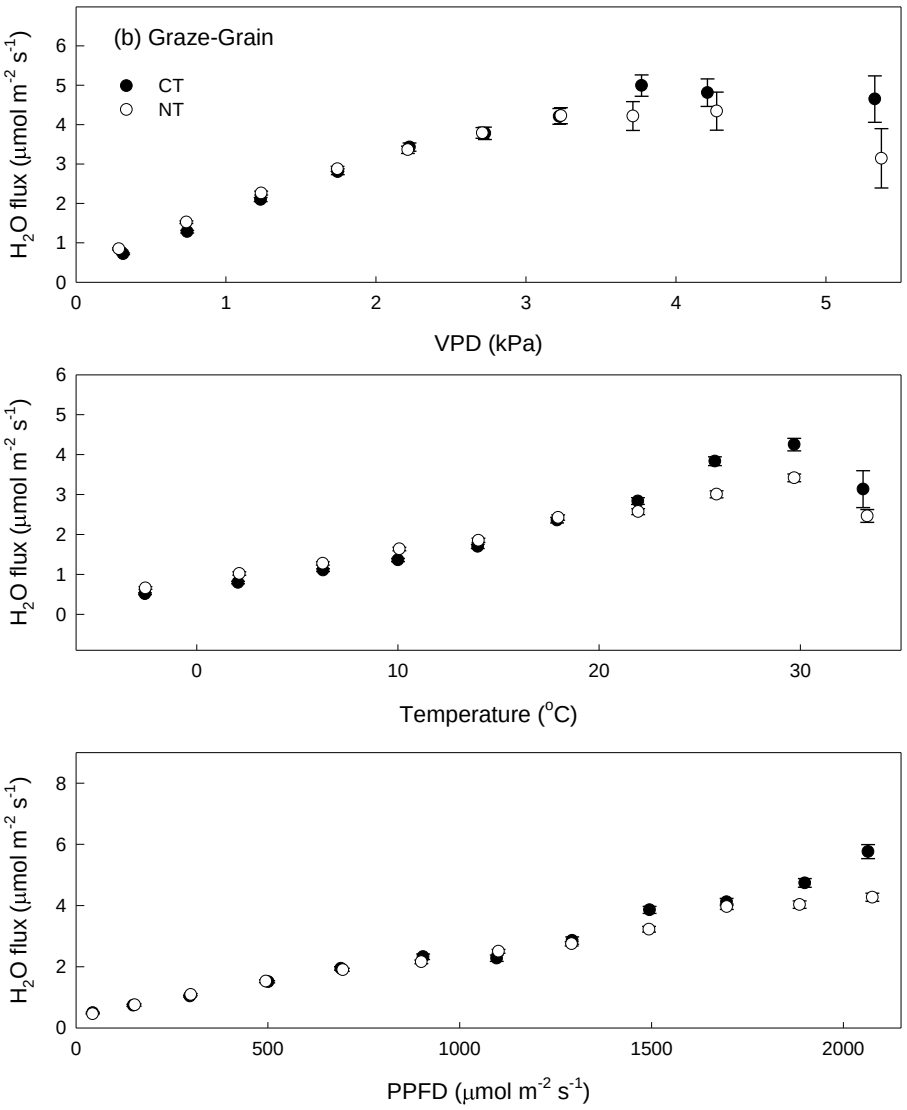

Fig. 10: Response of H_2O flux to vapor pressure deficit (VPD), air temperature (T_a), and photosynthetic photon flux density (PPFD) in conventional till (CT) and no-till (NT) winter wheat fields. Half-hourly H_2O fluxes for active growing seasons (October – May, 2018) were aggregated in classes of increasing PPFD, T_a, and VPD. Bars represent standard error of the means.

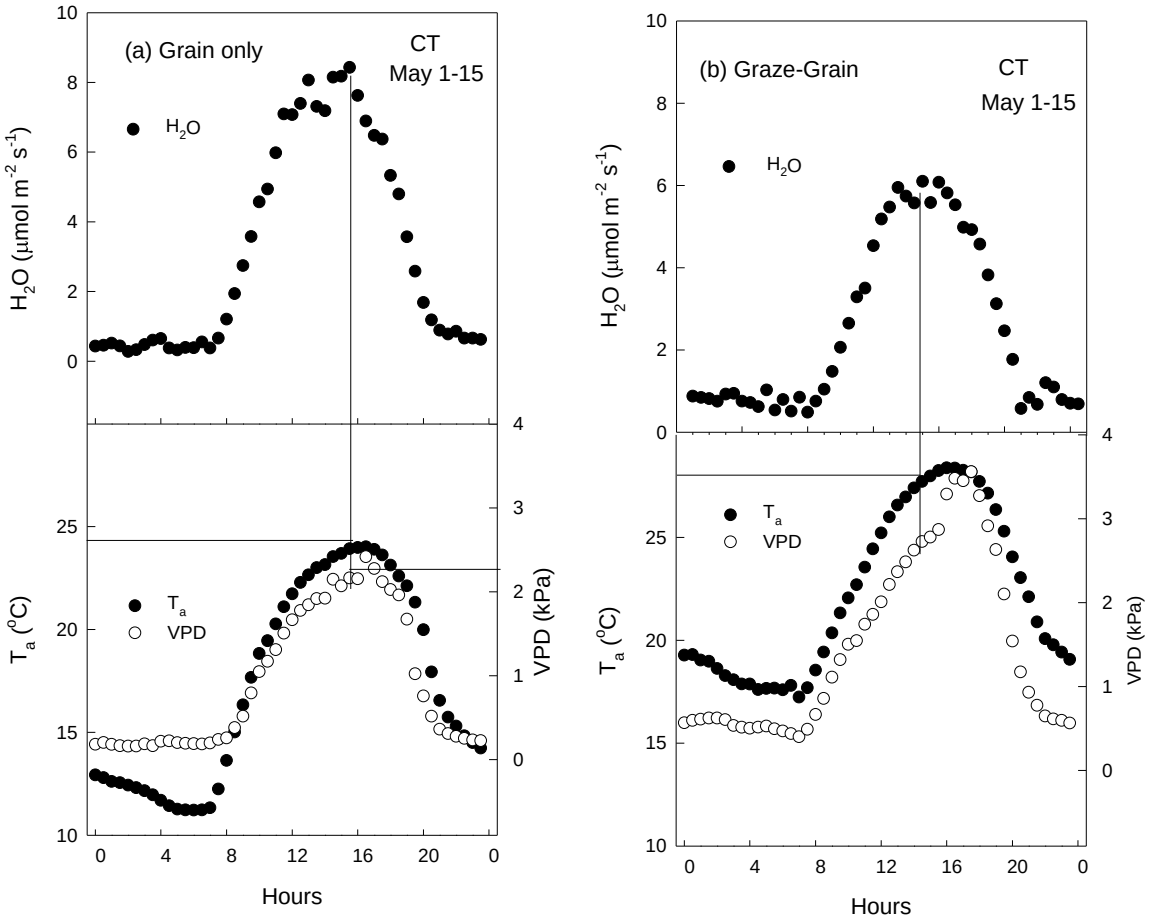

Fig. 11: Half hourly binned diurnal cycles of evapotranspiration (ET), air temperature (T_a), and vapor pressure deficit (VPD) for selected periods during the growing seasons [(a) May1-15, 2017 and (b) May1-15, 2018).

CHAPTER IV

ANNUAL DYNAMICS OF CO_2 AND H_2O FLUXES FROM CONVENTIONAL TILL AND NO-TILL CANOLA-FALLOW SYSTEMS IN THE U.S. SOUTHERN GREAT PLAINS

Abstract

A year-round fluxes of carbon dioxide (CO_2) and water vapor (H_2O) were measured over conventional till (CT) and no-till (NT) canola (*Brassica napus* L.) from planting through the end of following fallow period (DOY 289, 2016 – DOY 288, 2017). Daily magnitude (7-day average) of net ecosystem CO_2 exchange (NEE) reached -5.19 ± 0.49 and -4.66 ± 0.35 g C m^{-2} d^{-1} for CT and NT canola fields, respectively. The CT field was 1.8 times larger sink of carbon (-346 g C m^{-2}) than the NT field (-188 g C m-2) during the growing season (DOY 289, 2016 - 251, 2017), due to poor recovery of crop stand and shorter period (two months less) of carbon sink after winter damage at the NT field. During the fallow period, the NT field released more carbon (408 g C m^{-2}) than did the CT field (261 g C m^{-2}) due to offset of release of carbon by some uptakes due to regrowth of weeds at the CT field. Maximum daily evapotranspiration (ET, 7-day average) reached 4.69 ± 0.42 mm (CT) and 4.28 ± 0.36 mm (NT).

Cumulative ET for the growing season was similar (429 mm for CT and 415 mm for NT) between tillage systems, but cumulative ET for the fallow period was ~16 % lower in NT (254 mm) than in CT field (296 mm). At the growing season scale, ecosystem water use efficiency (EWUE) was 2.97 and 2.78 g C mm^{-1} ET and ecosystem light use efficiency (ELUE) was 0.19 and 0.16 g C mol^{-1} PAR for CT and NT fields, respectively. Since tillage practices were initiated just a year prior to this study period, long-term measurements will provide more insights into the influence of tillage practices and climatic conditions on carbon and ET dynamics of canola.

1. Introduction

Winter wheat (*Triticum aestivum* L.) is one of the major dryland crops grown in the Southern Great Plains (SGP) of the United States (U.S.) (Musick et al., 1994). Continuous wheat cropping systems are prone to failure due to yield-constraining insects and diseases (Duke et al., 2009). Italian ryegrass (*Lolium multiflorum* Lam.), introduced as a forage and erosion control grass, is also an important weed which has invaded many wheat fields and reduced wheat yields in Oklahoma (Barnes et al., 2001; Trusler et al., 2007). The application of herbicides to control weeds in wheat fields is limited by the cost, treatment efficiency, and grazing restrictions (Trusler et al., 2007) that can limit the use of wheat as pastures (Edwards et al., 2011; Redmon et al., 1995). Further, weeds decrease the value of the wheat crop by reducing its quality and yield. As a result, it is not viable for producers to grow continuous monocultures wheat (Barnes et al., 2001; Trusler et al., 2007).

Crop rotation involves growing different types of crops in the same land in a sequence and it has been a widely used strategy to minimize weed, insect, and disease problems in continuous winter wheat cropping systems (Duke et al., 2009; Liebman and Dyck, 1993). Canola (*Brassica napus* L.) has been identified as an economically viable crop to rotate with winter wheat in the

SGP (Duke et al., 2009; Gunstone, 2004). Bushong et al. (2012) and Duke et al. (2009) reported significantly higher wheat yield and net returns from a wheat-canola rotation as compared to a continuous wheat system. Furthermore, canola is the second most important oilseed crop in the world after soybean (*Glycine max L.*). Canola seeds contain an average of 45% oil, and can produce meal as animal feed with protein contents of ~21% (Johnston et al., 2002; Raymer, 2002). The global production of canola oilseed is forecast to rise 3.9 million tons in 2017-2018 (USDA, 2017). In the U.S., the consumption of domestic canola oil was approximately 2.74 million tons in 2017 (United States statistics, 2018).

Winter wheat production systems in the SGP have largely relied on different forms of conventional tillage (CT) to prepare land for planting and weed control during fallow periods. Surveys showed ~56% of croplands planted to wheat in Oklahoma was managed by CT (0 to 15% residual cover) (Hossain et al., 2004). However, conservation tillage (such as no-till (NT), or reduced tillage) are becoming more attractive to producers to reduce the production costs and increase soil water content during the fallow period, a critical component of wheat production (Patrignani et al., 2014). Both CT and NT are commonly used for production of canola in the region (Borstlap and Entz, 1994; De Vita et al., 2007).

Due to increasing atmospheric concentration of carbon dioxide (CO_2) and air temperature (T_a), the two major elements that contribute to global climate change, there has been a great interest in the measurement of net ecosystem exchange (NEE) of CO_2 and H_2O fluxes between atmosphere and various terrestrial ecosystems. Transferring CO_2 from the atmosphere to the terrestrial biosphere is an option to stabilize ever rising atmospheric CO_2 (West and Marland, 2002). As a result, the application of the eddy covariance (EC) technique to measure CO_2 and H_2O fluxes from a diverse range of terrestrial ecosystems has been rapidly increased (Baldocchi,

2014). However, EC-based measurements of CO_2 and H_2O fluxes is limited in canola (Taylor et al., 2013). Taylor et al. (2013) compared annual NEE budgets of three adjacent fields of hay [mix of timothy grass (*Phleum pretense L.*), rough fescue (*Festuca campestris Rydb*), and smooth brome (*Bromus inermis Leyss*)], oat (*Avena sativa L.*)-canola-oat, and hay-oat-fallow in Manitoba, Canada. They reported that canola had greater NEE than oat and smaller NEE than hay pastures. However, annual dynamics of CO_2 and H_2O fluxes from canola-fallow systems are lacking. In addition, comparative studies of the dynamics of CO_2 and H_2O fluxes between co-located CT and NT fields are scarce.

To achieve maximum production of agricultural systems, it is necessary to have an improved understanding of ecosystem water use efficiency (EWUE, the ratio of carbon gain to water loss) and ecosystem light use efficiency (ELUE, the ratio of carbon gain to radiation energy) (Wagle et al., 2016a). The EC measurements offer the opportunity to estimate NEE, ET, EWUE, and ELUE at the ecosystem level. Measurement of CO_2 and H_2O fluxes along with major climatic variables by the EC systems will also allow to investigate the functional responses of CO_2 and H_2O fluxes to changes in major climatic variables.

This is a pioneering study to thoroughly investigate annual dynamics of CO_2 fluxes and ET of economically important canola crop. The specific objectives of this study were to: 1) quantify year-round estimates of NEE and its components [gross primary production (GPP) and ecosystem respiration (ER)], and ET from co-located CT and NT canola-fallow systems, 2) investigate the responses of canola CO_2 and H_2O fluxes to changes in major climatic variables such as photosynthetically active radiation (PAR), vapor pressure deficit (VPD), and T_a, and 3) determine the seasonal dynamics of EWUE and ELUE at CT and NT canola fields.

2. Materials and methods

2.1. Field description

The study was conducted at the United States Department of Agriculture – Agricultural Research Service (USDA-ARS), Grazinglands Research Laboratory (GRL) in El Reno, Oklahoma. The experiment included two adjacent fields of winter canola under CT (19.8 ha, latitude: 35.5673, longitude: -98.0630, and elevation: 386 m above sea level) and NT (19.4 ha, latitude: 35.567922, longitude: -98.058708, and elevation: 384 m above seas level) systems. These fields have soil types of Renfrow-Kirkland silt loams, Bethany silt loams, and Norge silt loams (Mollisols) with an average pH ≤ 6.1 and organic matter < 2.8 % (USDA-NRCS, 1999). Canola (*cv.* DKW46-16) was sown at 6 kg seed ha^{-1} in rows spaced 19 cm apart during October 3-4, 2016 at both fields, and harvested during June 15-29, 2017. Flux data were collected from mid-October 2016 (after planting canola) through mid-October 2017 (end of the fallow period and start of the next cropping cycle for grain-only winter wheat). Tillage systems were initiated in 2015, a year prior to the study period. Additional information on management practices (e.g., tillage, applications of fertilizers and pesticides) are presented in Table 1.

2.2. Eddy fluxes and biometric measurements

Continuous measurements of CO_2 and H_2O fluxes were collected from both fields using EC systems. The EC systems were situated near the center of fields, and equipped with a three-dimension sonic anemometer (CSAT3, Campbell Scientific Inc., Logan, UT, USA) and an open path infrared gas analyzer (LI- 7500-RS, LICOR, Lincoln, NE, USA), mounted at a fixed height of 2.5 m. Other supplementary meteorological measurements such as PAR (using quantum sensor LI- 190, LICOR, Lincoln, NE, USA), T_a and relative humidity (using HPM45C, Vaisala, Helsinki, Finland), soil temperature at 2 and 6 cm depths (using thermocouples), soil heat flux

(G) at 8 cm depth (using HFT3, REBS Inc., Bellevue, WA, USA), soil water content (SWC) at 5 cm depth (using Hydra probe, Stevens Water Monitoring Systems Inc., Portland, OR, USA), and above canopy net radiation ($R_{n,}$ using NRLite, Kipp & Zonen, Delft, The Netherlands) were collected at 30-min intervals using Campbell Scientific data loggers.

The raw data collected at 10 Hz frequency were processed using the *EddyPro* (version 6.2) software (LICOR Inc., Lincoln, NE, USA) to get 30-min values of eddy fluxes. The *EddyPro* provides a quality flag, ranging from 0 (best quality fluxes) to 2 (bad quality fluxes that should be excluded). Data were excluded for periods of low turbulence (friction velocity, $u^* < 0.20$ m s^{-1}) and unreasonable fluxes. The fluxes were filtered to keep them within reliable ranges: sensible flux (H) from -200 to 500 Wm^{-2} and latent heat flux (LE) from -200 to 800 Wm^{-2} (Wagle and Kakani, 2014). Statistical outliers beyond ± 3.5 SD (standard deviation) based-on 14-day running windows were removed (Wagle and Kakani, 2014). The *REddyProc* (REddyProc, 2015) R–package, available online from the Max Planck Institute for Biogeochemistry, Germany, was used to fill gaps in data and to partition NEE into its two components: GPP and ER. The NEE sign conventions are considered negative if the ecosystems are carbon sinks and positive if the ecosystems are carbon sources.

Biometric measurements were collected at both fields at approximately two week intervals, which coincided with dates of Landsat overpass. The biometric measurements included leaf area index (LAI, using a LAI -2200C plant canopy analyzer, LICOR Inc., Lincoln, NE, USA), canopy height, and destructive biomass samples from five randomly located 0.5 × 0.5 m quadrats on each sampling date.

2.3. Examining the response of CO_2 and H_2O fluxes to major climatic variables (PAR, T_a, and VPD)

The response of CO_2 and H_2O fluxes to major climatic variables (PAR, T_a, and VPD) were compared across (2016-2017) growing season. Daytime CO_2 and H_2O fluxes (PAR > 5 µmol m^{-2} s^{-1}) for the growing season were binned into 12 classes of PAR (<100, 100-200, 200-400, 400-600, 600-800, 800-1000, 1000-1200, 1200-1400, 1400-1600, 1600-1800, 1800-2000, and >2000 µmol m^{-2} s^{-1}), 13 classes of T_a (<-5, -5-0, 0-3, 3-6, 6-9, 9-12, 12-15, 15-18, 18-21, 21-24, 24-27, 27-30 and >30°C), and 10 classes of VPD (<0.5, 0.5-1, 1-1.5, 1.5-2, 2-2.5, 2.5-3, 3-3.5, 3.5-4, 4-4.5, and > 4.5 kPa).

2.4. Ecosystem water use efficiency and ecosystem light use efficiency estimates

We estimated the seasonal distribution of EWUE and ELUE as the ratios of monthly sums of GPP to ET and GPP to PAR, respectively (Wagle et al., 2016a; Wagle et al., 2016b). We also determined seasonal and annual values of EWUE as the ratio between seasonal and annual sums of GPP to ET, respectively. The ELUE was computed at the seasonal scale as the ratio of seasonal sums of GPP to PAR.

3. Results and discussion

3.1. Weather conditions and crop growth

Because both fields were rainfed and co-located, they experienced similar weather conditions. The climate is temperate continental. Monthly mean T_a and total rainfall for the 2016-2017 study period in comparison with the 30-year means (1981-2010) are presented in Table 2. The annual average T_a and total rainfall during the 2016-2017 study period was ~15 °C and 1046 mm, respectively. The fields received ~1.13 times more annual rainfall from October 2016 to September 2017 as compared to the 30-year mean annual rainfall (926 mm). During the growing

season (October 2016 – May 2017), canola received 1.1 times more rainfall (517 mm) as compared to the 30-year mean (567 mm) for the same period. However, total rainfall was 74 % lower from October 2016 to January 2017, but it was 36 % higher from February to May 2017 as compared to the 30-year mean. During the fallow period (June – September 2017), both fields received 529 mm which was ~47 % higher than the 30-year mean precipitation for the same period (359 mm). During the fallow period, higher rainfall was recorded in all months except July as compared with the 30-year means.

Evolution of dry biomass, LAI, and canopy coverage during the 2016-2017 canola growing season is presented in Fig. 1. There was no substantial difference in dry biomass, LAI, and canopy coverage of CT and NT fields during fall 2016, but in spring 2017, they were substantially lower at the NT field due to poor recovery of crop stand after winter dormancy. Maximum dry biomass reached 0.82 and 0.41 kg m^{-2} in April, LAI reached 4.75 and 5.3 m^2 m^{-2} in December, and canopy coverage reached 97-98% in December at CT and NT canola fields, respectively. Grain yield approximated 0.91 t ha^{-1} and 0.97 t ha^{-1} for CT and NT fields, respectively. Bushong et al. (2012) reported mean canola yield of about 1.6 t ha^{-1} and 1.9 t ha^{-1} in 2009 at Chickasha and Perkins, Oklahoma, respectively, which were south (Chickasha, ~ 67 km) and northeast (Perkins, ~ 145 km) of the current study area. The lower grain yield in our study was attributed to the grain loss to shattering related to delayed harvesting caused by rains. If harvested on time, the tentative grain yield was estimated at 35 bu ac^{-1} (1.96 t ha^{-1}) for the CT field in this study.

Soil temperature (T_s) was lower (average of ~3 °C) throughout the growing season and relative soil water content [relative SWC = $(\theta - \theta_{min})/(\theta_{max} - \theta_{min})$] was higher (average of 0.4 m^3 m^{-3}), especially from mid-January through harvesting, at the NT field than the CT field (Fig. 2).

Note that our soil moisture measurements at 5-cm depth near the flux tower do not reflect the actual SWC of water logging conditions in micro-depressions in different parts of the NT field during higher rainfall in February-March. Lower T_s and poor drained condition could be the reasons for poor stand recovery after winter dormancy at the NT field since canola requires well-drained conditions to perform well (Agronomic recommendations, 2018). More winter kill problems have been observed in NT conditions by farmers in Oklahoma as well (South West farm press, 2018).

3.2. Diurnal patterns of NEE and ET

Diurnal trends of NEE and ET for few selected months, including both peak growth and dormant periods, are shown in Fig. 3 and 4, respectively. The NT field had slightly higher NEE rates in November 2016. However, the NEE rates were higher in CT field than in NT field from December 2016 to April 2017. This discrepancy can be attributed to differences in seasonal dynamics of dry biomass, LAI, and canopy cover % as shown in Fig. 1. The maximum diurnal peak NEE (monthly average) for the peak growing season were observed in April of -21.7 ± 1.34 and -15.9 ± 1.21 μmol m^{-2} s^{-1} at CT and NT fields, respectively. Diurnal peak NEE values were only -6.7 ± 1.21 (CT) and -5.8 ± 1.39 (NT) μmol m^{-2} s^{-1} during the period of winter dormancy in December. The magnitude of diurnal peak NEE (2-weeks period) reached up to -18.92 ± 1.07 μmol m^{-2} s^{-1} during November 1-15 at the NT field and -23.49 ± 1.66 μmol m^{-2} s^{-1} during March 16-31 at the CT field. The magnitude of NEE in canola in this study was similar (-23.18 ± 1.63 μmol m^{-2} s^{-1}) to the magnitude of NEE reported for soybean (*Glycine* max L.) in El Reno, Oklahoma (Wagle et al., 2017), but smaller than the magnitudes of NEE (~36 μmol m^{-2} s^{-1}) for switchgrass (*Panicum virgatum* L.) and high biomass sorghum (*Sorghum bicolor* L. Moench) in Chickasha, Oklahoma (Wagle et al., 2015a).

Peak diurnal ET (monthly average) for canola approximated 0.15-0.16 mm 30 min^{-1} in April at both fields. In contrast, the magnitude of diurnal ET in December was only 0.004-0.005 mm 30 min^{-1}. Diurnal peak ET (2-weeks period) reached 0.16 ± 0.016 (CT) and 0.19 ± 0.018 (NT) during April 16-30. The magnitude of canola ET in this study was substantially smaller than the ET for rainfed switchgrass (0.31 ± 0.02 mm 30 min^{-1}) and sorghum (0.28 ± 0.02 mm 30 min^{-1}) in Chickasha, Oklahoma (Wagle et al., 2016b).

3.3. Seasonal patterns and sums of NEE, GPP, ER, and ET

The seasonal courses of daily (7-day average) NEE, GPP, ER, and ET for both fields followed the similar seasonal dynamics (Fig. 5). As expected, CO_2 fluxes and ET increased with increasing crop growth after planting, declined during their dormant stage in winter, started increasing again after mid-January with increasing temperature and crop growth. Fluxes peaked during the period that corresponded to peak growth, and declined rapidly during the late growing season due to senescence.

The maximum NEE (7-day average) reached -5.19 ± 0.49 and -4.66 ± 0.35 g C m^{-2} d^{-1} at CT and NT fields during the growing season, respectively. The seasonal sums of NEE were -346 g C m^{-2} (CT) and -188 g C m^{-2} (NT). Based on monthly sums of NEE, the CT field was a carbon sink for six and half months, from mid-October to December and February to May. In contrast, the NT field was a carbon sink for four and half months, from mid-October to December and March to April (Table 3). The rates of CO_2 fluxes were very similar until end of January. Due to differences in winter recovery, as reflected in dry biomass, LAI, and canopy cover (Fig. 1), large differences in NEE and GPP occurred from end of February to end of April. As a result, CT field gained about 50% more carbon during the growing season. Chi et al. (2016) and Montanaro et al. (2017) reported more carbon sequestration in NT wheat and peach (*Prunus persica* L.

Batsch) fields than CT fields. In contrast, more carbon was sequestered by CT canola field in our study because of the better crop stand after winter dormancy. For the same study area during the same study period (2016-2017), Wagle et al. (2018b) reported maximum (7-day average) NEE of -7.79 ± 1.08 and -8.68 ± 0.87 g C m^{-2} d^{-1} and seasonal NEE sums of -542 and -469 g C m^{-2} for grain-only winter wheat under CT and NT systems, respectively. The results showed that canola fields were smaller sinks of carbon as compared to winter wheat fields.

Maximum daily (7-day averages) GPP reached ~12.5 g C m^{-2} d^{-1} at both fields. The magnitudes (7-day averages) of ER reached 9.74 ± 0.34 and 13.4 ± 1.2 g C m^{-2} d^{-1} at CT and NT fields, respectively. In comparison, the 7-day averages of GPP were ~16.62 ± 0.95 and 16.92 ± 0.49 g C $m^{-2}d^{-1}$, and ER were ~9.47 ± 0.23 and 9.98 ± 0.51 g C $m^{-2}d^{-1}$ for grain-only winter wheat under CT and NT systems, respectively (Wagle et al., 2018b). The seasonal sums of GPP were 1322 and 1214 g C m^{-2}, and seasonal sums of ER were 1002 and 1055 g C m^{-2} at CT and NT canola fields, respectively. Wagle et al. (2018b) reported seasonal GPP sums of 1643 and 1571 g C m^{-2} and seasonal ER sums of 1101 and 1102 g C m^{-2} for grain-only winter wheat under CT and NT systems, respectively. The results showed GPP sums were substantially lower (~20-22%) but ER sums were similar or slightly lower (4-8%) in canola, compared to those of grain-only winter wheat for the same study area and study period.

Magnitude of daily ET (7-day average) reached 4.69 ± 0.42 mm d^{-1} and 4.28 ± 0.36 mm d^{-1} at CT and NT fields, respectively, during the growing season. Monthly ET sums at CT and NT fields were similar during the growing season, ranging from 20-22 mm in December and January to >110 mm in May (Table 3). As a result, cumulative growing season ET (October 2016-May 2017) was similar between both fields (429 mm for CT and 415 mm for NT). These seasonal ET sums were slightly smaller than those (460-470 mm) for grain-only winter wheat CT and NT

fields for the same study area and study period (unpublished data). Similar cumulative ET despite large differences in canopy stand and CO_2 fluxes during spring 2017 indicated more evaporative loss of water from the NT field due to sparse vegetation after winter dormancy.

3.4. Variability in NEE, GPP, ER, and ET during the fallow period.

The cumulative NEE for the fallow period was 250 and 401 g C m^{-2} at CT and NT fields, respectively. The results showed the NT field released 38% more carbon during the fallow period. Less release of carbon by the CT field can be attributed to the offset of release of carbon by some uptakes due to regrowth of weeds. As a result, cumulative GPP for the fallow period was 18% higher at the CT than the NT field. In comparison, cumulative ER for the fallow period was ~7% higher at the NT field than the CT field. Decomposition of the crop stubble and more residues, and higher microbial activities could also be attributed to relatively higher ER at the NT field (Al-Kaisi and Yin, 2005; Linn and Doran, 1984).

Maximum daily ET rates (7-day average) were 4.42 ± 0.39 mm d^{-1} and 3.11 ± 0.18 mm d^{-1} during the fallow period at CT and NT fields, respectively. Monthly ET values during the fallow period were higher at the CT field than the NT field (Table 3). The highest difference in monthly ET was observed in August (~29 % higher for CT than NT) when monthly rainfall was higher (252 mm). Overall, cumulative ET for the fallow period was ~14 % higher at the CT field (296 mm) than the NT field (254 mm). The residue on the surface served as a barrier to minimize ET loss from NT field. Cumulative ET for a complete year (from mid-October 2016 to mid-October 2017) was 725 mm at the CT field compared to 669 mm at the NT field. Burba and Verma (2005) reported similar annual ET (714 to 750 mm) during 1996-2000 for grain-only winter wheat in north-central Oklahoma.

Tillage practices and rainfall events also influenced dynamics of CO_2 fluxes and ET during the fallow period. For example, daily NEE rates increased from ~3 g C m^{-2} to ~9-10 g C m^{-2} in both fields after rainfall event of 20 mm on July 3. Similarly, rates of ET also increased after the rainfall event. At the CT field, ET rates decreased and the field switched from sink of carbon to source of carbon due to removal of weeds after tillage during June 28-30.

3.5. Response of NEE and H_2O fluxes to T_a, VPD, and PAR

Response of NEE and H_2O fluxes to major climatic variables are presented in Figs. 6 and 7, respectively. Both NEE and H_2O fluxes exhibited similar responses to T_a, VPD, and PAR at both fields. Optimum thresholds of T_a and VPD for H_2O fluxes were approximately 25° C and 2.7 kPa, respectively (Fig. 7). The H_2O flux did not decrease with increasing PAR > 2050 μmol m^{-2} s^{-1}. The results showed that NEE was more sensitive to major climatic variables than H_2O fluxes, consistent with the findings of previous studies (Wagle et al., 2018a; Wagle et al., 2015b). Wagle et al. (2018 b) reported optimum threshold T_a of 22 $^{\circ}$ C, VPD of 1.25 kPa, and PAR of 1500 μmol m^{-2} s^{-1} for NEE of winter wheat at the same study area and study period. The results indicated a similar threshold value of T_a (22-23° C) for NEE in winter wheat and canola, but thresholds of VPD and PAR for NEE were higher in canola than in winter wheat.

There were different responses of H_2O fluxes to T_a and VPD beyond the threshold values at CT and NT fields. The H_2O fluxes declined beyond threshold T_a and VPD at the CT field, but not at the NT field. This discrepancy can be explained by higher contribution of evaporation to ET at the NT field due to sparse vegetation. Transpiration rate increases as VPD increases, which leads to a reduction in leaf water potential resulting in stomatal closure, thereby reducing ET at higher T_a and VPD (Monteith, 1995).

To further examine the responses of NEE and H_2O fluxes to T_a and VPD, we created diurnal trends of NEE, H_2O, T_a, and VPD for selected periods of growing season at the CT field (Fig. 8). Since the NT field had sparse vegetation and resulted higher contribution of evaporation to ET, we only examined for the CT field. Results illustrated that NEE exhibited symmetrical diurnal patterns (reaching peak values at around 2:00 pm) in November and March when T_a and VPD were below thresholds by 2:00 pm. However, NEE showed an asymmetric diurnal pattern in May. The NEE peaked at 12:00 pm when T_a and VPD were close to thresholds (T_a of ~23 $^{\circ}$ C and VPD of ~1.7 kPa). However, H_2O fluxes showed symmetric diurnal pattern (reaching peak values at around 2:00 pm) for all selected periods due to higher thresholds of T_a and VPD. These results further confirmed the smaller threshold values of T_a and VPD for NEE than for H_2O fluxes.

We further evaluated the response of daytime NEE (PAR > 5µmol m^{-2} s^{-1}) to PAR for different periods of the growing season at CT and NT fields (Fig. 9). Results showed that NEE increased with the observed ranges of increasing PAR for all selected periods (~1300 µmol m^{-2} s^{-1} in November, ~1800 µmol m^{-2} s^{-1} in March, and ~2000 µmol m^{-2} s^{-1} in April), except in May. In May, NEE reached a maximum at around 1000 µmol m^{-2} s^{-1} PAR and did not increase much when PAR increased further due to senescence of vegetation.

3.6. Seasonal trends and magnitudes of EWUE and ELUE

Both EWUE and ELUE increased with increasing crop growth during October-November, decreased during December-January due to the decline in carbon uptake caused by low solar radiation and winter temperature, then increased with crop growth from February to April (Fig. 10). The monthly EWUE ranged from 1.69 to 3.82 g C mm^{-1} ET at the CT field and from 1.18 to 3.95 g C mm^{-1} ET at the NT field. The magnitude of monthly EWUE reached 3.82 g C mm^{-1} ET

in March and 3.95 g C mm^{-1} ET in November at CT and NT fields, respectively. Minimum monthly EWUE of 1.69 and 1.18 g C mm^{-1} ET were observed in January at CT and NT fields, respectively. Growing season EWUE (October 2016 – May 2017) was 1.13 times higher at the CT field than the NT field, most likely caused by higher proportion of evaporation (waste water) loss due to sparse canopy at the NT field during spring 2017.

The monthly ELUE ranged from 0.05 to 0.32 g C mol^{-1} PAR at the CT field and from 0.03 to 0.28 at g C mol^{-1} PAR at the NT field (Fig. 10). Maximum ELUE reached about 0.32 g C mol^{-1} PAR in April at the CT field and 0.28 g C mol^{-1} PAR in November at the NT field. Minimum ELUE rates were 0.05 (CT) and 0.03 (NT) g C mol^{-1} PAR in January. The ratio of seasonal sums of GPP to PAR yielded higher ELUE at the CT field (0.19 g C mol^{-1} PAR) than at the NT field (0.16 g C mol^{-1} PAR), due to higher photosynthetic activity and carbon sink potential at the CT field. The maximum ELUE (monthly) of 0.32 g C mol^{-1} PAR in canola was higher than the maximum ELUE (weekly) reported in rainfed soybean (0.22 g C mol^{-1} PAR) for the same location (Wagle et al., 2017). The growing season ELUE values of 0.16-0.19 g C mol^{-1} PAR in canola were smaller than those reported growing season ELUE values of 0.23-0.24 g C mol^{-1} PAR in grain-only winter wheat for the same study period and study area (Wagle et al., 2018b).

4. Conclusions

The seasonal sums of NEE were -346 g C m^{-2} and -188 g C m^{-2} at the CT and NT canola fields, respectively. Sums of NEE for mid-October-December period were -91 and -100 g C m^{-2}, but for January-May period were -254.97 and -88.23 g C m^{-2} at the CT and NT fields, respectively. The large discrepancy in NEE for the January-May period was due to poor recovery of crop stand after winter damage at the NT field. During the fallow period, NT field released 38% more carbon than did the CT field. Cumulative seasonal ET during the growing season was

similar for both fields (429 mm for CT and 415 mm for NT). Similar seasonal cumulative ET despite large differences in canopy stand during spring 2017 indicated more evaporative loss of water from the NT field due to sparse vegetation. Cumulative ET for the fallow period (June-October 2017) was 1.16 times higher at the CT field than the NT field. Overall, cumulative ET for a complete year (from mid-October 2016 to mid-October 2017) was 725 mm at the CT field and 669 mm at the NT field. Optimum values of T_a, VPD, and PAR for NEE were approximately 23° C, 1.7 kPa, and 1700 μmol m^{-2} s^{-1}, respectively. Optimum values of T_a and VPD were higher for H_2O fluxes (~25° C and 2.7 kPa, respectively) than for CO_2 fluxes. Poor canopy stand after winter dormancy at the NT field caused lower ELUE and EWUE.

Large differences in CO_2 fluxes and ET during the growing season between CT and NT fields were mainly caused by differences in stand establishment after winter dormancy rather than by tillage treatment since tillage experiment was initiated just a year prior to this study. However, the impact of tillage on CO_2 fluxes and ET was more evident during the fallow period. Long term measurements will provide further insights on the influence of tillage practices and climatic conditions on CO_2 and ET dynamics of canola.

REFERENCES

Al-Kaisi, M. M., & Yin, X. (2005). Tillage and crop residue effects on soil carbon and carbon dioxide emission in corn–soybean rotations. *Journal of Environmental Quality*, *34*(2), 437-445.

Baldocchi, D. (2014). Measuring fluxes of trace gases and energy between ecosystems and the atmosphere–the state and future of the eddy covariance method. *Global change biology*, *20*(12), 3600-3609.

Barnes, M. A., Peeper, T. F., Epplin, F. M., & Krenzer, E. G. (2001). Effects of herbicides on Italian ryegrass (Lolium multiflorum), forage production, and economic returns from dual-purpose winter wheat (Triticum aestivum). *Weed technology*, *15*(2), 264-270.

Borstlap, S., & Entz, M. H. (1994). Zero-tillage influence on canola, field pea and wheat in a dry subhumid region: Agronomic and physiological responses. *Canadian journal of plant science*, *74*(3), 411-420.

Bushong, J. A., Griffith, A. P., Peeper, T. F., & Epplin, F. M. (2012). Continuous winter wheat versus a winter canola–winter wheat rotation. *Agronomy Journal*, *104*(2), 324-330.

Chi, J., Waldo, S., Pressley, S., O'Keeffe, P., Huggins, D., Stöckle, C., ... & Lamb, B. (2016). Assessing carbon and water dynamics of no-till and conventional tillage cropping systems in the inland Pacific Northwest US using the eddy covariance method. *Agricultural and forest meteorology*, *218*, 37-49.

De Vita, P., Di Paolo, E., Fecondo, G., Di Fonzo, N., & Pisante, M. (2007). No-tillage and conventional tillage effects on durum wheat yield, grain quality and soil moisture content in southern Italy. *Soil and Tillage Research, 92*(1-2), 69-78.

Duke, J. C., Epplin, F. M., Vitale, J. D., & Peeper, T. F. (2009). Canola-Wheat Rotation versus Continuous Wheat for the Southern Plains. In *Selected paper. Atlanta: Southern Agricultural Economics Association Annual Meeting, Atlanta, Georgia, January*.

Edwards, J. T., Carver, B. F., Horn, G. W., & Payton, M. E. (2011). Impact of dual-purpose management on wheat grain yield. *Crop Science, 51*(5), 2181-2185.

Gunstone, F. D. (Ed.). (2004). *Rapeseed and canola oil: production, processing, properties and uses*. CRC Press.

Hossain, I., Epplin, F. M., Horn, G. W., & Krenzer Jr, E. G. (2004). Wheat production and management practices used by Oklahoma grain and livestock producers. *Oklahoma Agricultural Experimental Station, B-818. Oklahoma State University, Stillwater*.

Johnston, A. M., Tanaka, D. L., Miller, P. R., Brandt, S. A., Nielsen, D. C., Lafond, G. P., & Riveland, N. R. (2002). Oilseed crops for semiarid cropping systems in the northern Great Plains. *Agronomy Journal, 94*(2), 231-240.

Liebman, M., & Dyck, E. (1993). Crop rotation and intercropping strategies for weed management. *Ecological applications, 3*(1), 92-122.

Linn, D. M., & Doran, J. W. (1984). Effect of water-filled pore space on carbon dioxide and nitrous oxide production in tilled and nontilled soils 1. *Soil Science Society of America Journal*, *48*(6), 1267-1272.

Liu, M., Wu, J., Zhu, X., He, H., Jia, W., & Xiang, W. (2015). Evolution and variation of atmospheric carbon dioxide concentration over terrestrial ecosystems as derived from eddy covariance measurements. *Atmospheric Environment*, *114*, 75-82.

Montanaro, G., Tuzio, A. C., Xylogiannis, E., Kolimenakis, A., & Dichio, B. (2017). Carbon budget in a Mediterranean peach orchard under different management practices. *Agriculture, Ecosystems & Environment*, *238*, 104-113.

Monteith, J. L. (1995). A reinterpretation of stomatal responses to humidity. *Plant, Cell & Environment*, *18*(4), 357-364.

Musick, J. T., Jones, O. R., Stewart, B. A., & Dusek, D. A. (1994). Water-yield relationships for irrigated and dryland wheat in the US Southern Plains. *Agronomy Journal*, *86*(6), 980-986.

Patrignani, A., Lollato, R. P., Ochsner, T. E., Godsey, C. B., & Edwards, J. (2014). Yield gap and production gap of rainfed winter wheat in the southern Great Plains. *Agronomy Journal*, *106*(4), 1329-1339.

Raymer, P. L. (2002). Canola: an emerging oilseed crop. *Trends in new crops and new uses*, *1*, 122-126.

Redmon, L. A., Horn, G. W., Krenzer, E. G., & Bernardo, D. J. (1995). A review of livestock grazing and wheat grain yield: Boom or bust?. *Agronomy Journal*, *87*(2), 137-147.

REddyProc. 2015. Department Biogeochemical Integration. https://www.bgc-jena.mpg.de/bgi/index.php/Services/REddyProcWebR.

Taylor, A. M., Amiro, B. D., & Fraser, T. J. (2013). Net CO 2 exchange and carbon budgets of a three-year crop rotation following conversion of perennial lands to annual cropping in Manitoba, Canada. *Agricultural and forest meteorology*, *182*, 67-75.

Trusler, C. S., Peeper, T. F., & Stone, A. E. (2007). Italian ryegrass (Lolium multiflorum) management options in winter wheat in Oklahoma. *Weed Technology*, *21*(1), 151-158.

USDA- FAS. 2017. USDA global oilseed demand growth forecast datanase. http://usda.mannlin.cornell.edu/usda/fas/oilseed-trade//2010s/2017/oilseed-trade-05-10-2017.pfd (accessed April 15, 2018).

United States Canola oil consumption staticts database. 2017. https://www.statista.com/statistics/301036/canola-oil-consumption-united-states (accessed April 15, 2018).

Wagle, P., Gowda, P. H., Anapalli, S. S., Reddy, K. N., & Northup, B. K. (2017). Growing season variability in carbon dioxide exchange of irrigated and rainfed soybean in the southern United States. *Science of the Total Environment*, *593*, 263-273.

Wagle, P., Gowda, P. H., Moorhead, J. E., Marek, G. W., & Brauer, D. K. (2018). Net ecosystem exchange of CO 2 and H 2 O fluxes from irrigated grain sorghum and maize in the Texas High Plains. *Science of the Total Environment*, *637*, 163-173.

Wagle, P., Gowda, P. H., Northup, B. K., Turner, K. E., Neel, J. P., Manjunatha, P., & Zhou, Y. (2018). Variability in carbon dioxide fluxes among six winter wheat paddocks managed under different tillage and grazing practices. *Atmospheric Environment*, *185*, 100-108.

Wagle, P., Gowda, P. H., Xiao, X., & Anup, K. C. (2016). Parameterizing ecosystem light use efficiency and water use efficiency to estimate maize gross primary production and evapotranspiration using MODIS EVI. *Agricultural and forest meteorology*, *222*, 87-97.

Wagle, P., & Kakani, V. G. (2014). Seasonal variability in net ecosystem carbon dioxide exchange over a young Switchgrass stand. *Gcb Bioenergy*, *6*(4), 339-350.

Wagle, P., Kakani, V. G., & Huhnke, R. L. (2015). Net ecosystem carbon dioxide exchange of dedicated bioenergy feedstocks: Switchgrass and high biomass sorghum. *Agricultural and forest meteorology*, *207*, 107-116.

Wagle, P., Kakani, V. G., & Huhnke, R. L. (2016). Evapotranspiration and ecosystem water use efficiency of switchgrass and high biomass sorghum. *Agronomy Journal*, *108*(3), 1007-1019.

Wagle, P., Xiao, X., Scott, R. L., Kolb, T. E., Cook, D. R., Brunsell, N., ... & Bajgain, R. (2015). Biophysical controls on carbon and water vapor fluxes across a grassland climatic gradient in the United States. *Agricultural and forest meteorology*, *214*, 293-305.

West, T. O., & Marland, G. (2002). A synthesis of carbon sequestration, carbon emissions, and net carbon flux in agriculture: comparing tillage practices in the United States. *Agriculture, Ecosystems & Environment*, *91*(1-3), 217-232.

Table 1. Management practices applied to conventional till (CT) and no-till (NT) canola fields.

Fields	Date	Event	Product	Rate
CT field	9/6/2016	Broadcast Fertilizer	Dry 46-00-00	112 kg ha^{-1}
	10/4/2016	Fertilizer in Furrow	Dry 18-46-00	49 kg ha^{-1}
	11/4/2016	Herbicide	Glyphosate, Insecticide	
	3/3/2017	Herbicide	Glyphosate, Insecticide	
	2016 (7/13, 8/12)	Tillage (tandem disc harrow)	10-13 cm	
	9/7/2016	Tillage (field cultivator)	10-13 cm	
	10/4/2016	Sowing		
	6/15/2017	Harvest		
Fallow period tillage at CT field	2017 (6/28-6/30)	Tandem disc harrow	10-13 cm	
	2017 (7/29-7/31)	Vertical till	5 cm	
	9/5/2017	Vertical till	5 cm	
	2017 (9/23-9/24)	Seedbed preparation	8-10 cm	
NT field	8/19/2016	Broadcast Fertilizer	Dry 46-00-00	112 kg ha^{-1}
	Date	Event	Product	Rate
	10/3/2016	Fertilizer in Furrow	Dry 18-46-00	49 kg ha^{-1}

	9/19/2016	Herbicide	Glyphosate	
	10/27/2016	Herbicide	Glyphosate, Insecticide	
	3/3/2017	Herbicide	Glyphosate, Insecticide	
	2016 (9/20, 10/3)	Vertical Tillage	5 cm	
	10/3/2016	Sowing		
	6/29/2017	Harvest		

Table 2. Monthly total rainfall and average air temperature (T_a) for the 2016-2017 study period in comparison with the 30-year Normals (1981-2010).

Month	2016-2017		30-Year Normals	
	T_a (°C)	Rainfall (mm)	T_a (°C)	Rainfall (mm)
October 2016	11.00	15	15.91	95
November	11.98	15	9.25	59
December	2.60	23	3.62	46
January 2017	3.49	7	2.85	33
February	8.95	114	5.33	48
March	12.49	50	10.04	80
April	14.99	227	15.13	82
May	18.78	66	20.14	124
June	24.44	136	24.63	113
July	27.43	22	27.43	65
August	23.90	252	27.02	87
September	21.59	119	22.21	94

Table 3. Monthly sums of net ecosystem CO_2 exchange (NEE, g C m^{-2}), gross primary production (GPP, g C m^{-2}), ecosystem respiration (ER, g C m^{-2}), and evapotranspiration (ET, mm) for the study period.

	NEE		GPP		ER		ET	
Month	CT	NT	CT	NT	CT	NT	CT	NT
October 15-31, 2016	-5	-10	42	71	37	61	15	24
November	-70	-90	161	196	91	107	43	50
December	-17	-3	71	72	54	70	23	24
January 2017	12	26	39	24	51	50	23	20
February	-24	15	111	59	86	73	39	30
March	-140	-53	292	161	152	108	76	60
April	-99	-85	341	274	242	189	97	92
May	-4	9	216	295	212	303	111	113
June	-1	59	168	109	168	168	72	64
July	53	77	81	84	133	160	16	32
August	126	150	84	67	210	217	104	75
September	47	77	76	59	124	136	45	44
October 1-15	34	43	19	31	53	74	54	35

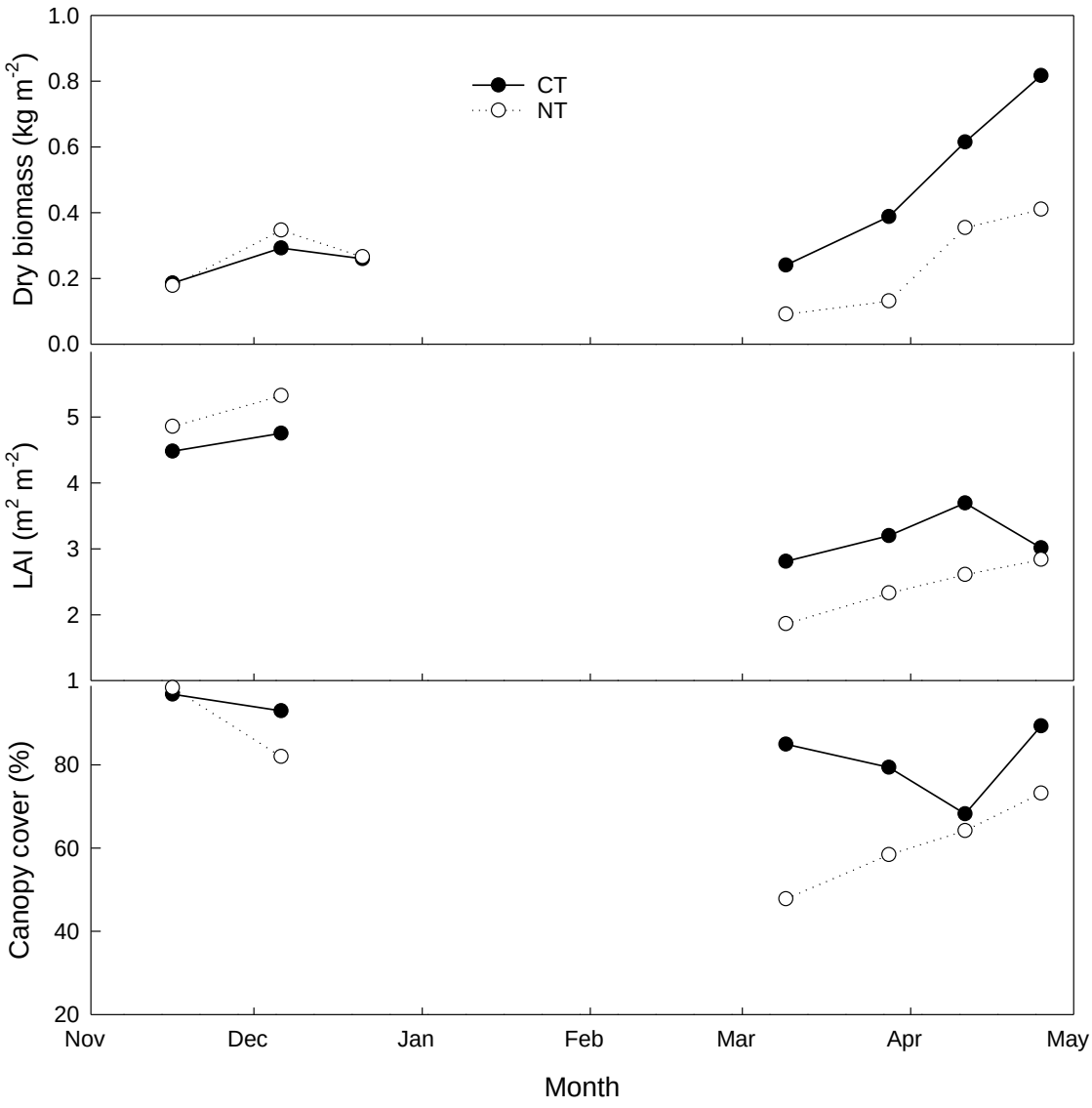

Fig. 1. Seasonal change in aboveground dry biomass, leaf area index (LAI), and percent of canopy coverage for the 2016-2017 growing season in conventional till (CT) and no-till (NT) canola fields.

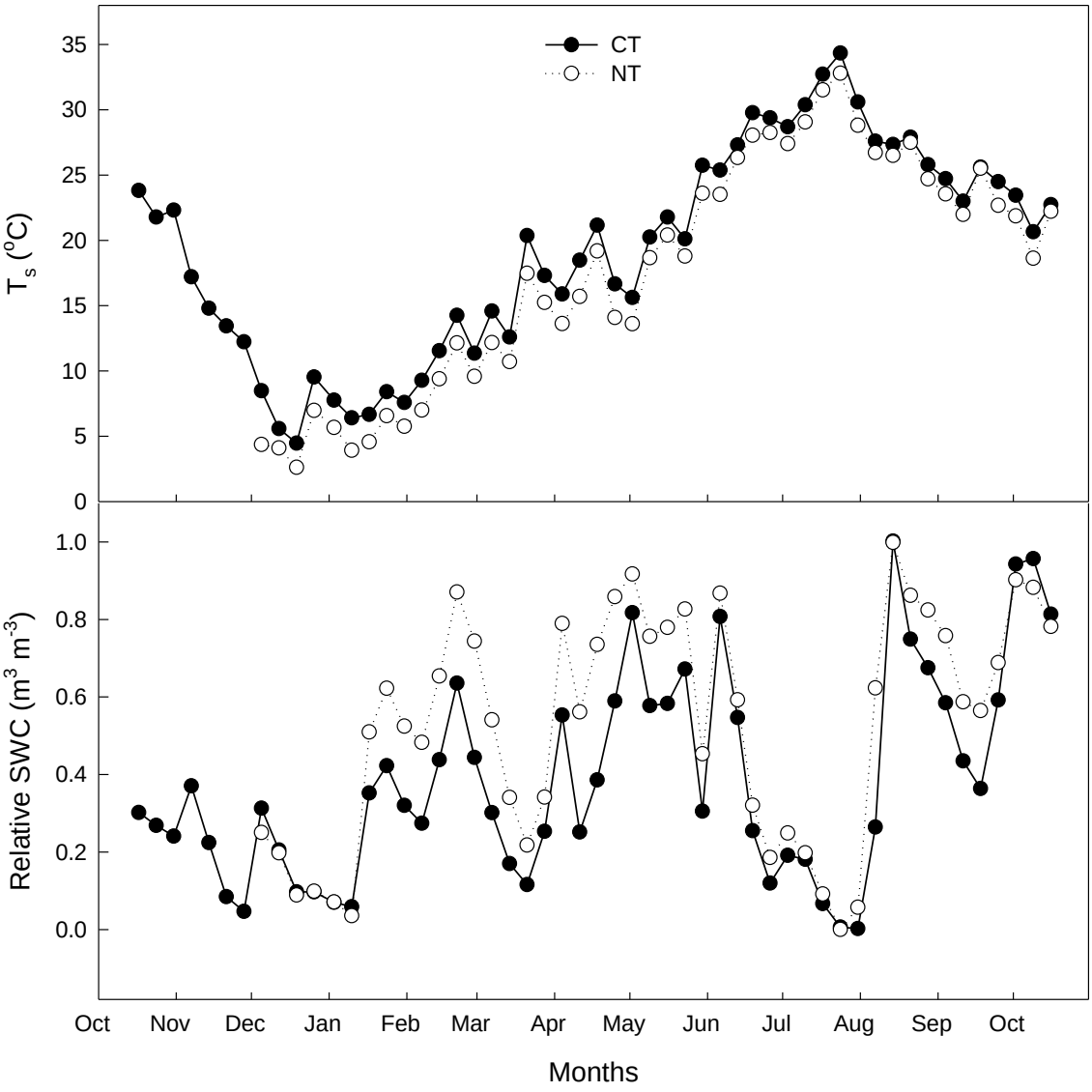

Fig. 2: Soil temperature (T_s) and relative soil water content (SWC) for the study period in conventional till (CT) and no-till (NT) canola fields.

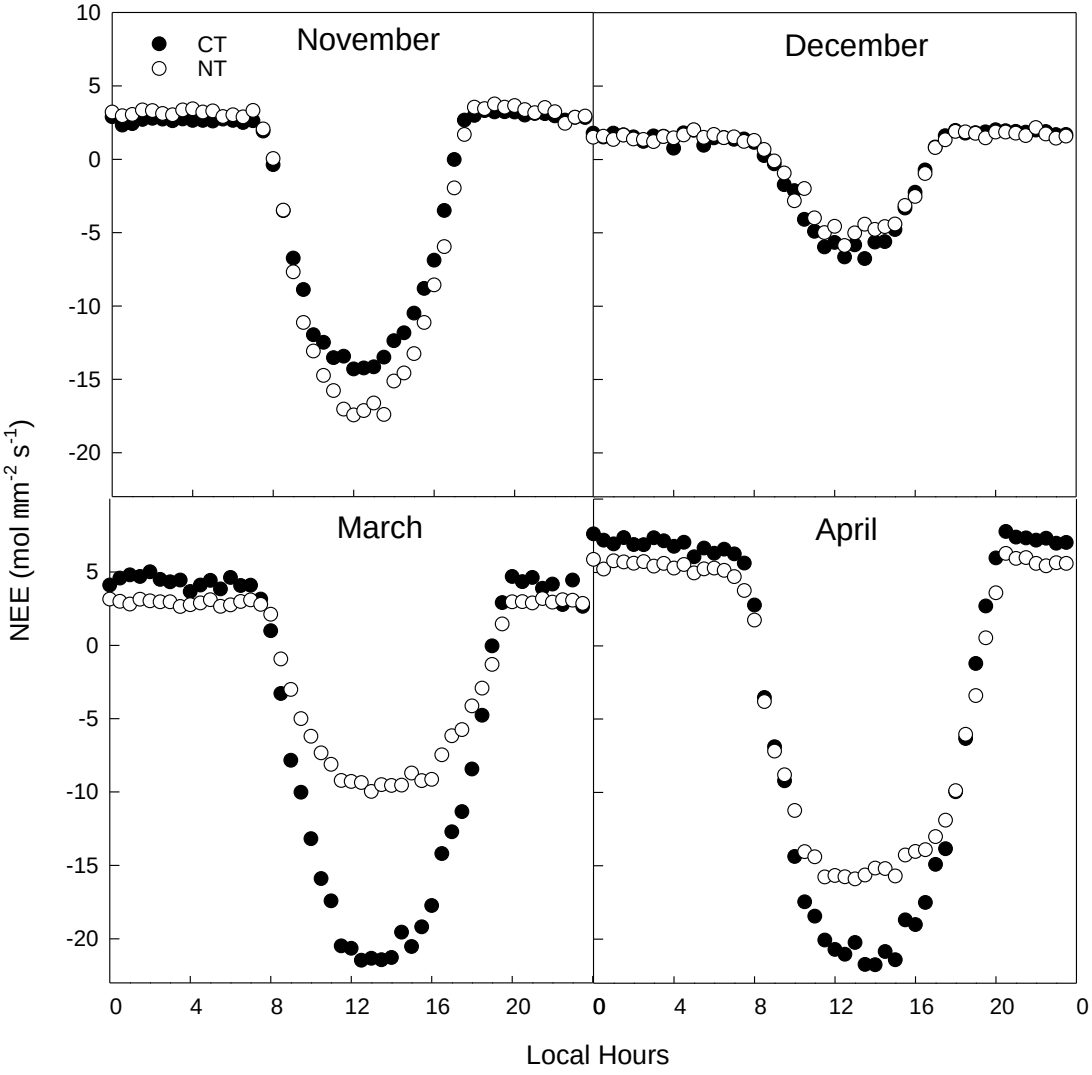

Fig. 3: Half-hourly binned diurnal courses of net ecosystem CO_2 exchange (NEE) for selected months in conventional till (CT) and no-till (NT) canola fields.

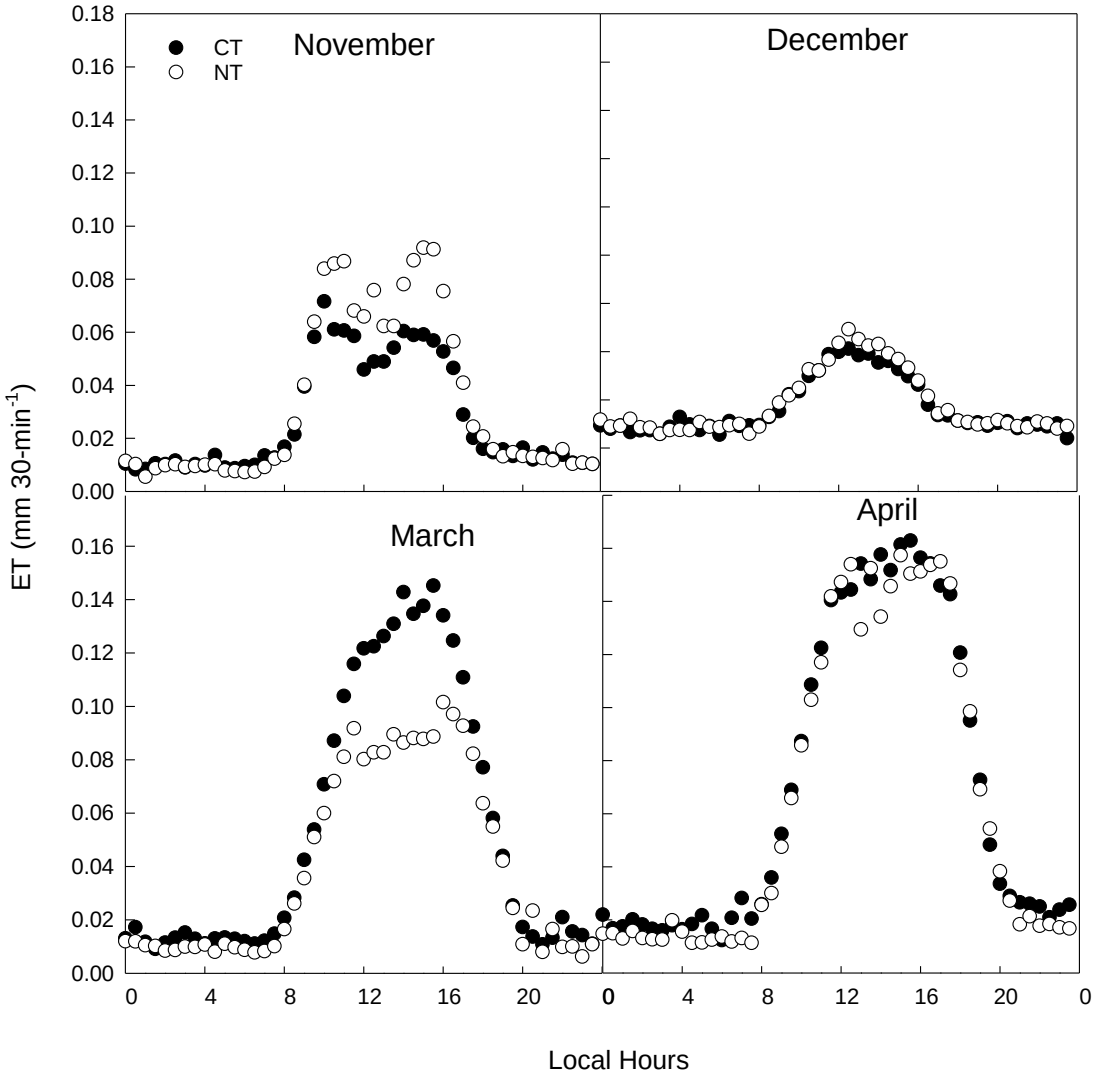

Fig. 4: Half-hourly binned diurnal courses of evapotranspiration (ET) for selected months in conventional till (CT) and no-till (NT) canola fields.

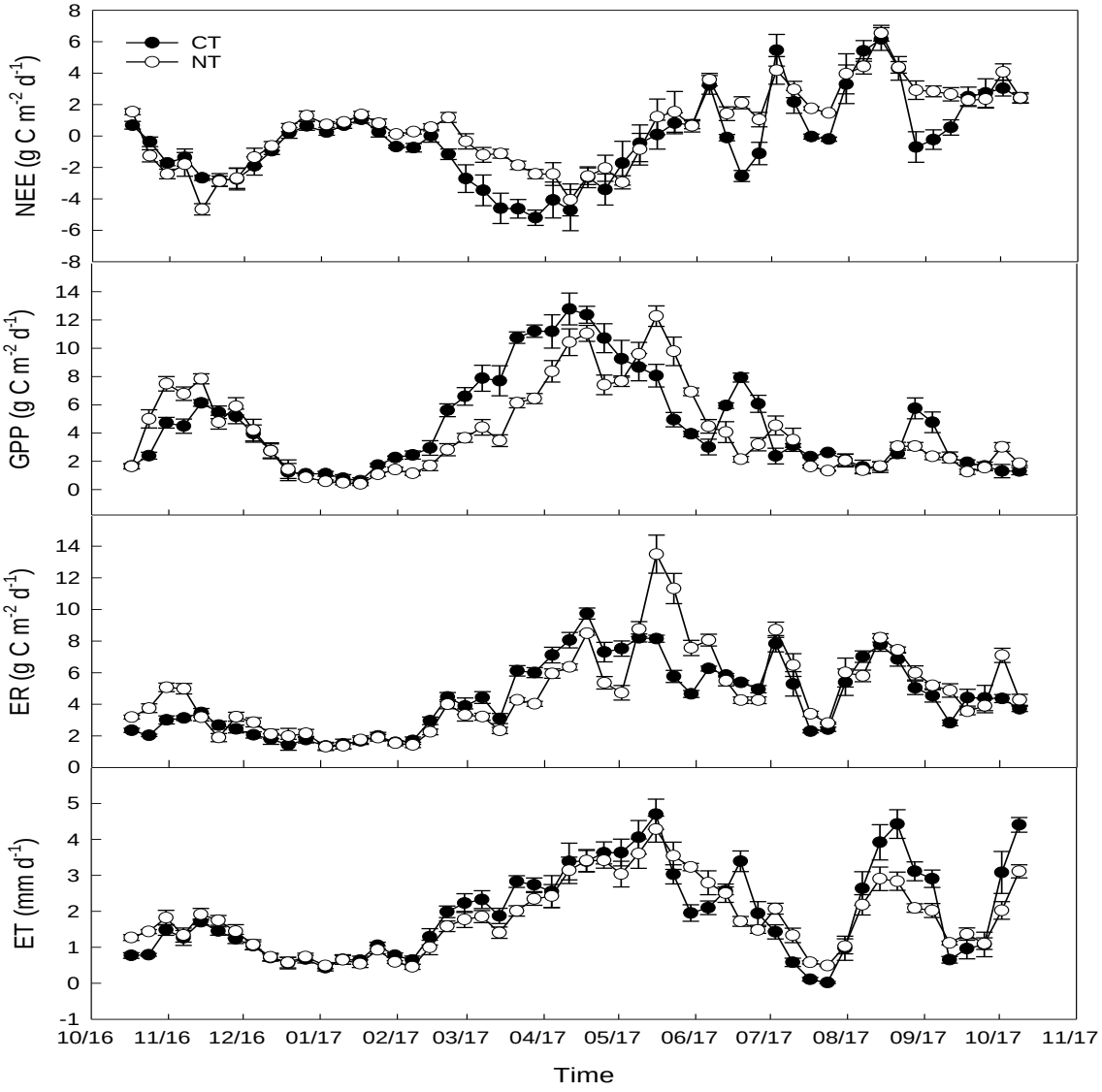

Fig. 5: Seasonal changes (7-day averages) of net ecosystem CO_2 exchange (NEE), gross primary production (GPP), and ecosystem respiration (ER), and evapotranspiration (ET) in conventional till (CT) and no-till (NT) canola fields. Bars represent standard errors of the means.

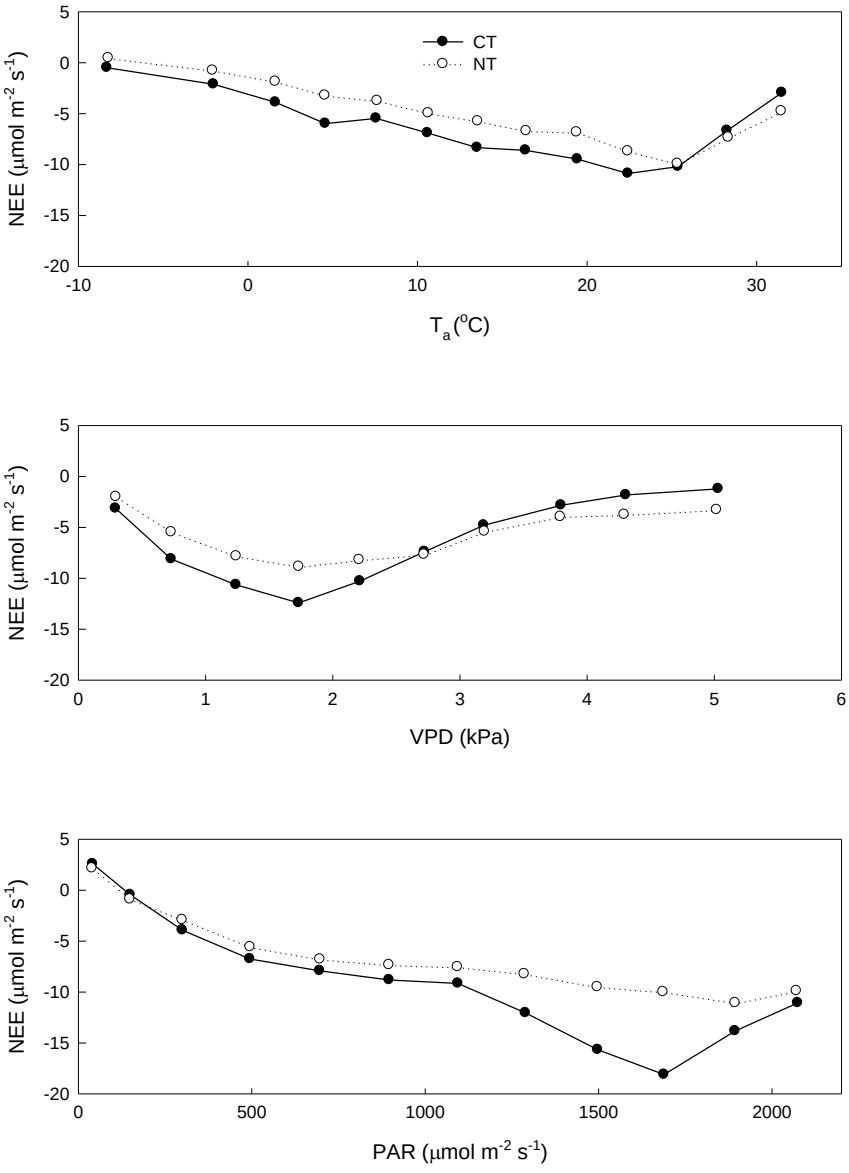

Fig. 6: Response of net ecosystem CO_2 exchange (NEE) to air temperature (T_a), vapor pressure deficit (VPD), and photosynthetically active radiation (PAR) in conventional till (CT) and no-till (NT) canola fields. Half-hourly NEE data for the growing season (November 2016-May 2017) were aggregated in classes of increasing T_a, VPD, and PAR.

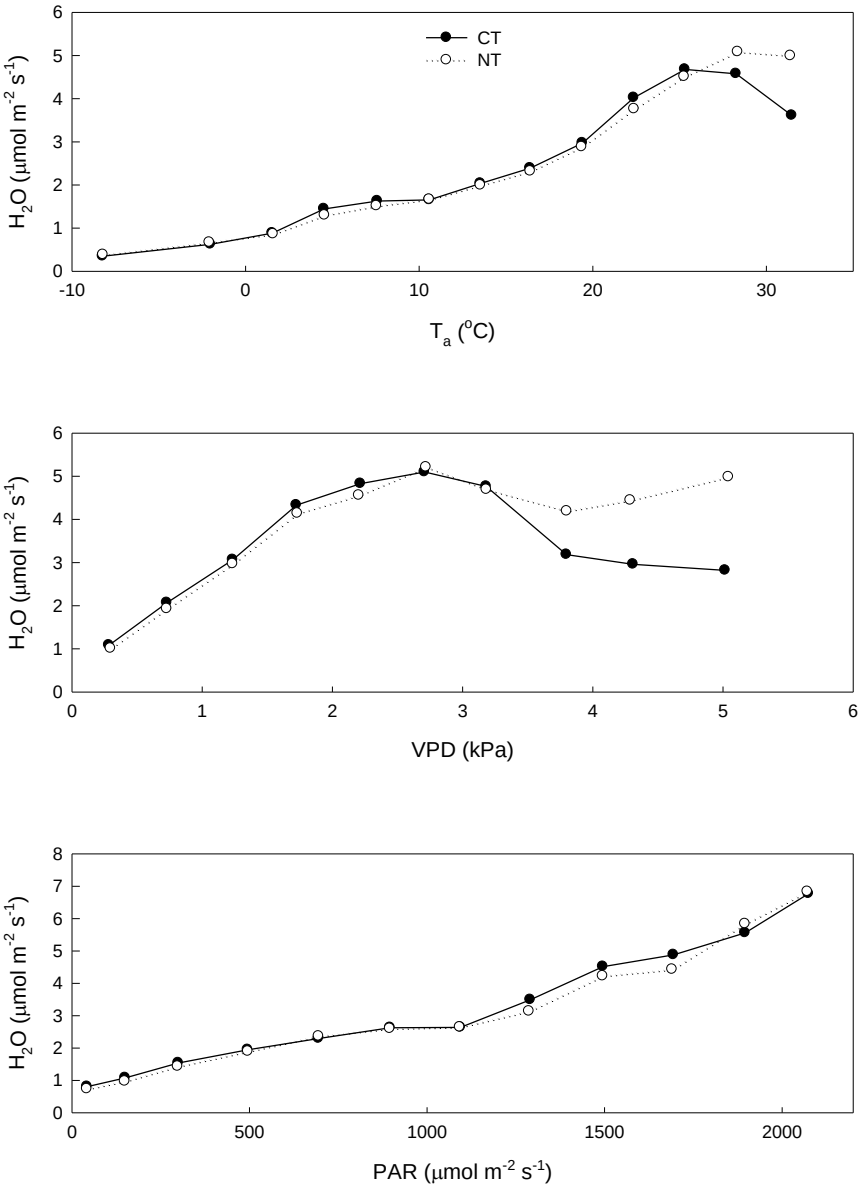

Fig. 7: Response of water vapor (H_2O) flux to air temperature (T_a), vapor pressure deficit (VPD), and photosynthetically active radiation (PAR) in conventional till (CT) and no-till (NT) canola fields. Half-hourly H_2O data for the growing season (November 2016-May 2017) were aggregated in classes of increasing T_a, VPD, and PAR.

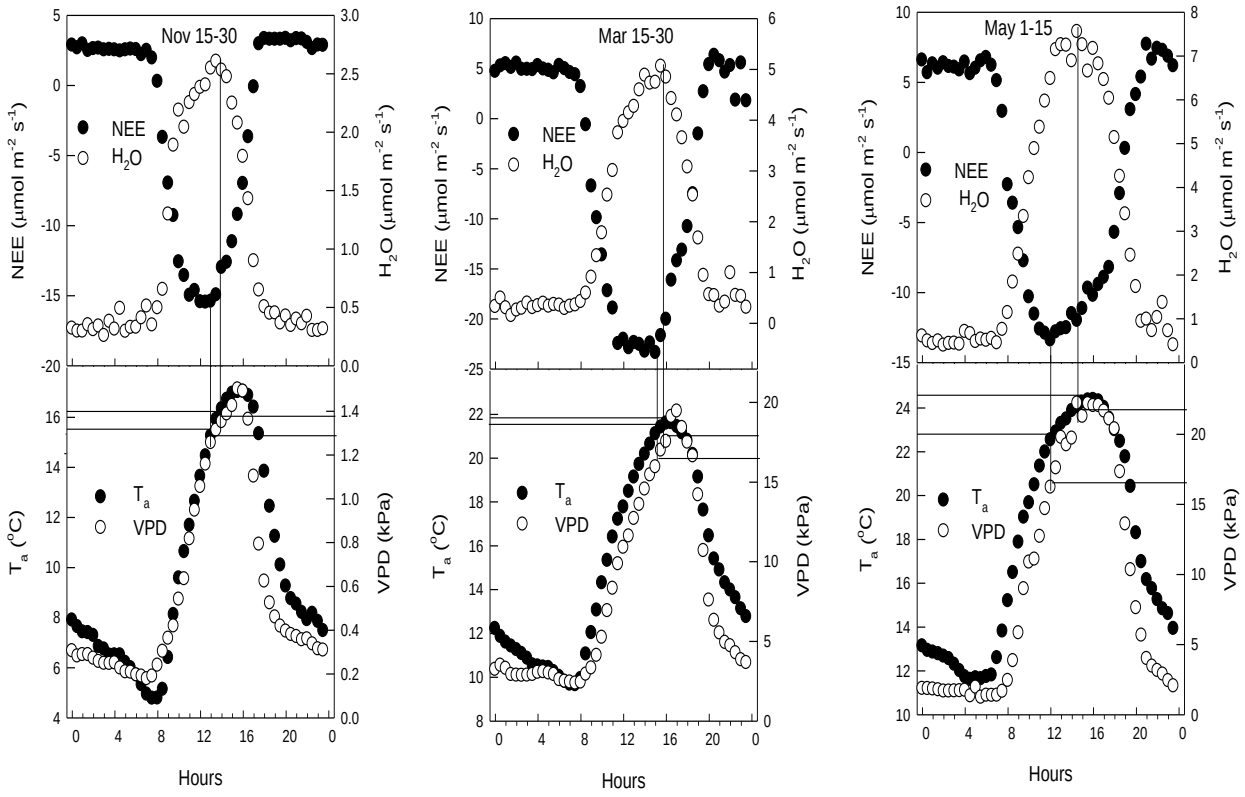

Fig. 8. Half hourly binned diurnal cycles of net ecosystem CO_2 exchange (NEE), evapotranspiration (ET), air temperature (T_a), and vapor pressure deficit (VPD) for selected periods during the growing season.

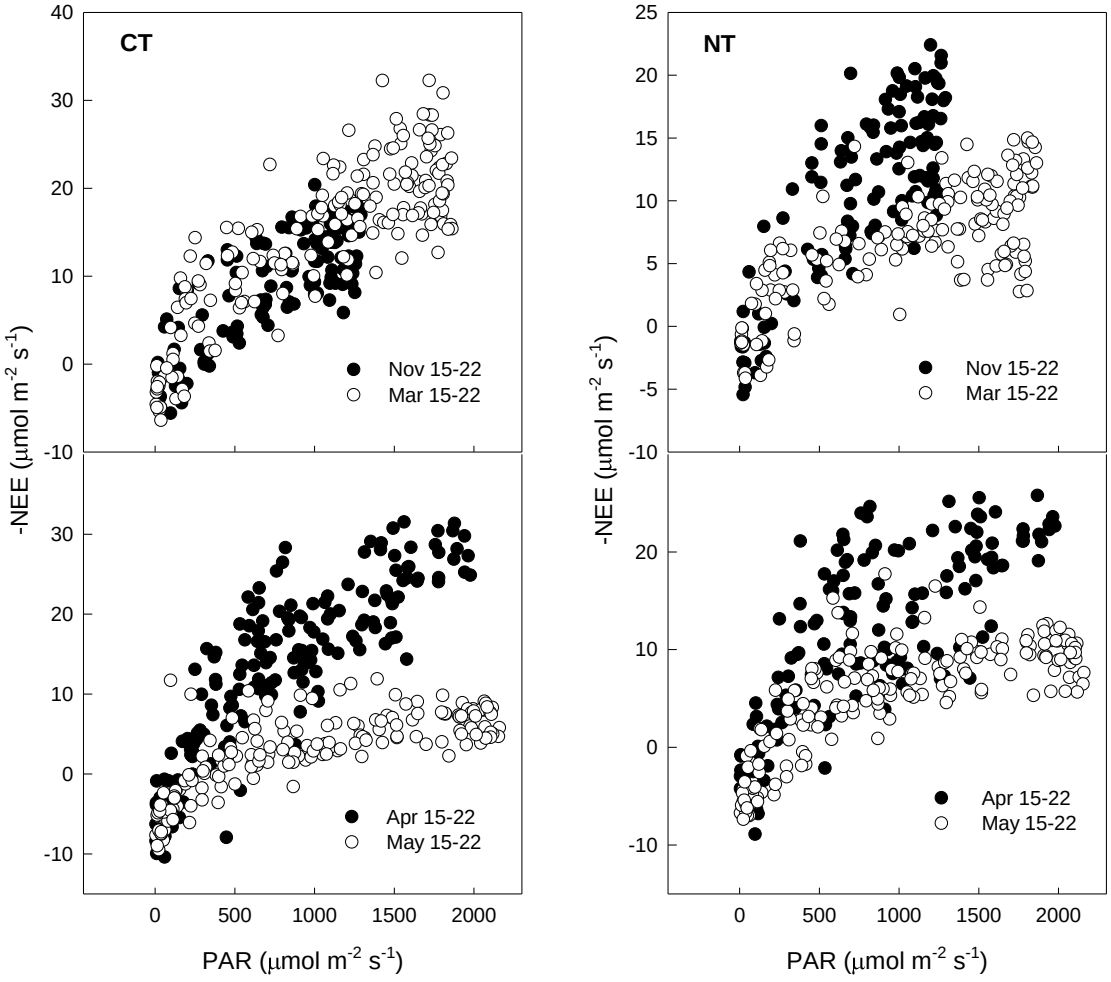

Fig. 9: Comparison of the response between net ecosystem CO_2 exchange (NEE) and photosynthetically active radiation (PAR) for selected periods during the growing season.

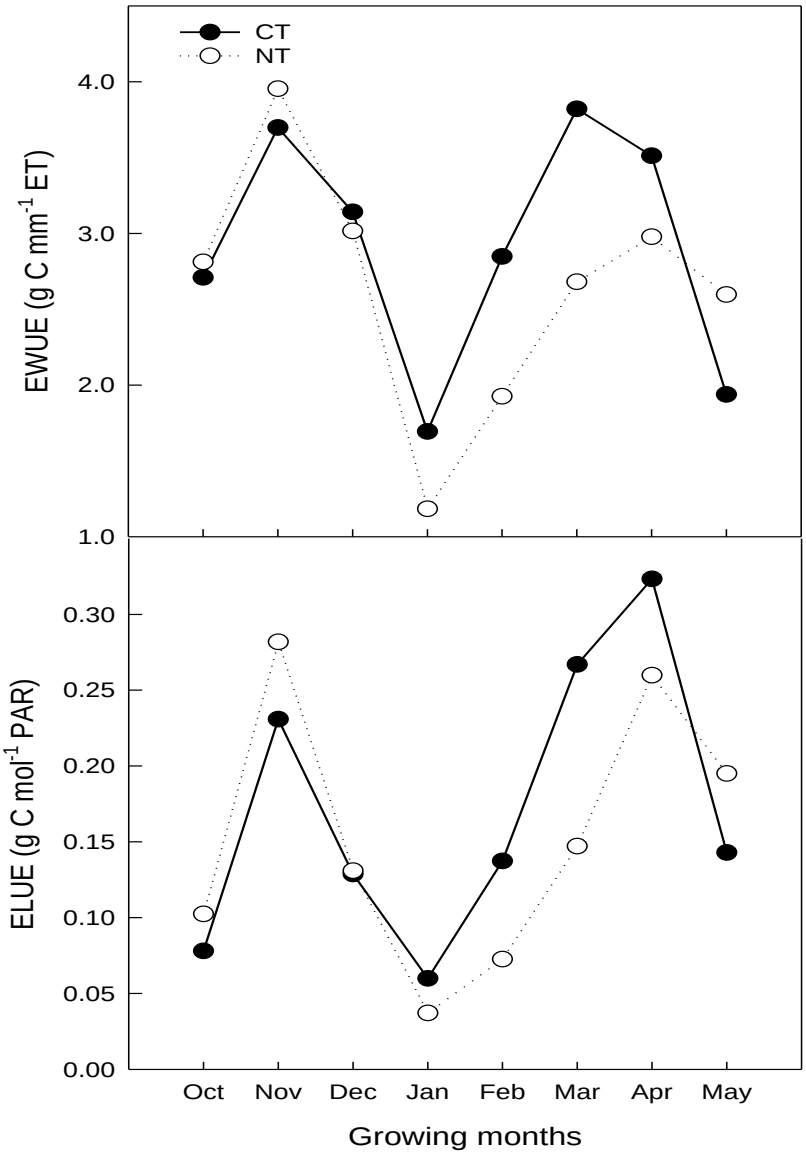

Fig. 10: Monthly values of ecosystem water use efficiency (EWUE) and ecosystem light use efficiency (ELUE) for the 2016-2017 growing season in conventional till (CT) and no-till (NT) canola fields.

CHAPTER V

GENERAL CONCLUSIONS

Eddy covariance (EC) system was used to measure ecosystem level CO_2 and H_2O fluxes from neighboring wheat and canola ecosystems in El Reno, Oklahoma, USA. The study period for wheat spanned from 2016 to 2018, where the 2016-2017 growing season was grain-only and the 2017-2018 growing season was graze-grain wheat. The major objectives of this study were to determine the seasonality of net ecosystem CO_2 exchange (NEE), evapotranspiration (ET), and ecosystem water use efficiency (EWUE) over wheat and canola ecosystems in response to change in environmental factors and management practices.

The energy balance closure (EBC) for the November 2016 – September 2017 period was 0.74 for conventional till (CT) field and 0.76 for NT field. For the 2017-2018 wheat growing season (October 2017 – May 2018), it was 0.75 for CT field and 0.85 for no-till (NT) field. Diurnal peak values of sensible heat (H) decreased as the growing season progressed, then increased after crop senescence and harvesting. In contrast, diurnal peak values of latent heat (LE) increased as the growing season progressed and decreased after crop senescence and harvesting. The ET rates were higher in the 2016-2017 wheat growing season due to more favorable climatic conditions and the management practice (grain-only) that was applied. Daily ET during the 2016-2017 growing season reached ~6.0 mm d^{-1} in both fields. Daily ET for the

2017-2018 growing season reached up to 4.6 mm d^{-1} and 5.3 mm d^{-1} in NT and CT fields, respectively. Lower magnitudes of daily ET in grazed fields than in grain-only fields was due to reduced transpiration from plants related to dry conditions and biomass removal by grazing. Cumulative ET was similar during the 2016-2017 growing season (grain-only wheat) in both systems (459 mm for CT and 469 mm for NT). Cumulative ET during the 2017-2018 growing season (graze-grain wheat) was 365 mm for CT and 404 mm for NT fields. Cumulative ET during the fallow period was substantially higher under CT (216 mm) than NT (146 mm) management. Annual ET for the November 2016 – October 2017 period for grain-only winter wheat in this study was 755 mm for CT field and 684 mm for NT field. The growing season average EWUE was 3.49 and 3.27 g C mm^{-1} ET for the 2016-2017 growing season and 2.82 g C mm^{-1} ET and 2.99 g C mm^{-1} ET for the 2017-2018 growing season for CT and NT fields, respectively. Large differences in ET and EWUE during two growing seasons were attributed to different climatic conditions, 2016-2017 growing season received higher amount of rainfall that resulted in higher ET and EWUE, whereas 2017-2018 growing season was dry with less rainfall that contributed less ET and EWUE. In grain-only management both evaporation and transpiration contributed to ET as a result ET was higher during the 2016-2017 growing season, and lower ET and EWUE during the 2017-2018 graze-grain management was due to reduced transpiration from plants to biomass removal by grazing. The H_2O flux increased rapidly with increasing T_a, VPD, and PPFD, and reached a maximum at optimum T_a of ~24°C and VPD of ~2.25 kPa in CT and NT fields during the 2016-2017 wheat growing season. Optimum values of T_a and VPD for the 2017-2018 growing season were approximately 29°C and 3.5 kPa in CT and NT fields, respectively. We further examined the response of H_2O flux to T_a and VPD by creating diurnal trends of H_2O, T_a, and VPD for two selected weeks (May 1-15) of both grain-

only and graze-grain growing seasons. Daily H_2O patterns during 2017 were symmetrical in grain-only when T_a and VPD was ~24°C and ~2.25 kPa. In comparison, daily H_2O patterns were still symmetrical in graze-grain fields when T_a was ~28°C and VPD was ~2.7 kPa. Higher thresholds of T_a and VPD for the graze-grain growing season could be due to two factors, 1) thresholds of T_a and VPD are generally higher in dry seasons due to adaptation to dry conditions, and 2) higher contribution of evaporation to ET due to sparse vegetation during the graze-grain growing season.

The seasonal sums of NEE were -346 g C m^{-2} and -188 g C m^{-2} at the CT and NT canola fields, respectively. Sums of NEE for mid-October-December period were -91 and -100 g C m^{-2}, but for January-May period were -254.97 and -88.23 g C m^{-2} at the CT and NT fields, respectively. The large discrepancy in NEE for the January-May period was due to poor recovery of crop stand after winter damage at the NT field. During the fallow period, NT field released 38% more carbon than did the CT field. Cumulative seasonal ET during the growing season was similar for both fields (429 mm for CT and 415 mm for NT). Tillage practices and rainfall events also influenced dynamics of CO_2 fluxes and ET during the fallow period. Optimum thresholds of T_a and VPD for H_2O fluxes were approximately 25° C and 2.7 kPa, respectively. The H_2O flux did not decrease with increasing PAR > 2050 μmol m^{-2} s^{-1}. The results showed that NEE was more sensitive to major climatic variables than H_2O fluxes. To further examine the responses of NEE and H_2O fluxes to T_a and VPD, we created diurnal trends of NEE, H_2O, T_a, and VPD for selected periods of growing season at the CT field. Results illustrated that NEE exhibited symmetrical diurnal patterns (reaching peak values at around 2:00 pm) in November and March when T_a and VPD were below thresholds by 2:00 pm. However, H_2O fluxes showed symmetric diurnal pattern (reaching peak values at around 2:00 pm) for all selected periods due to higher

thresholds of T_a and VPD. The monthly EWUE ranged from 1.69 to 3.82 g C mm^{-1} ET at the CT field and from 1.18 to 3.95 g C mm^{-1} ET at the NT field. Growing season EWUE (October 2016 – May 2017) was 1.13 times higher at the CT field than the NT field, most likely caused by higher proportion of evaporation (waste water) loss due to sparse canopy at the NT field during spring 2017. The monthly ecosystem light use efficiency (ELUE) ranged from 0.05 to 0.32 g C mol^{-1} PAR at the CT field and from 0.03 to 0.28 at g C mol^{-1} PAR at the NT field. Large differences in CO_2 fluxes and ET during the growing season between CT and NT fields were mainly caused by differences in stand establishment after winter dormancy rather than by tillage treatment since tillage experiment was initiated just a year prior to this study. However, the impact of tillage on CO_2 fluxes and ET was more evident during the fallow period.

VITA

Priyanka Aggalaiah Manjunatha

Candidate for the Degree of

Master of Science

Thesis: NET ECOSYSTEM EXCHANGE OF CARBON DIOXIDE AND WATER VAPOR FLUXES IN WINTER WHEAT AND CANOLA UNDER CONVENTIONAL TILL AND NO-TILL SYSTEMS

Major Field: Plant and Soil Sciences

Biophysical:

Education:

Completed the requirement for the Master of Science in Plant and Soil Sciences at Oklahoma State University, Stillwater, Oklahoma in May 2019.

Completed the requirement for the Master of Science in Civil Engineering at University of Texas at Tyler, Tyler, Texas in August 2015.

Completed the requirement for the Bachelor of Engineering in Civil Engineering at Nitte Mahalinga Adyanthaya Memorial Institute of Technology, Karkala, India in 2013.

Experience:

Graduate Research Assistant at Oklahoma State University Department of Plant and Soil Sciences from August 2016 to December 2019.

Graduate Research Assistant at University of Texas at Tyler Department of Civil Engineering from January 2014 to August 2015.

Professional Memberships:

American Geophysical Union

American Society of Civil Engineering